Universidade de Aveiro: Departamento de Ciências Médicas
2021

Gonçalo Filipe Giesta de Sousa

Mapeamento da resistência a antifúngicos em *Candida albicans* por abordagens genómicas

Mapping antifungal drug resistance in *Candida albicans* by genomic approaches

Universidade de Aveiro: Departamento de Ciências Médicas
2021

Gonçalo Filipe Giesta de Sousa

Mapeamento da resistência a antifúngicos em *Candida albicans* por abordagens genómicas

Mapping antifungal drug resistance in *Candida albicans* by genomic approches

Dissertação apresentada à Universidade de Aveiro para cumprimento dos requisitos necessários à obtenção do grau de Mestre em Biomedicina Molecular, realizada sob a orientação científica do Doutora Ana Rita Macedo Bezerra, Investigador Doutorado (Nível 1) do Instituto de Biomedicina da Universidade de Aveiro e coorientação e coorientação do Doutor Miguel Monsanto Pinheiro, Investigador auxiliar do Instituto de Biomedicina da Universidade de Aveiro.

This work was supported by the Portuguese Foundation for Science and Technology through UIDB/04501/2020, GenomePT POCI-01-0145-FEDER-022184, and project PTDC/BIA-MIC/1141/2021.

o júri

presidente

Prof. Doutor Ramiro Daniel Carvalho de Almeida
Professor Auxiliar da Universidade de Aveiro

Doutora Ana Rita Macedo Bezerra
Investigador Doutorado (Nível 1) do Instituto de Biomedicina da Universidade de Aveiro

Doutor João Manuel Salvador Simões
Investigador Auxiliar do Centro de Engenharia Biológica da Universidade do Minho

agradecimentos

À minha família pelo suporte dado ao longo desta jornada.

À minha orientadora Doutora Ana Rita Bezerra pela orientação, disponibilidade, apoio e todo o conhecimento que me transmitiu ao longo destes 2 anos.

Ao grupo RNA Biology Laboratory pelo suporte dado em especial à Ana Poim, Carla Oliveira, Rita Guimarães e Inês Sousa por todo o apoio e ajuda que forneceram ao longo deste trabalho.

palavras-chave *Candida albicans*, candidíase, antifúngicos, evolução da resistência, variação genómica, variação fenotípica, erros de tradução, ambiguidade do codão

resumo *Candida albicans* é o principal agente causador de infeções fúngicas invasivas potencialmente fatais vida e com taxas de mortalidade associadas que se aproximam dos 40%, apesar do tratamento. A resistência aos azóis comumente usados está a aumentar e os antifúngicos alternativos, como a anfotericina B ou as equinocandinas, aumentam significativamente o custo da terapia antifúngica. Apesar da relevância económica e clínica da resistência aos antifúngicos, este tópico ainda é pouco estudado. Neste estudo, investigou-se o papel dos erros de tradução do mRNA em proteínas, um mecanismo característico usado por *C. albicans* para diversificar o seu proteoma, na evolução da resistência a antifúngicos. A sequenciação do genoma completo de isolados submetidos a evolução experimental com polienos e azoís foi usada para compreender os caminhos evolutivos que levam ao aparecimento de resistências em estirpes de *C. albicans* com elevado erro de tradução do mRNA, denominadas "hypermistranslators". Os resultados demonstraram que elevados níveis de erro aceleram a aquisição de resistência a azóis, mas não a resistência a polienos. "Hypermistranslation" causou um aumento da frequência de aquisição de resistência ao fluconazol através de CNVs que afetam genes de efluxo, alvos da droga e biossíntese de ergosterol, enquanto no itraconazole as aneuploidias afetaram genes de transporte. Na evolução com o polieno, "hypermistranslation" retardou a aquisição de resistência com as alterações genómicas a resumirem-se a SNPs e INDELs em genes de filamentação.

keywords *Candida albicans*, candidiasis, antifungals, resistance evolution, genomic variation, phenotypic variation, mistranslation, codon ambiguity

abstract *Candida albicans* is the leading cause of life-threatening invasive fungal infections with mortality rates approaching 40%, despite treatment. Resistance to the commonly used azoles is increasing and alternative antifungals, such as amphotericin B or echinocandins, increase the cost of antifungal therapy. Despite the economic and clinical relevance of antifungal drug resistance, this subject remains poorly studied. Here, we investigated the role of protein mistranslation, a characteristic mechanism used by *C. albicans* to diversify its proteome, in the evolution of antifungal resistance. We used whole-genome sequencing to unravel the evolutionary paths leading to the emergence of resistance in hypermistranslating *C. albicans* strains subjected to experimental evolution with drugs from two major classes of antifungals (polyenes, azoles). Results showed that high levels of mistranslation accelerate the acquisition of azole resistance, but not polyene resistance. Hypermistranslation caused more rapid and frequent evolution of fluconazole resistance mediated through CNVs affecting the classical drug efflux and ergosterol biosynthesis pathways, while itraconazole resistant isolates showed aneuploidies affecting transport. In the evolution with the polyene Amphotericin B, hypermistranslation seemed to delay acquisition of resistance with genome changes summed up to SNPs and INDELs in filamentation genes.

Index

Index of Figures

Index of Tables

Abbreviations

VVC - Vulvovaginal candidiasis

Als - Agglutinin-like sequence

GPI - glycosylphosphatidylinositol

Hwp1 - Hyphal Wall Protein 1

Eap1 - Increased Adherence to Polystyrene

rDNA - ribosomal DNA

SNP - Single nucleotide polymorphism

INDELs - Small insertions and deletions

CNV - Copy number variations

LOH - Loss of heterozygosity

CCL - Concerted chromosome loss

MRS - Main repeat sequence

RPS - Repeat sequence arrays

TLO - Telomere-associated gene

MTL - Mating-Like-Type

GOF – Gain of Function

CDR1 - Candida drug resistance 1

CDR2 – Candida drug resistance 2

MIC - Minimum inhibitory concentration

WSG - Whole genome sequencing

YPD - Yeast Peptone Dextrose

PGA – Predicted Gpi-Anchored

LIP – Lipase

SAP – Secreted Aspartyl Proteinase

ERG – Ergosterol Biosynthesis

TAC1 – Transcriptional Activator of CDR genes

MRR1 – Multidrug Resistance Regulator 1

MRR2 - Multidrug Resistance Regulator 2

CDR4 – Candida drug resistance 4

HSP – Heat shock proteins

ALS – Agglutinin-Like Sequence

FGR - Filamentous Growth Regulator

I. INTRODUCTION

Global mortality associated with fungal diseases exceed that of tuberculosis or malaria. Estimates suggest that fungi are responsible for over 1.6 million deaths annually and over one billion people suffer from chronic or allergic infections[1]. Species of *Aspergillus*, *Cryptococcus* and *Candida* are the main causative agents of fungal infections in humans, with *Candida albicans* serving as leading agent of life-threatening invasive infections in developed countries[2]. Amongst the factors contributing to the severity of *C. albicans* infections is the rapid acquisition of antifungal drug resistance. There is also a stark rise in infections caused by *Candida* species that are intrinsically resistant to azole antifungals, including *Candida glabrata*, *Candida krusei* and *Candida auris*[1]. In Europe, antifungal drugs cost €8.4 billion annually and the societal costs in terms of quality of life are severe[1,2]. Despite the economic and clinical relevance of antifungal drug resistance, this subject remains poorly studied in comparison with the similar issue of antibiotic resistance in bacterial pathogens. Mechanisms of antifungal drug resistance are being intensively studied, but progress has been rather slow.

1. Pathobiology of *Candida albicans*: from commensal to pathogen

1.1. Taxonomy and epidemiology

Candida albicans is a species of the Fungi kingdom, phylum Ascomycota, subphylum Saccharomycotina, and class Saccharomycetes[3]. This diploid polymorphic fungus is part of the human microflora and can be found in the gastrointestinal, respiratory, and urogenital tract, as a harmless commensal resident[4–7]. In certain circumstances, this harmless commensal fungus can turn into an opportunistic organism causing various infections that can range from superficial skin infections to life-threatening systemic infections[4,5,8].

Among species of Candida, *Candida albicans* is responsible for 46,3% of cases of invasive candidiasis, mostly in clinical environments. However, the epidemiology of the infection has been changing over the years, due to the appearance of infections related to other species of the genus *Candida*, such as *Candida glabrata* in 24.4% of cases and *Candida parapsilosis* in 8.1% of cases[4,9,10]. Infections caused by *C. albicans* are mainly superficial,

however systemic infections can occur in severely immunocompromised patients with a mortality rate associated of approximately 40% despite the existence of treatment[4,6,11,12]. *C. albicans* is also responsible for a wide variety of mucous infections that occur due to an environmental imbalance such as lowering the pH, or due to weakened immunity caused by HIV infection, which can lead to oral or vaginal candidiasis[4,13]. The most diagnosed infection is vulvovaginal candidiasis (VVC), with approximately 10–15% of asymptomatic women infected with *Candida*, 70–75% of women will have a VVC event in their lifespans, 50% of initially infected women will have a second VVC event, and 5–10% of all women will develop recurrent VVC[12,14]. This disease presents a set of clinical manifestations such as vaginal discharge, pain accompanied with burning and vaginal irritation, leading to dyspareunia and dysuria, vulvar and vaginal erythema, edema and fissures[12,15].

1.2. Virulence attributes

Candida albicans exhibits several characteristics that allow this pathogen to adapt and cope with different conditions within the host, namely in terms of temperature, pH, nitrogen, oxygen and carbon dioxide levels and availability of nutrients. These environmental changes are a source of stress, requiring the activation of regulatory pathways and transcription circuits that impact the morphology of *C. albicans*, promoting its survival within the host[16].

The cell wall of *C. albicans* is a structure in constant evolution, which is approximately 0.5 mm thick, has the function of protecting the cell and is responsible for most of the interactions of the cell with its host and with the surrounding yeasts and bacteria. The innermost layers are formed by a dense network of polysaccharides comprising about 5% of chitin, 40% of β-1,3 glucan and 20% of β-1,6 glucan, and the rest is composed of mannosylated proteins that are found in the outermost layers. The surface is covered by a fibrillar layer whose thickness varies according to the growth medium in which the cells develop[17].

This fungus can be found in different morphologies, such as in the form of yeast, hyphae, pseudo-hyphae, chlamydospore, white, opaque, grey, and GUT[16,18] (Figure 1).

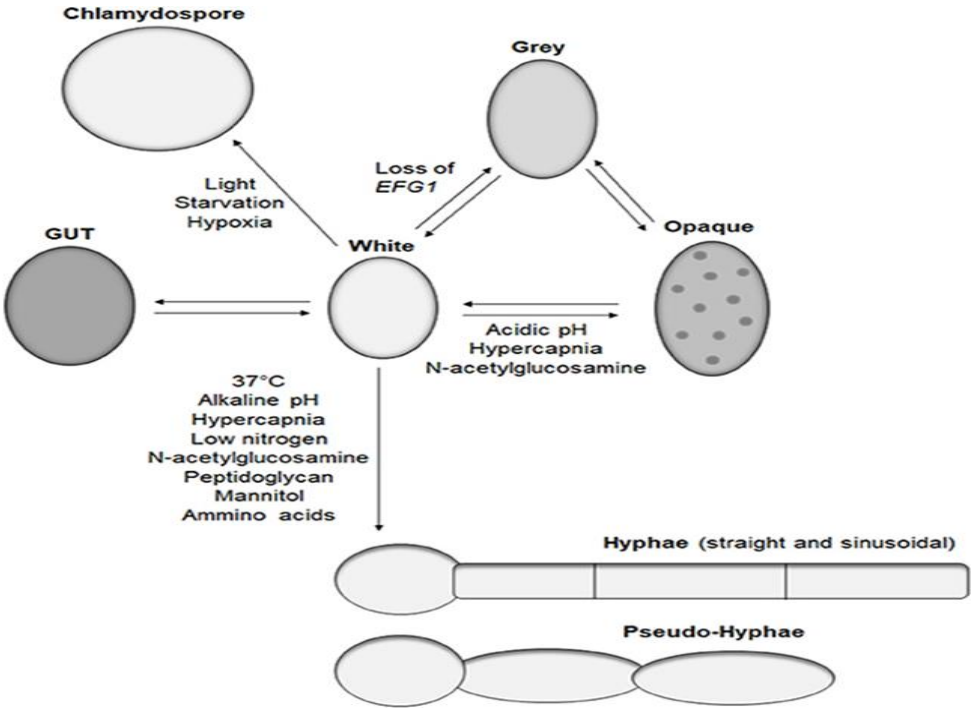

Figure 1 **-** *Candida albicans* morphologies and morphological switches triggered by recognised stimuli. Adapted from Cottier & Hall, 2020[19]

The yeast phenotype has a round to oval cell morphology, like that of the *Saccharomyces cerevisiae* species[18]. It reproduces by budding, the nuclear division occurs at the junction between the mother and daughter cells, and as the descending cells completely detach from the mother cells after cytokinesis these are considered unicellular[18,20,21].

Hyphal cells are highly elongated cells in the form of adherent tubes that can produce complex and branched filamentary networks[18,22]. The nuclear division occurs inside daughter cells, followed by the migration of a nucleus from the progeny back to mother cells; they remain attached after the cytokinesis, so that iterative cycles of cell division produce branched multicellular filamentary structures called mycelia[18]. Hyphal cells are naturally invasive, penetrating the host's epithelial and endothelial barriers by expressing specific virulence factors such as degradative enzymes, cell surface adhesins and Candidalisin (a pore-forming toxin)[22].

Pseudo-hyphal cells share characteristics of yeast and hypha phenotypes. Controversy over this phenotype remains, on whether it represents a type of genuine terminal cell or an intermediate phase in the transition from yeast to hypha when it changes from commensal to pathogenic state[18,23]. Just like hyphae, pseudo-hyphal cells remain attached

after cytokinesis and generate mycelia after several cell divisions[18]. As in yeasts, nuclear division occurs at mother-daughter junctions, and has an ellipsoid shape[18].

Chlamydospores are large spherical cells with thick walls observed *in vitro* under certain adverse conditions, such as starvation and hypoxia[18,24]. They are very rarely found *in vivo*, being generated by cells at the distal ends of mycelial filaments, called suspension cells[18]. The nuclear division occurs inside the parental suspension cell, followed by the migration of a progeny nucleus to the nascent chlamydospore, which remains linked to the parent suspension cell[18,25].

The white phenotype has a morphology like yeast, they form similar domed colonies, creamy white and shiny[18]. However, these colonies can give rise to opaque cells that are slightly darker, matte, and flattened[18]. These are more elongated cells compared to white ones, with more pronounced vacuoles and protrusions on the cell surface[18,26,27]. These cells are related to the *C. albicans* parasexual cycle (described in section 2.2).

Grey cells are smaller than conventional yeasts, don't have protuberances as opaque, have a very low mating efficiency and their morphology is induced when they grow in a nutrient-rich medium[18,28]. These cells can acquire mutations in the transcription factor EFG1, which is well recognised for its role in morphogenesis, because of a genetic change, such as transit through the human gastrointestinal system[19,29]. A *C. albicans* strain that is hemizygous for EFG1 produces white cells morphology, but any functional loss of the remaining EFG1 wild-type allele causes grey cells to develop[19,29]. Grey cells with mutations in EFG1 have been recovered from clinical samples, indicating that such occurrences occur in the human host[19,29].

The GUT phenotype is found within the gastrointestinal tract of mammals[18,30]. They are like the opaque ones, are more elongated than the white ones and they generate darker and flatter colonies[18]. They do not show protuberances on the surface, and they are unable to mate[18].

Besides polymorphism and phenotypic switching, *C. albicans* has other elaborate mechanisms capable of overcoming the barriers raised by the host's body[5]. Adhesion to epithelial cells is a crucial occurrence in both the pathogenic and commensal states[31,32]. It is necessary for colonisation and the subsequent development of mucosal illness, which might result in disseminated candidiasis[31,33]. While passive forces like as van der Waals forces and hydrophobic interactions mediate initial cell-cell contact, adhesion necessitates the

interaction of *Candida* adhesins with host cell receptors[8,34,35]. The Als (agglutinin-like sequence) family of adhesins is the most well-studied[5]. The eight members of the ALS gene family (ALS1-7 and ALS9) are cell surface proteins related to the ß-1,6-glucans of the fungal cell wall via glycosylphosphatidylinositol (GPI)[8,36–38]. Als5-7 and Als9 are adhesins present on the surface of yeast cells, whereas ALS1-4 encode adhesins specialised for germ tubes and hyphae[8,39]. Another hypha-associated GPI-linked protein, Hyphal Wall Protein 1 (Hwp1), also plays a significant role in mediating adhesion to host cells[8]. Aside from Hwp1 and Als proteins, several *C. albicans* adhesins are known, including the morphology-independent Eap1 (increased adherence to polystyrene), which was discovered due to its resemblance to a *Saccharomyces cerevisiae* GPI-linked protein[8].

C. albicans relies on two complementary pathways to invade host cells: induced endocytosis and active penetration[8,40]. The pathways depend on the host's epithelial lineage, as *C. albicans* uses both pathways to invade oral epithelial cells[8,32,40], but active penetration is the only way to get into gastrointestinal epithelial cells[8,41]. The fungus causes induced endocytosis by expressing specific proteins on the cell surface (invasins) that facilitate binding to host ligands (such as E-cadherin on epithelial cells[42] and N-cadherin on endothelial cells[43]), causing the fungal cell to be engulfed by the host cell[5]. So far, Als3 and Ssa1 have been identified as invasins[42,44]. Ssa1 is a heat shock protein family member that is expressed on the cell surface[44]. Als3 and Ssa1 bind to host E-cadherin and are thought to trigger endocytosis through a clathrin-dependent mechanism. Nevertheless, macropinocytosis has also been linked to *C. albicans* induced endocytosis[41,42]. Active penetration, on the other hand, is a fungal-driven process that necessitates the presence of *C. albicans* hyphae[32,41]. The mechanisms that mediate this second pathway of invasion into host cells are mostly unknown[5]. *C. albicans* hyphae can produce hydrolases after attachment to host cell surfaces and hyphal development, which has been hypothesised to aid active penetration into these cells[40]. Furthermore, secreted hydrolases are considered to improve extracellular nutrient acquisition efficiency[45]. *C. albicans* produces three types of secreted hydrolases: proteases (Sap1–10), phospholipases (Plb1–5), and lipases (Lip1–10)[5].

Contact sensing is an essential environmental signal that causes *C. albicans* to produce hyphae and biofilms[5]. Yeast cells transition to hyphal development when they come into touch with a surface[46]. These hyphae can then infiltrate on specific substrates, such as agar or mucosal surfaces[5]. Biofilms are formed when cells encounter solid surfaces[46].

Thigmotropism, directional hyphal growth, can develop on surfaces with certain topologies (such as the presence of ridges)[47]. This is regulated by extracellular calcium uptake through the calcium channels Cch1, Mid1, Fig1[47] and additional mechanisms include the polarisome Rsr1/Bud1-GTPase module[48]. This specific direction is required for full damage of epithelial cells[49]. As a result, pathogenicity depends on accurate sensing and responsiveness to both biofilm development and invasion surfaces[5].

Furthermore, binding of yeast cells to abiotic or biotic surfaces can give rise to the formation of biofilms. Biofilms come into form by a sequential process that includes the adherence of yeast cells to the substrate, their proliferation, hyphal cell formation in the upper part of the biofilm, accumulation of extracellular matrix material and the dispersion of yeast cells from the biofilm complex[50,51]. This is an important virulence factor since it confers resistance to antifungal agents, host defence mechanisms and physical and chemical stresses[5].

In addition to these virulence factors, several fitness traits influence fungal pathogenicity, including a robust stress response mediated by heat shock proteins, auto-induction of hyphal formation through amino acid absorption, ammonia excretion and concomitant extracellular alkalinization, metabolic flexibility, absorption of different compounds as carbon and nitrogen sources, and absorption of essential metals such as iron, zinc, copper, and manganese[5].

Overall, it is clear that *C. albicans* has evolved a variety of mechanisms to allow the fungus to fine-tune its response to specific microenvironments in the host and switch from harmless commensal to invasive pathogen. Among such mechanisms are epigenetic regulation, niche-specific patterns of gene expression, stress-induced mutagenesis, and the ability to generate large-scale genetic variation.

2. Genomic plasticity of *Candida albicans*

2.1. Genome and types of genetic diversity

C. albicans has its diploid genome composed of eight chromosomes, numbered 1 to 7 and one called R, which encodes the ribosomal DNA (rDNA) locus. In research studies, *C. albicans* SC5314 is widely used as the reference genome with a size of 14.3 Mb encoding approximately 6400 genes[52]. It contains 43,665 heterozygous positions, with a single nucleotide polymorphism (SNP) every 330 bp between homologous chromosomes, which are not distributed uniformly across the genome, and whose frequency varies among isolates[52]. Although *C. albicans* is heterozygous diploid, it can propagate with altered ploidy, with copy number variants and different patterns of heterozygosity, which provides selective advantages for specific *in vitro* and *in vivo* conditions that contribute to successful colonization, persistence, and adaptability in diverse hosts[53].

Genome plasticity is a distinctive feature of *C. albicans* due to DNA small insertions and deletions (INDELs), copy number variations (CNV), loss of heterozygosity (LOH) and karyotypic variation due to segmentation and aneuploidies of whole chromosomes. These genomic alterations occur often in response to environmental stresses such as heat shock, host interactions and in the presence of antifungals[53,54]. The parasexual cycle of *C. albicans* also contributes to genomic plasticity through the concerted chromosome loss (CCL) that produces genetically diverse products (described in section 2.2), in part due to the formation of multiple aneuploid forms[11,52].

In the *C. albicans* genome, several repetitive loci have been identified that serve as hotspots for genome rearrangements that contribute to genomic and phenotypic plasticity[53,54]. The four main repetitive regions are the telomeres, subtelomeres, the main repeat sequence (MRS) and the rDNA locus[53,54]. These repetitive loci can have one or more copies that encode identical or nearly identical tandem-repeated sequences of length ranging from one to thousands of nucleotides[53,54]. This makes these loci prone to recombination, which results in indels and translocations between adjacent and distal repeats [53,54]. Adjacent recombination alters copy number variants as well as promoting de novo and non-inherited mutations due to errors in DNA exchange and repair [53,54]. Also, recombination between distal and non-allelic repeats can result in large-scale chromosomal aberrations such as fusion events, truncations, and translocations [53,54].

MRSs are involved in many of the translocations and rearrangements that are detected in *C. albicans* chromosomes. They are the largest non-telomeric homologous sequences present on each chromosome, one on chromosomes R, -1, -2, -5 and -6, and two on chromosomes -4 and -7. Chromosome -3 only contains a portion of the sequence[55,56]. An MRS is composed of several large 2 kb repeat sequence arrays (RPS), which are between two non-repeating sequences, the RB2 and the HOK with 6 kb and 8 kb, respectively[11]. The MRS main unit (RPS-1) is composed of smaller repetitive segments of about 80 – 170 bp, which are separated into two families of ordered segments, REP1 and REP3 that contain the common 29 bp sequence COM29 (5'- CAAAAAAGGCCGTTTTGGCCATAGTTAAG-3')[53]. Due to its size and presence on all chromosomes, it becomes a potential hotspot for reciprocal recombination events between non-homologous chromosomes, generally resulting in the formation of two new chromosomal bands. The expansion and contraction of MRS caused by intrachromosomal recombination also contribute to the chromosome size polymorphism, however this recombination only affects a homolog[53]. Changes in MRS size are detected more frequently on the smaller chromosomes and their length affects chromosomal segregation, with homologues with a larger MRS having a higher rate of chromosomal non-disjunction than the same homologue with a shorter MRS[53]. Size variations also occur on chromosome R due to the frequency of recombination between the rDNA *locus*, producing extrachromosomal rDNA circles and extrachromosomal linear rDNA plasmids[53].

The telomeric region is divided into two distinct parts, the telomeres and the subtelomeres. Telomeres in *C. albicans* have 23 bp (5'-ACTTCTTGGTGTACGGATGTCTA-3') which are substantially divergent from other *Candida* species, being more complex and larger in size[53]. Their maintenance through recombination plays a critical role in genome instability[53]. During alternative telomere elongation, a telomerase-independent and recombination-dependent process adds telomeric repeats to chromosome ends, and a by-product can be produced[53]. These by-products are characterized by telomeric circles that are somehow involved in genomic instability[53]. However, in *C. albicans*, very little experimental work has been carried out in relation to telomeres and genome plasticity in recent decades[53].

Subtelomeres are genomic regions adjacent to telomeres that are enriched with repetitive sequences such as transposons and expanded genes family members[52,53]. Approximately 50 protein-coding genes were annotated in the SC5314 reference genome, associated with several roles linked to virulence and pathogenicity [52,53]. Most of these genes belong to the telomere-associated gene (TLO) family, and participate in the regulation of several functions, including growth, resistance to stress factors and biofilm formation. In subtelomeres there are also several repetitive elements of DNA that contribute to genomic plasticity, such as the long terminal repeats, the unique non-LTR retrotransposon Zorro2, TLO recombination element and the Bermuda Triangle sequence that is within the TRE sequence [52,53]. These elements have a high probability of undergoing recombination, the most frequent being the loss of heterozygosity (LOH). LOH occurs when heterozygous positions between two homologous chromosomes are lost, making these regions homozygous [52,53]. This event can involve chromosome segments of various lengths or even the entire chromosome, however LOH in entire chromosomes is a rare event compared to segmental events. Large-tract LOH are attributed to mitotic crossovers or break-induced replication, and usually lie between the site of the DNA break to the end of the respective chromosome arm [52,53]. Short-tract LOH occur via gene conversion or double crossovers and are mainly located in the telomeric region, in regions with repeats and in genes with repetitive elements [52,53].

The rDNA repeats are a matrix located on the right arm of the R chromosome at the RDN1 locus, with a length between 11.6 kb to 12.5 kb[53]. The rDNA unit repeats vary between 21 and 176 copies, depending on the strain and the growth conditions[53]. The size of RDN1 varies to a large extent due to the high frequency of intrachromosomal recombination between the rDNA repeats, which contribute approximately 92% of the chromosomal variation and instability of the morphology of mutant colonies of *C. albicans*[53].

In addition to the four main repeat regions described above, there are still other regions that contribute to genomic plasticity such as the ALS gene family, centromeres and other long repeat sequences that have not yet been characterized[53]. ALS genes are part of the adhesin group, and can be found in eight distinct loci, each producing a glycoprotein capable of forming amyloid-like aggregates[53]. Mutation and LOH rates within this gene family are also remarkably high compared to the four major repeat regions[53]. Within each ALS *locus*, there is a conserved Ser/Thr-rich domain that is prone to intergenic recombination between

ALS homologues, but intragenic recombination may also occur, producing new genetic variants[53]. In *C. albicans* the centromeres are between inverted repeats that, when recombined, lead to the formation of isochromosomes (chromosomes being composed of two identical arms joined in a functional centromere)[53,54].

2.2. Parasexual cycle

Candida albicans was considered asexual for a long time, until the discovery of a highly complex parasexual cycle (Figure 2).

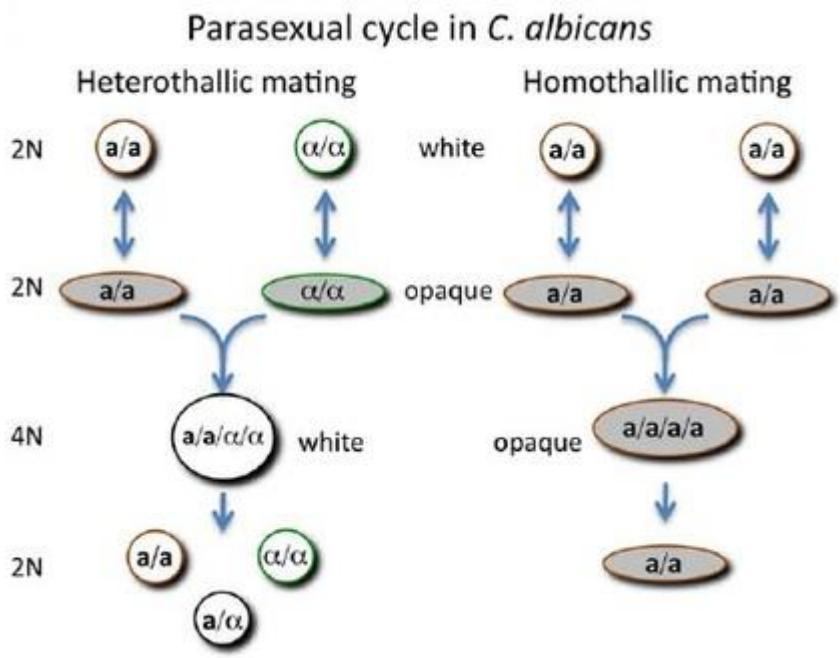

Figure 2 - C. albicans **heterothallic and homothallic mating cycles.** To become mating competent, cells must transform from a white to an opaque condition in both mating cycles. The merging of diploid a and alpha cells to generate a white tetraploid a / alpha cell is known as heterothallic mating. Under some circumstances, homothallic mating between two opaque a cell (or two alpha cells) might result in the formation of an opaque tetraploid cell. Adapted from Bennett, 2010[144]

This cycle is regulated by the Mating-Like-Type (MTL) locus, located in a region of chromosome 5[18,57]. The configuration of the MTL locus controls the phenotypic change between White to Opaque [18,57]. The reversible exchange between the two cellular states occurs stochastically under specific environmental conditions [18,57]. This change is regulated by the transcription factor Wor1, whose expression is necessary and sufficient for the

formation of the opaque phenotype[18]. The two phenotypes differentially express 16% of the genome, which gives them distinct functional attributes[18].

The MTL locus has two distinct configurations, called a and α, encoding genes that specify two types of cells[58]. In the clinical isolates of *C. albicans*, the majority are diploid and have a heterozygous MTL configuration (a/α), however some isolates were found in a homozygous MTL configuration (a/a or α/α)[58]. Heterozygous strains express the sexual genes MTLa1 and MTLα2, in which their protein products form a heterodimer that directly represses the change from white to opaque phenotype by binding to the Wor1 promoter region, while homozygous MTL strains contain the MTLa1 gene or MTLα2, but not both, so that the production of heterodimers that repress the expression of Wor1 does not occur, causing a change of state from white to opaque[58].

In the parasexual cycle there are two types of mating, heterothallic and homothallic mating. Heterothallic mating occurs between MTL-homozygous a / a cells and MTL-homozygous α / α cells[58,59]. These homozygous cells switch from white to opaque and secrete specific pheromones, activated through the MAPK signalling pathway[58]. Cells with the a / a configuration secrete pheromones a encoded by the MFa1 gene and those with the α / α configuration secrete α pheromones encoded by the MFα1 gene. This promotes the development of mating projections towards the greatest pheromone concentration gradient[29,58]. When the two mating projections come together, it allows nuclear fusion and the formation of a tetraploid nucleus that undergoes a process of loss of combined chromosomes (CCL) to generate diploid progenies[58]. Unlike heterothallic mating, homothallic mating occurs between MTL-homozygous cells with the same configuration[58]. This event is only possible when opaque cells do not have Bar1 protease that inactivates α pheromone, which results in fusion between opaque cells a[58,59]. As mentioned above, *C. albicans* returns its tetraploid products to the diploid state through the non-meiotic depolyploidization process, CCL[57]. However, this process is not always carried out properly, which leads to the generation of aneuploids[57]. As explained in the previous section, variations in chromosome organization and copy number are a common mechanism used by *C. albicans* to rapidly generate diversity in response to stressful growth conditions, including, but not limited to, antifungal drug exposure.

3. Antifungal drug resistance in *Candida*

3.1. Mechanisms of action of antifungal drugs

Currently, there are only 5 classes of antifungal agents: polyenes (amphotericin B, nystatin and natamycin), azoles (fluconazole, itraconazole, posaconazole, voriconazole and isavuconazole), echinocandins (caspofungin, micafungin and anidulafungin), allylamines (terbinafine) and antimetabolites (flucytosine)[60]. The fact that there are only five classes of antifungals can be explained by the eukaryotic nature of both fungal pathogens and their hosts, which explains the lack of specific targets and subsequently limits the effectiveness of these antifungal agents[61,62].

Polyenes have a unique mechanism of action compared to other classes of antifungal agents[63]. They do not have a specific enzyme as their target but interact with an essential molecule of the cell membrane, ergosterol[63]. Currently, four distinct models of polyene action are proposed: the pore forming model, the surface adsorption model, the sterol sponge model, and the oxidative damage model[63]. In the model of pore formation, polyenes and ergosterol interact to form a complex like an ion channel in the cell membrane, so that ions and small organic molecules leak from the cell, leading to cell death[63]. Surface Adsorption and Sterol Sponge Models both hypothesize that, by adsorption or extraction of ergosterol from the membrane, the phospholipid membrane is destabilized and essential cellular processes such as endocytosis and regulation of membrane protein function are disturbed[63]. In the oxidative damage model, polyenes induce oxidative stress and cause DNA damage, protein carbonylation and lipid peroxidation, eventually leading to or contributing to cell death[63].

Azoles interfere with the ergosterol biosynthesis pathway through the inhibition of the enzyme lanosterol 14-a-desmethylase (encoded by ERG11), which has the function of converting lanosterol into ergosterol. Inhibition of this enzyme leads to the accumulation of a toxic sterol (14- α-methyl-3,6-diol) in the fungal cellular membrane, which results in loss of membrane integrity, inhibiting cellular growth[64].

Echinocandins are lipopeptides modified from pneumocandins which target the 1,3-β-d-glucan synthase enzyme, composed of transmembrane catalytic Fsk and intracellular regulatory Rho1 subunits. The antifungal inhibits the Fsk1 subunit, preventing the conversion of glucose uridine diphosphate into a β-d-glucan (polymer in fungal cell walls)[65].

The disruption of the structure of growing cell walls results in osmotic instability and fungal cells death[65].

Allylamines interfere with ergosterol biosynthesis by inhibiting squalene and epoxidase[60]. This inhibition leads to the accumulation of the ergosterol precursor squalene that increases membrane permeability and consequently promotes membrane rupture[60]. Antimetabolites are pyrimidine analogues and selectively interfere with nucleic acid synthesis, however their use as monotherapy is rare due to the rapid development of resistance and is therefore mainly used as a component of combined therapy[60].

3.2. Antifungal resistance mechanisms

Due to the implications of fungal drug resistance for human health, it is important to understand the molecular mechanisms behind the acquisition of resistance. Most known mechanisms involve mutations, ranging from chromosomal re-arrangements to point mutations, that alter the binding of the drug to its target. Other mutations cause gene expression changes that reduce drug susceptibility by inducing drug transporters or strong stress responses[6,66] (Figure 3).

Of all antifungal classes, azoles are the most used against infections from *C. albicans*. Fluconazole is widely used in the clinical setting due to its great efficiency, low toxicity, excellent bioavailability, and low cost. However, the extensive use of fluconazole and its fungistatic nature has increased resistance to azoles[67,68]. Various pathways can contribute to azole resistance, including sterol biosynthesis changes, resulting in sterols being substituted for ergosterol; overexpression of the target enzyme, resulting in adequate activity when the antifungal drug is present; upregulation of drug efflux pumps, which lowers the drug's intracellular concentration; alterations in the target gene sequence, resulting in a decrease in the protein's drug binding affinity (Figure 3)[66,69,70].

Point mutations in the ERG11 gene, which encodes the enzyme targeted by azoles, are frequently linked to resistance[66,71,72], with 21 of the 140 point mutations identified for this gene linked to fluconazole resistance[66,73]. Azole resistance has also been discovered to be conferred by inactivation of the protein expressed by the ERG3 gene[66,74]. ERG3 mutations also cause a decrease in ergosterol and an increase in other sterols, which can contribute to cross-resistance to polyenes[66,75]. Increased expression of ERG11 due to activating mutations

in the gene encoding its zinc-finger transcriptional regulator UPC2 is another mechanism leading to reduced azole sensitivity[66,76].

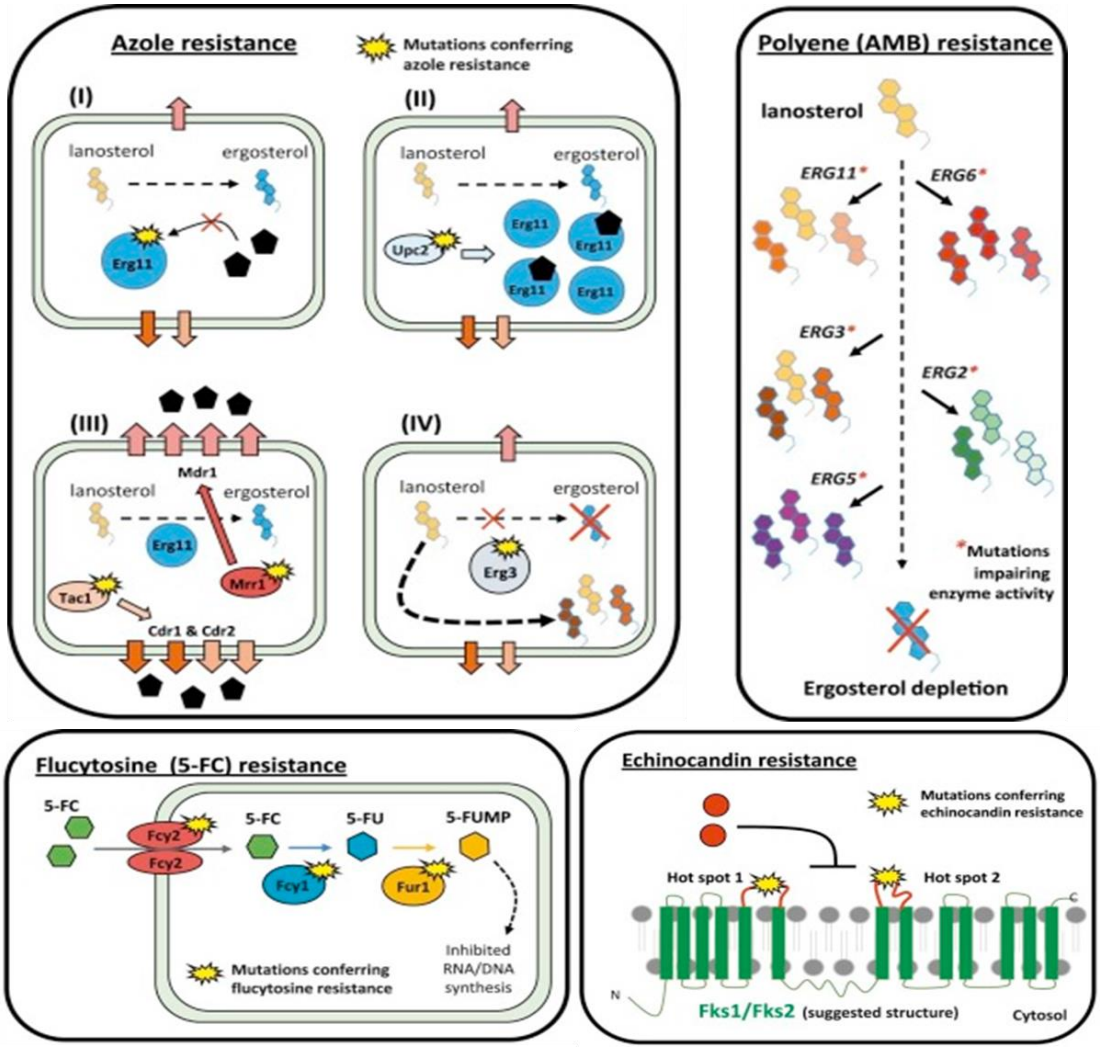

Figure 3 **- Molecular resistance mechanisms to antifungal drug classes. Azole resistance** is frequently caused by a complex interplay of processes. **(I)** Changes in the structure of the azole drug target Erg11 reduce affinity. **(II)** Increased transcription (Gain of function (GOF) mutations in UPC2) or more ERG11 gene copies (genome plasticity) upregulate the pharmacological target. **(III)** GOF mutations in MRR1 or TAC1 or extra TAC1 gene copies (genome plasticity) cause upregulation of drug efflux transporters. **(IV)** The ergosterol pathway is bypassed, resulting in the production of alternative sterols that are not reliant on Erg11. **Flucytosine resistance** can be caused through the drug's absorption (Fcy2) or metabolism (Fcy1 or Fur1). **Echinocandin resistance** has almost completely been associated with natural variations or mutations within conserved hot-spot regions of the FKS encoded protein. **Polyene resistance** occurs when the ergosterol biosynthetic pathway is disrupted, resulting in the build-up of alternative sterols at the expense of ergosterol. Adapted from Morio *et al*, 2017[145]

Overexpression of drug efflux pumps, as well as the multidrug resistance gene MDR1, which is regulated by the transcription factor MRR1, [66,77] and Candida drug resistance 1 and Candida drug resistance 2 (CDR1/CDR2) genes[66,78] are other pathways to acquire resistance. The overexpression of these pumps is linked to at least 17 distinct mutations in their transcriptional regulator TAC1[66,79,80] and the deletion of either of the CDR1/2 genes results in the loss of the resistance phenotype[66,79].

Lastly, substantial genomic alterations such as aneuploidy or loss of heterozygosity have been linked to enhanced azole resistance. Aneuploidy in chromosome 5, which contains ERG11, its transcriptional regulator UPC2, and the efflux pump regulator TAC1, changes the susceptibility of the fungal cells[66,81], as well as the loss of heterozygosity in regions encoding ERG11, TAC1, or MRR1[66,82]. Increased copy numbers of chromosomes 3 and 6 were recently added to the list of genomic rearrangements linked to fluconazole resistance in *C. albicans*[66,83].

The acquisition of resistance to Echinocandins is acquired through mutations in specific regions, hotspots, in the FKS1 gene (Figure 3)[84]. These mutations result in decreased affinity between the drug and the 1,3-β-d-glucan synthase enzyme, such as amino acid substitutions S641P and S645Y[66,85]. Resistance is also linked to stress responses that result in the paradoxical growth of the fungus at high drug concentrations and high cell wall chitin content[86,87].

The most common mechanism of acquired resistance to Polyenes is the alteration of the cell membrane sterol composition, through mutations in genes belonging to the ergosterol biosynthesis pathway (Figure 3). In *C. albicans*, there is a loss of function of the genes ERG11 (14α-desmethylase lanosterol) and ERG3 (C-5 sterol desaturase) that results in the exchange of ergosterol by alternative sterols such as lanosterol, eburicol and 4,14-dimethyl- membrane zymosterol[63]. Other mutations that can occur are in the ERG2[88], ERG5[89] and ERG6[90] genes, which lead to cross-resistance with the azole class[66].

In Flucytosine (antimetabolites), the decrease in susceptibility is associated with point mutations in the FCY1 and FUR1 genes that inactivate the enzymes involved in the pyrimidine pathway, mutations in the FCY2 gene that interferes with drug uptake and the deletion of the FPS1 and FPS2 genes that reduce intracellular drug concentrations (Figure 3)[66,91,92].

3.3. Evolutionary pathways for the emergence of resistance

Inherent resistance, also known as primary resistance, refers to isolates with intrinsic resistance, prior to antifungal exposure[93] (Figure 4). Target incompatibility, stress response signalling, and efflux pump overexpression are just a few of the processes that contribute to this type of resistance[93]. Furthermore, the development of fungal biofilms also reduces overall fungal drug sensitivity due to the glucan matrix that can function as a physical barrier, preventing antimicrobial chemicals from being bioavailable and reaching its target[93]. On the other hand, the prolonged exposure to antifungals leads to the development of secondary resistance (Figure 4). Processes that drive genome evolution like single-point mutations, gene duplications, deletions, inversions and insertions, chromosomal rearrangements, aneuploidies, heterozygosity loss, horizontal gene transfer and/or hybridization are responsible for the appearance of secondary resistance phenotypes[66]. Certain genomic re-arrangements may occur before point mutations, resulting in more effective and durable resistance[66]. Large genomic re-arrangements, such as aneuploidies, are good candidates in this regard because they cause coordinated over- or under-expression of several genes, they are well tolerated by cells, and they are relatively common under stress[66]. Alternative genomic alterations such as copy number variation (CNV), especially short segmental CNV[55], and loss of heterozygosity (LOH) in heterozygous species such as *C. albicans*, have also been hypothesized to promote rapid adaptation[66,94]. Additionally, how a drug affects the pathogen may restrict the ways in which cells can adapt to it. For example, fungistatic drugs that inhibit growth but do not kill fungal cells open a window of opportunity for mutations to appear.

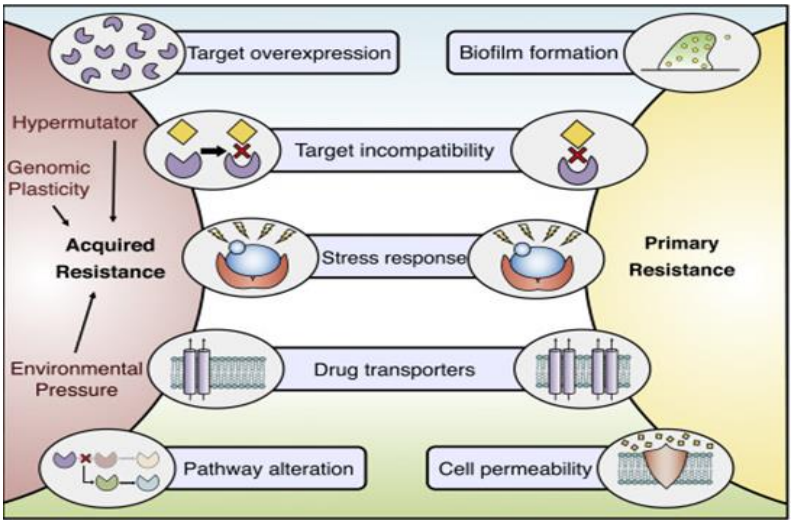

***Figure 4* - Primary resistance vs Secondary resistance.** Target incompatibility, stress response signalling, and efflux pump overexpression are some of the processes involved in primary resistance, which overlap with those involved in acquired resistance. A variety of pathways can lead to the development of acquired resistance or second resistance. Overexpression of the drug target, amino acid modifications in the drug target that prevent drug binding, signalling via stress response pathways, activation of efflux pumps, and changes in cellular pathways are all examples. Multiple factors, including but not limited to an organism's genetic plasticity, the existence of hypermutator strains, or environmental pressures can accelerate acquired resistance in fungal pathogens. Adapted from Revie *et al*, 2018[93].

Whole genome sequencing of serial clinical isolates and *in vitro* evolution studies have been used to investigate the evolutionary pathways that contribute to the emergence of resistance. While *in vivo* research on patient samples is more therapeutically relevant than *in vitro* studies, they have drawbacks[66]. An example for a *in vivo* study is the work of Ford et al[95]. In this work, they used next generation sequencing to examine 43 isolates from 11 patients with oral candidiasis[95]. They discovered novel mutations, such as single-nucleotide polymorphisms (SNPs), copy-number variations, and loss-of-heterozygosity (LOH) events[95]. SNPs in 240 genes may be connected to host adaptation, and LOH events were typically associated with acquired resistance[95]. Most aneuploidies, on the other hand, were temporary and had nothing to do with drug resistance[95]. Their findings also revealed that isolates differed in terms of adhesion, filamentation, and pathogenicity[95]. Their research shows common molecular processes between drug resistance acquisition and host adaption evolution[95].

However, the findings of *in vivo* experiments are not easily reproducible, the population size parameters are not regulated, and the mutational makeup of the final isolate is generally the only thing examined[66]. Due to these constraints, alternative *in vitro* methods are a viable tool for deciphering the evolutionary pathways that contribute to the establishment of resistance[66]. This "experimental evolution" method allows for precise measurement of important factors and adjustment of circumstances[66]. Furthermore, samples may be saved at intermediate time periods, and the experiment can be restarted at any moment with different conditions, allowing researchers to realign the evolution[66]. Additionally, the evolutionary trajectory, for example, may be followed by tracking the order in which adaptive mutations occur[66]. Several investigations with yeasts such as *C. albicans*[96] and *S. cerevisiae* [97] have found a high degree of concordance between *in vivo* and *in vitro* findings[66]. For example, Cowen and colleagues studied adaptation to inhibitory doses of the antifungal fluconazole in replicated experimental populations derived from a single drug-sensitive *Candida albicans* cell and grown for 330 generations[96]. The resistant populations showed unique overexpression patterns of four genes implicated in azole resistance: the ATP-binding cassette transporter genes CDR1 and CDR2, the gene encoding the azole target enzyme in the ergosterol biosynthesis pathway, ERG11, and the major facilitator gene MDR1[96]. Their findings suggest that chance, in the form of adaptive mutations, plays a role in the evolution of azole drug resistance in *C. albicans* populations[96]. Another work of Cowen and colleagues also revealed that changes in gene expression occurred throughout 330 generations of evolution in four replicate populations of the pathogenic fungus *C. albicans* in the presence of the antifungal drug fluconazole[98]. Their cluster analysis revealed an up-regulation of the multidrug ATP-binding cassette transporter gene CDR2, and the up-regulation of the multidrug major facilitator transporter gene MDR1[98]. These alterations in gene expression were also found in fluconazole-resistant clinical isolates, indicating that they are part of common fluconazole adaption processes[98].

In vitro evolution experiments coupled with whole genome sequencing is a useful tool that can be used to study antifungal drug resistance, and this is a research topic in great development[66].

4. Non-standard translation of CUG codon in *C. albicans*

4.1. Ambiguous translation of the CUG codon

One of the most intriguing features of *C. albicans* is the fact that it belongs to the so-called fungal CTG-clade group, where all members translate the CUG codon into serine instead of leucine[62,99,100]. However, in *C. albicans* the CUG codon is ambiguously translated as serine, 97% of the time, and leucine, 3% of the time, because the Ser-tRNA$_{CAG}$ is recognized by two aminoacyl-tRNA synthetases, seryl - and leucyl-tRNA synthetases[101]. Therefore, *C. albicans* is an organism known to have a basal level of mistranslation (3% Leu).

Mistranslation is a term used to refer to errors that occur during protein synthesis that results in the sequence of amino acids in a newly synthesized protein being different to the genetically encoded sequence[102]. Recent data suggests that cells not only tolerate, but actively produce, specific amounts and types of mistranslation under certain conditions[102]. To this aim, dedicated biological mechanisms have recently been discovered to lower translational fidelity, indicating that mistranslation is not always a bad thing and can even be beneficial to cells in some cellular settings[102].

In the case of *C. albicans*, under normal standard growth conditions (30ºC), the levels of leucine incorporated into CUG sites is 2.96%[103]. These levels, however, fluctuate depending on the environmental conditions. For example, it increases to 3.9% at 37ºC, 4.95% at pH 4, and 4.03% in the presence of hydrogen peroxide (H2O2)[103]. Gomes and colleagues estimated that the 6,438 *C. albicans* genes may generate $6x10^6$ and $40x10^6$ novel proteins for CUG mistranslation percentages of 2.96% and 28.1%, respectively[103]. Considering that it is estimated that 13,074 CUG codons are distributed in 66% of *C. albicans* genes, it is expected that these variable values of translational ambiguity impact the biology of this pathogen[100,103].

4.2. Phenotypic and genomic impact of CUG ambiguity

Rocha and colleagues examined the impact of CUG codon ambiguity on the proteome of *C. albicans* by aligning 680 sequenced proteins with CUG-encoded residues with orthologs of six other fungal species, demonstrating that 90% of CUG codons are

localized in non-conserved positions[100,104]. These CUG-encoded residues are uniformly distributed in several functional categories, but the remaining 10% located in conserved positions are in proteins related to signal transduction, biofilm formation, mating, morphogenesis, and adhesion indicating that CUG decoding ambiguity plays an important role in pathogen–host interactions[100,104].

Previous work by Bezerra et al. led to the construction of a series of strains with different levels of Leu misincorporation (3-98%) by incorporating one or two copies of a mutant Leu-tDNA$_{CAG}$ gene into the genome of *C. albicans* SN148 strain and deleting the endogenous Ser-tRNA$_{CAG}$[105]. Recombinant *C. albicans* cells incorporating 28% of Leu at CUG sites exhibited a wide range of morphologies, including ovoid opaque cells, pseudo-hyphal, and hyphal morphologies[100]. The phenotypes seen in highly ambiguous cells resembled those caused by environmental cues including high temperature, low pH, and serum[100]. High-level CUG codon ambiguity increased extracellular hydrolase activity (aspartic proteinases and phospholipases), induced mating by upregulating the key regulator of white-opaque switching, and up-regulated expression of genes involved in cell adhesion and hyphal development[100,106]. These hypermistranslating cells also exhibited better fibronectin and gelatin adhesion[101]. This could be explained by the fact that most CUG-encoded residues are found on the surface of proteins, and CUG codons are particularly abundant in membrane and cell wall genes[104]. Therefore, CUG mistranslation may enhance cell surface hydrophobicity by increasing the substitution of polar Ser for non-polar Leu[101]. Also, the presence of Leu at two CUG-encoded residues in the adhesin Als3, in positions 379 and 433, changed its activity, increasing cell flocculation and substrate adherence[101]. Furthermore, compared to wild-type cells, high levels of Leu-CUG translation caused heterogeneity in the cell wall proteome, which changed the cell surface exposure of 1,3-glucan and decreased macrophage phagocytosis[101]. These findings suggest that codon ambiguity in *C. albicans* might be a method for generating cell surface diversity and perhaps contributing to antigenic variation to escape immune identification, which is especially important in the fungal-host relationship[100].

Increased levels of CUG ambiguity also have a dramatic influence on the genome of this pathogen[100,105]. Indeed, higher levels of CUG-Leu translation caused loss of heterozygosity (LOH) in a 300-kb area of chromosome V in strains incorporating 80% and 99% of Leu, as well as the whole chromosome R in the strain with 80% of Leu at CUG sites

[100,105]. The LOH events that were identified mostly affected genes with unclear functions, but they also affected genes involved in biological process control, organelle structure, and stress response [100,105]. The number of SNPs was also higher in hypermistranslating cells, affecting genes related with filamentous development, cell adhesion, metabolic activities, and transcription control [100,105]. Consequently, several phenotypes observed in these recombinant cells may be linked to chromosomal alterations [100,105]. Overall, codon ambiguity can lead to genomic and phenotypic diversity with significant adaptability potential[100].

One of the phenotypes observed in hypermistranslating strains was their tolerance to antifungals, particularly fluconazole. In a previous study by Weil et al., researchers compared the resistance trajectories of high-level Leu-CUG translating and wild-type strains in the absence and presence of fluconazole to see how CUG non-standard translation contributes to the acquisition of antifungal resistance[107]. Greater levels of mistranslation resulted in increased tolerance and hasten the establishment of fluconazole resistance[107]. Genome sequencing, array-based comparative genome analysis, and transcriptional profiling indicated that the spectrum of mutational and gene dysregulation changes in strains that contain Leu at a high degree were distinctly different and wider over evolution with fluconazole[107]. While the ergosterol production pathway, which encodes the fluconazole's molecular target, was increased in both wild-type and high-mistranslating resistant strains, the drug efflux route was impacted differently[107]. The wild-type strain acquired a previously described A736V gain-of-function mutation in TAC1[108,109], the transcriptional activator of the CDR1 and CDR2 genes, while the high-level Leu-CUG translating strain acquired a previously described A736V gain-of-function mutation in MRR1[77,110], a positive transcriptional regulator of the multidrug efflux pump gene MDR1. Overall, both strains triggered the conventional mechanisms of azole resistance, although through distinct drug efflux routes, despite the stochastic nature of mutations[100].

Nevertheless, dissection of the genes necessary for evolution of resistance requires additional studies. Particularly, parallel evolution of multiple isolates of both hypermistranslating and wild-type strains is necessary to clarify the adaptive and mechanistic relevance of the multiple mutations identified in the study by Weil et al. This constitutes the starting point of the work developed during this master´s thesis.

5. Hypothesis and objectives

In this work we propose the hypothesis that mistranslation in *C. albicans* accelerates the acquisition of resistance to antifungal drugs through genomic alterations. To test this hypothesis, we took advantage of previously constructed strains with varying levels of Leu-CUG incorporation: T0 (wild-type strain) and T1 and T2 (hypermistranslating strains incorporating 20% and 67% of Leu at CUGs, respectively). Using these strains, we addressed the following specific objectives:

1. *In vitro* evolution of hypermistranslating and wild-type strains in the absence and presence of antifungal drugs;

2. Determination of the minimum inhibitory concentration (MIC) during experimental evolution to detect isolates resistant to the antifungal agents;

3. Whole genome sequencing (WGS) of susceptible and resistant isolates using the Illumina platform;

4. Bioinformatic analysis of WGS and variant calling: SNPs (Single nucleotide polymorphisms), INDELs (Small insertion and deletion) and copy number variation (CNVs).

II - Materials and methods

1. Strains and growth conditions

In this study, strains of *C. albicans* with different levels of leucine incorporation at CUG sites were used. Strains T0, T1 and T2 were previously built by Bezerra *et al* (Table - 1) and were grown in commercially available Yeast Peptone Dextrose (YPD) medium (Formedium), containing 2% glucose, 1% yeast extract and 1% peptone. Strains were grown at 30ºC, unless otherwise specified.

Table 1 - *Candida albicans* strains used in this study

Strains	**Genotype**	**Description**	**% Mistranslation (Leu misincorporation)**
T0	arg4Δ/arg4Δ leu2Δ/leu2Δ his1Δ/his1Δ ura3Δ::imm434/ura3Δ::imm434 iro1Δ::imm434/iro1Δ::imm434 RPS1/rps1Δ::pUA709 (URA3)	Naturally ambiguous strain; wt strain carrying a mistranslation reporter system	1.45
T1	arg4Δ/arg4Δ leu2Δ/leu2Δ his1Δ/his1Δ ura3Δ::imm434/ura3Δ::imm434 iro1Δ::imm434/iro1Δ::imm434 RPS1/rps1Δ::pUA702 (URA3, Sc tLCAG)	Hypermistranslating strain carrying a mistranslation reporter system	20.61
T2	arg4Δ/arg4Δ leu2Δ/leu2Δ his1Δ/his1Δ ura3Δ::imm434/ura3Δ::imm434 iro1Δ::imm434/iro1Δ::imm434 RPS1/rps1Δ::pUA706 (URA3, Sc tLCAG, Sc tLCAG)	Hypermistranslating strain carrying a mistranslation reporter system	67.29

2. Experimental evolution *in vitro*

18 isolates of each strain (T0, T1 and T2) were subjected to *in vitro* experimental evolution under two different conditions - evolution with and without antifungal drug (Figure - 5). For the evolution with antifungals, two drugs from the azole class (Fluconazole and Itraconazole), and one drug from the polyene class (Amphotericin B) were used. In total, 4 different evolutions were performed in 96-well plates with YPD medium at 37ºC. Every two days an aliquot of the stationary phase culture was transferred to fresh media. During evolution with drug, at each passage the drug concentration of the liquid growth media was adjusted to twice the last measured minimal inhibitory concentration (MIC). The drug passages were repeated until cells reached approximately 200 generations. All isolates were stored at -80°C in 40% glycerol.

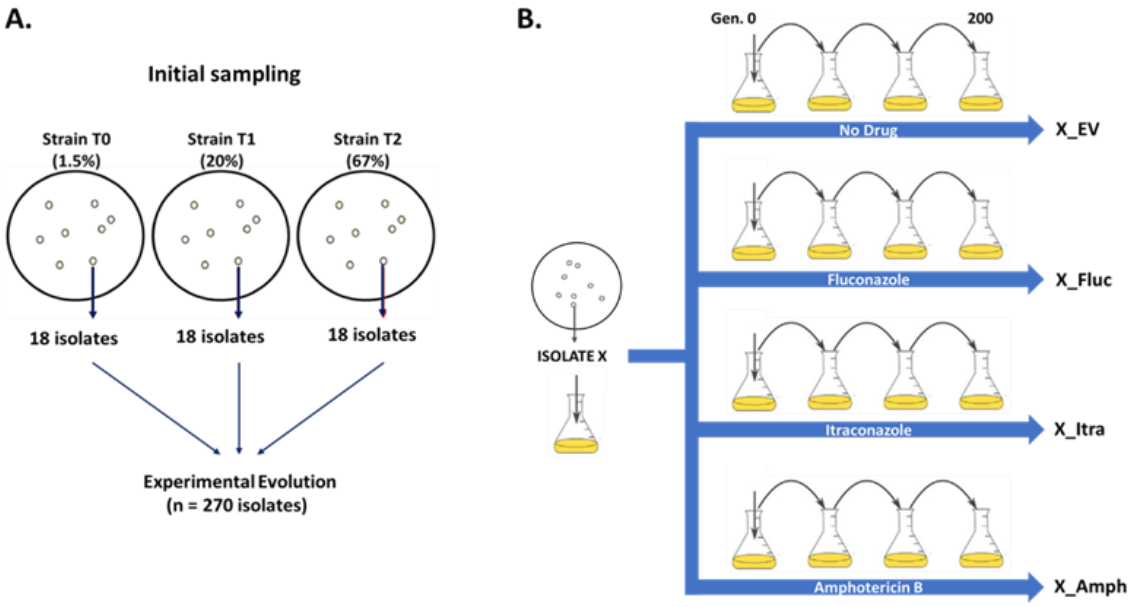

***Figure 5* - Overview of the experimental evolution. A.** Control strain T0 and hypermistranslating strains T1 and T2 were used for the initial sampling. 18 isolates from each strain were selected to *an in vitro* experimental evolution. **B.** Each isolate was evolved until reaching 200 generations, and under 4 different conditions: without drug, with Itraconazole, Fluconazole and Amphotericin B. In each passage, drug concentration was adjusted to double the concentration of the last minimal inhibitory concentration (MIC) measured.

3. Determination of minimal inhibitory concentration (MIC)

The MIC was determined using the European Committee on Antimicrobial Susceptibility Testing (EUCAST protocol) which is a broth microdilution assay. This test is performed in 96-well plates and is based on the preparation of 100 µL of antifungal agent solutions per well and the addition of 100 µL of inoculum. The inoculum was made from a colony grown in YPD medium in a Petri dish, subcultured in RPMI-1640 2% G liquid medium, constituted by RPMI-1640, 3-(N-morpholino) propanesulphonic acid (MOPs) and Glucose. The cell culture was incubated overnight at 30ºC with 180 rpm. The BioRad's TC10 Automated cell counter was used to count calls and prepare an inoculum with $5x10^5$ cells/ml. 96-well plates with the antifungal agent solution were prepared with RPMI-1640 2% G and with different concentrations of Fluconazole (0.125-256 µg/ml), Amphotericin B (0.0312-16 µg/ml) and Itraconazole (0.0156-8 µg/ml). In these plates, an inoculum of *Candida parapsilopsis*, susceptible to fluconazole, was used as a control. Plates were incubated for 24-48h at 30°C without agitation. The absorbance was read at 595 nm using the iMARK Microplate Reader, and if at 24 hours there was no conclusive reading, the next reading was taken after 48 hours of incubation. The MIC value was defined by the concentration that was needed to prevent 50% growth when compared to the drug-free control.

4. Whole-genome sequencing

4.1. DNA extraction

DNA was extracted from drug resistant clones and their respective susceptible controls at initial generation of strains T0, T1 and T2. The protocol used was from Lucigen's MasterPure Yeast DNA Purification Kit with modifications. A 20 ml culture, in mid-log phase (OD: 1-1.5), was centrifuged at 4000g, 4°C, for 10 minutes and the pellet washed with 4 ml of 1x TE (10 mM Tris-HCl, pH 8.0; 1mM EDTA, pH 8.0). For lysis, 300 µL of Yeast Cell Lysis Solution (supplied by the kit) and 10 µL RNAse A (100 mg/ml, Qiagen) were used and then incubated for 2.5-3 hours at 50ºC. The suspension was placed on ice for 5 minutes and 150 µL of MPC Protein Precipitation Reagent (provided by the Kit) was added and vortexed for 10 seconds. The suspension was then centrifuged for 10 minutes at 13,000 rpm at 4°C. The supernatant was removed to a new tube and the process repeated, reducing

the centrifugation time to 2-3 minutes. 500 µL of isopropanol was added at room temperature and mixed by inversion for 30-40 times. The suspension was centrifuged for 10 minutes at 13,000 rpm at 4°C and the isopropanol was removed. The remaining pellet was washed with 500 µl ethanol 70% and centrifuged for 2 minutes at 13,000 rpm at 4°C and the ethanol removed. The above process was repeated, and the pellet was allowed to dry for 5 minutes at room temperature. The pellet was then suspended in 23 µL of TNE Buffer 1x and left overnight at 4°C. 1 µL of RNAse A (100 mg/mL) from Qiagen and RNAse I (3 U/µL) was added and incubated at 37ºC overnight. After incubation, 25 µL of Yeast Cell Lysis Solution was added and placed on ice for 5 minutes. 50 µL of MPC Protein Precipitation Reagent was added, vortexed for 10 seconds and centrifuged at 13,000 rpm, at 4°C for 10 minutes. The supernatant was removed into a new tube and the process repeated with a 2–3 minute centrifugation. 100 µl of isopropanol was added and mixed by inversion for 30-40 times and centrifuged at 13,000 rpm at 4°C for 10 minutes. Isopropanol was removed and the pellet washed with ethanol 70% twice by performing 2-3 minute centrifugations. Ethanol was removed and allowed to dry for 5 minutes, and the DNA was suspended with 35 µL of mQH2O and stored at 4°C overnight. Quality was measured by assessing A260/A280 and A260/230 ratios on the Denovix DS-11 Spectrophotometer and by running the DNA samples in a 1% agarose gel. Quantification of total DNA was performed using the Qubit 2.0 Fluorometer Assay.

4.2. Library preparation

DNA libraries were prepared using the Illumina DNA Prep protocol (Figure - 6). Each library is prepared with an insert size of ~600 bp. DNA is diluted in mQH2O until it has a DNA input for sequencing between 100-500 ng. The first step of the protocol is the Tagment Genomic DNA, which fragments and tags the DNA with adapter sequences. To do so, samples were incubated in the BioRad thermal cycler for 15 minutes at 55ºC, with a mix of BLT (Bead-Linked Transposomes) and TB1 (Tagmentation Buffer 1). After that, TSB (Tagmentation Stop Buffer) was added to stop the tagmentation reaction and samples were incubated for another 15 minutes at 37ºC. The next step is a clean-up to wash the adapter-tagged DNA before performing PCR amplification. Samples were transferred to a 96-well plate that was placed on a magnetic stand and the supernatant was discarded. Then, samples

were washed two times with TWB (Tagment Wash Buffer), and afterwards, beads were resuspended in TWB. The following step is the amplification of the tagmented DNA. After discarding the supernatant, a PCR master mix (EPM -Enhanced PCR Mix) and water were added to the samples along with the index adapters. The PCR program ran on the Biorad Thermal Cycler using the program described on the protocol. After the PCR cycle, the amplified libraries were purified. The supernatant was removed and transferred to a new plate, using the magnetic stand. Diluted SPB (Sample Purification Beads) was added to the samples and the supernatant was transferred to a new plate, to which was again added SPB. The supernatant was removed, and samples were washed twice with EtOH 80%, which was carefully removed. Then, beads were resuspended in RSB (Resuspension Buffer), and the supernatant was transferred to a new plate. The last step is checking the quantity and quality of the DNA libraries. Libraries were quantified using the Qubit fluorometric assay and samples were ran on the Agilent 2100 Bioanalyser to obtain the library size profile.

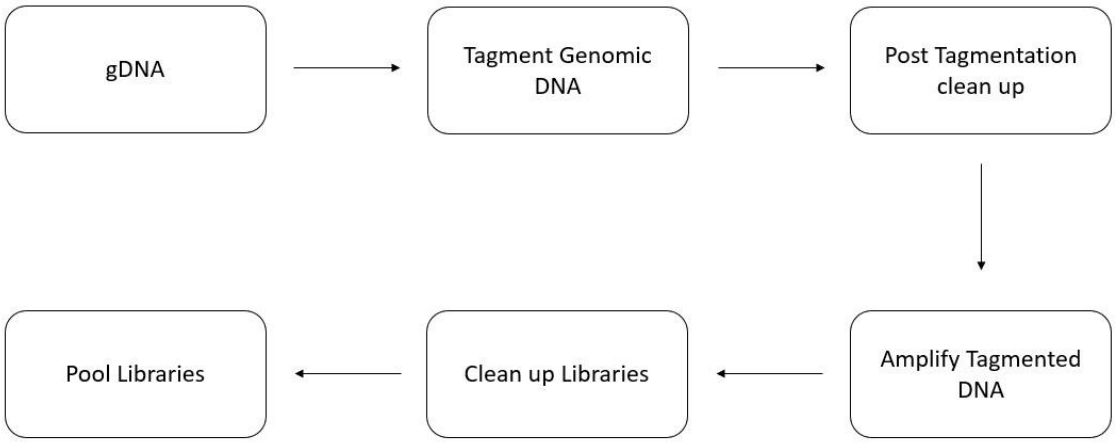

***Figure 6* - Illumina DNA Prep Workflow**. The procedure for Illumina DNA Prep is depicted in the diagram below. Between are designated safe stopping places.

4.3. Sequencing

DNA libraries were sequenced using the NextSeq 550 System by Illumina following the manufacturer's guide protocol. Before loading, samples were diluted to 1μM and denatured with 0.1N NaOH. Denatured libraries were further diluted to 1.8pM with HT1 (Hybridization Buffer). For quality control, PhiX was used. Libraries were then loaded in the reagent cartridge and after checking the run and system status, the run was started.

5. Bioinformatic analysis

The bioinformatic pipeline adopted for the analysis of DNA sequencing raw data was theWGS-Seq pipeline that was developed and validated by the bioinformatics facility of iBiMED (Figure - 7). This pipeline allowed the analysis of variants such as SNPs, Indels and CNVs. LOH analysis was not performed in this work.

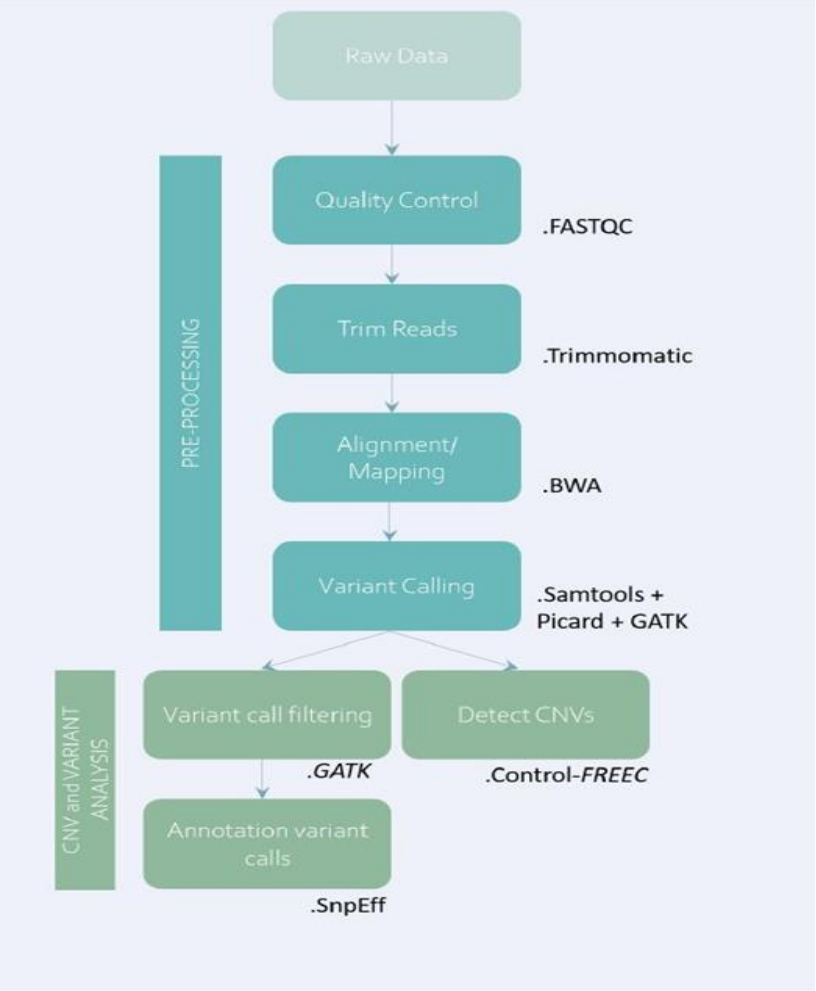

***Figure 7* - Workflow used for the WGS sequencing analysis.** The picture below demonstrates the workflow used in analysis with the programs used in each step.

5.1. Single Nucleotide Polymorphisms (SNPs) and Small Insertions/Deletions (INDELs)

Initial quality check of the raw reads was performed with FASTQC v0.11.7[111] and parameters were adjusted to improve the quality of the reads with Trimmomatic v0.36[112]. Reads were mapped against the SC5314 reference genome (Candida Genome Database Assembly 22, haplotype A) using BWA v0.7.17[113] with default options. Coverage of the mapped reads were checked with an in-house script (calculate_coverage.py). Bam files containing all mapped reads were sorted and PCR duplicates filtered using Samtools v1.12[114] and Picard v2.21.3[115]. Base quality score recalibration (BQSR) was performed using GATK v4.1.3.0[116], which detects and corrects systematic errors in the original base accuracy scores. Variant calling was also performed using GATK detecting SNPs and INDELS. Low-quality

variant calls were filtered using GATK with parameters "QD < 2.0 || FS > 60.0 || MQ < 40.0 || MQRankSum < -12.5 || ReadPosRankSum < -8.0" for SNPs variants and "QD < 2.0 || FS > 200.0 || ReadPosRankSum < -20.0" for INDELS. All variants were further filtered, according to Selmecki et al, 2015[117], for alternative allele support and allelic frequency (more than two reads supporting an alternative allele for coverage 10× to 20×, and more than four reads supporting an alternative allele for coverage more than 20×). Variants were classified using SnpEff v4.3[118]. Finally, an in-house python script (progression_time_points.py) was ran to group variants from the same sample between time-points.

5.2. Copy Number Variations (CNV)

For the CNV analysis the Control-FREEC v11.6 program[119] was used to detect CNVs per sample. A 100bp window was set to search for the CNVs in each chromosome and these were considered significant for p-value < 0.05 for Wilcoxon Rank Sum test and Kolmogorov–Smirnov test.

5.3. Functional enrichment and analysis

A list of genes with mutations was obtained for each sample and the CGD Gene Ontology (GO) tool in Candida Genome Database was used for functional enrichment with the GO Term finder tool and functional analysis with the GO SlimMapper tool. GO term enrichment was carried out according to Skrzypek and colleagues[120], applied over GO biological process, and then selecting GO terms enriched with a p-value lower than 0.01.

III – RESULTS

1. *In vitro* experimental evolution and antifungal susceptibility assessment

To clarify the role of mistranslation in the acquisition of antifungal resistance, an *in vitro*, evolution of 18 isolates from each strain (control T0, and hypermistranslating strains T1 and T2) under 4 different conditions: without drug, with Itraconazole, Fluconazole and Amphotericin B was performed and is described in the materials and methods section (Figure 5). The determination of the minimum inhibitory concentration (MIC) was performed using the European Committee on Antimicrobial Susceptibility Testing (EUCAST protocol), in order to unveil the susceptibility of the isolates at the beginning and after 200 generations of evolution with or without drug.

For each drug there is a specific test range, with Amphotericin B having a range from 0.0312 to 16 mg/L, Itraconazole from 0.0156 to 8 mg/L, and Fluconazole from 0.125 to 64 mg/L. The MIC of isolates treated with Amphotericin B is determined when there is more than 90% growth inhibition. If this inhibition is found below or equal to 1 mg/L, the isolate is considered susceptible and if it is greater than 1 mg/L it is considered resistant. In the case of Fluconazole and Itraconazole, the MIC is determined when there is 50% growth inhibition, so that in Fluconazole if the MIC is equal to or below 2 mg/L the isolate is considered susceptible and if it is above 4 mg/ L is considered resistant; in Itraconazole if the MIC is equal to or below 0.06 mg/L the isolate is susceptible and if it is above 0.06 mg/L the isolate is resistant[121].

Table 2 shows the number of isolates of each strain that were assessed as susceptible (S) or resistant (R) in the different experimental conditions. In the experimental evolutions with Itraconazole and Amphotericin B, there was loss of isolates due to contaminations during the evolution process, leaving only half of the isolates for the determination of MIC. The data presented in Table 2 also demonstrates that isolates from the three strains at the beginning of evolution (non-evolved) and after the drug-free evolution process (evol. no drug) were all susceptible. In evolution with drugs, the appearance of isolates that acquire resistance to the drugs used was observed and these are highlighted in red in Table 2. The exact value of MIC for each isolate of each strain at the beginning and end of the evolution is presented in annex A.

Table 2 - Number of isolates that acquired resistance during evolution

Antifungal Therapy		T0 (1.5%)		T1 (20%)		T2 (67%)	
		S	**R**	**S**	**R**	**S**	**R**
Fluconazole	**Non-Evolved**	18	0	18	0	18	0
	Evol. No Drug	18	0	17*	0	17*	0
	Evol. Fluconazole	13	5	6*	7	8	10
Itraconazole	**Non-Evolved**	9	0	9	0	9	0
	Evol. No Drug	9	0	9	0	9	0
	Evol. Itraconazole	4	5	2	7	2	7
Amphotericin B	**Non-Evolved**	9	0	9	0	9	0
	Evol. No Drug	9	0	9	0	9	0
	Evol. Amphotericin B	5	4	8	1	6	3

* Due to cell-cell aggregation and the presence of hypha and pseudohypha phenotypes it was not possible to determine the exact value of MIC of the missing isolates.

In evolutions with Fluconazole and Itraconazole, results show that increasing the mistranslation increases the frequency of isolates acquiring resistance. T0 strain, which has 1.5% mistranslation, had the lowest number of isolates that acquired resistance (5 in both fluconazole and itraconazole) and the T2 strain with the highest percentage of mistranslation (67%) had the highest number of isolates that acquired resistance (10 isolates in fluconazole and 7 in itraconazole). However, in the evolution with Amphotericin B, the strain with the lowest mistranslation (T0) had the highest number of resistant isolates (4) compared to the hypermistranslating strains T1 and T2 with 1 and 3 resistant isolates, respectively. These results indicate that there is a relationship between mistranslation and the frequency in the acquisition of antifungal resistance. Also, increased levels of mistranslation appear to speed up the emergence of azole resistance but not polyene resistance. For genomic analysis only isolates with precise MIC were sequenced.

2. Genomic alterations induced by mistranslation and antifungal therapy

Resistant isolates, and their respective non-evolved and drug-free evolved isolates, were sequenced using Illumina sequencing (40 - 190 X coverage), described in the materials and methods section 4. Number of reads, percentage of mapped reads and genome coverage from each isolate that was sequenced is shown in annex B. The sequencing data were subjected to a bioinformatics analysis, described in the Materials and Methods section 5, which analyzed the genomic alterations induced by mistranslation and antifungal therapy in the context of Single Nucleotide Polymorphisms (SNPs), Small Insertions/deletions (INDELs), and copy number variation (CNV).

The approach used to analyse the data was to find the genomic variations common among all resistant isolates from each strain and at each of the four conditions of experimental evolution, making it a very restrictive approach. This approach aimed to compare the impact of mistranslation and the effects of stress produced by antifungal therapy between the wild-type strain (T0) and the hypermistranslating strains (T1, T2), through the various mutations that occurred in genes that were common among all isolates.

2.1. Single Nucleotide Polymorphisms (SNPs) and Small Insertions/Deletions (INDELs)

The average total number of SNPs found in isolates of the three strains before the experimental evolution is close to 69.000 (Figure - 8A.). These values are consistent with the estimated >48.000 SNPs in strain SC5413[122]. In the case of Indels, the average total number was approximately 12.000, similar in all three strains (Figure 8B.). In both cases, variations were distributed in the same way per chromosome and no difference between control and hypermistranslating strains was detected.

SNPs and INDELs were then analysed using the same approach (Figure - 8C.), in which for each evolved resistant isolate, the mutations that were present in the corresponding non-evolved and evolved isolate without drug (background mutations – black variant in Fig. 8C) were removed, so that the only mutations left are linked to antifungal resistance (red variant in Fig. 8C). To find out the changes caused by mistranslation in drug-free evolution (yellow variant in Fig. 8C), the background variant from the non-evolved isolates were removed. Results from these analyses are described in the following sections 2.1.1 and 2.2.2.

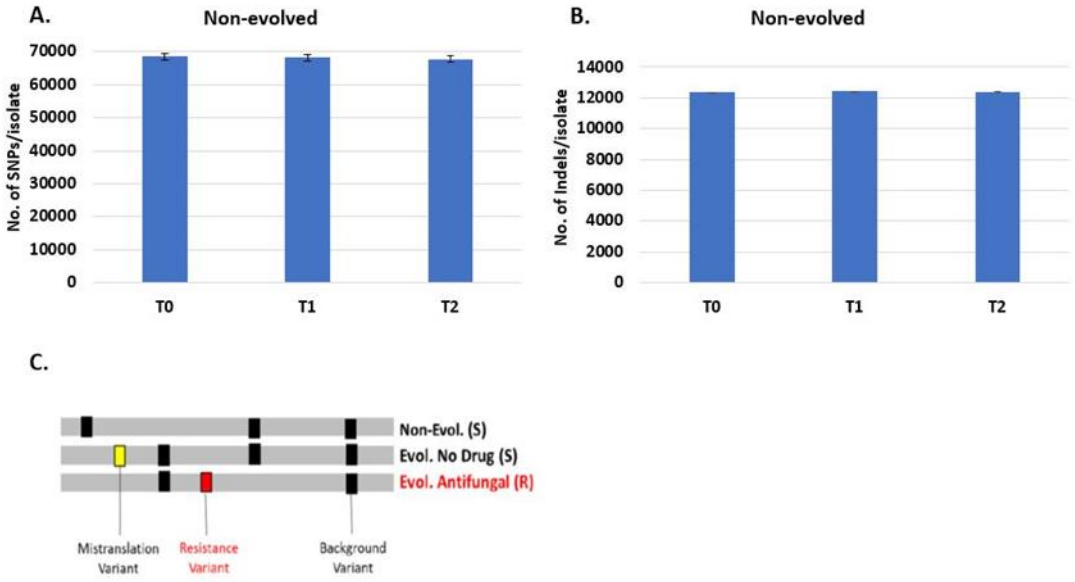

***Figure 8* - Average number of SNPs and INDELs per isolate. A-B.** Average total number of SNPs and Indels before experimental evolution. No statistically significant differences were detected between control T0 and hypermistranslating strains T1 and T2. **C.** For each resistant isolate, background variants that are present in the corresponding non evolved and evolved without drug isolate were removed. The same for mistranslation variant.

2.1.1. Single Nucleotide Polymorphisms (SNPs)

The first step in the analysis of SNPs was to compare the average number of SNPs per isolate in strains T0, T1 and T2, in the four different conditions of evolution, with strain T0 being the control of the analysis. By analysing the data shown below (Figure 9), after the exclusion of background mutations, it was observed that in the drug-free evolution (Figure 9A.) there was a significant increase of SNPs in strains T1 (1711 SNPs) and T2 (1970 SNPs) compared to strain T0 (1521 SNPs). In the case of evolution with antifungal drugs, results show that with Itraconazole (Figure 9C.) there is a small non-significant increase among the three strains (T0 – 630 SNPs; T1 – 636 SNPs; T2 – 665). In the evolution with Fluconazole (Figure 9B.) there is an increase in the average number of SNPs per isolate in strains T1 (1085 SNPs) and T2 (1222 SNPs) compared to T0 (749 SNPs), although not statistically significant. In contrast, evolution with Amphotericin B (Figure 9D.) resulted in a significant decrease in the mean number of SNPs per isolate in strains T1 (402 SNPs) and T2 (340 SNPs) compared to strain T0 (632 SNPs).

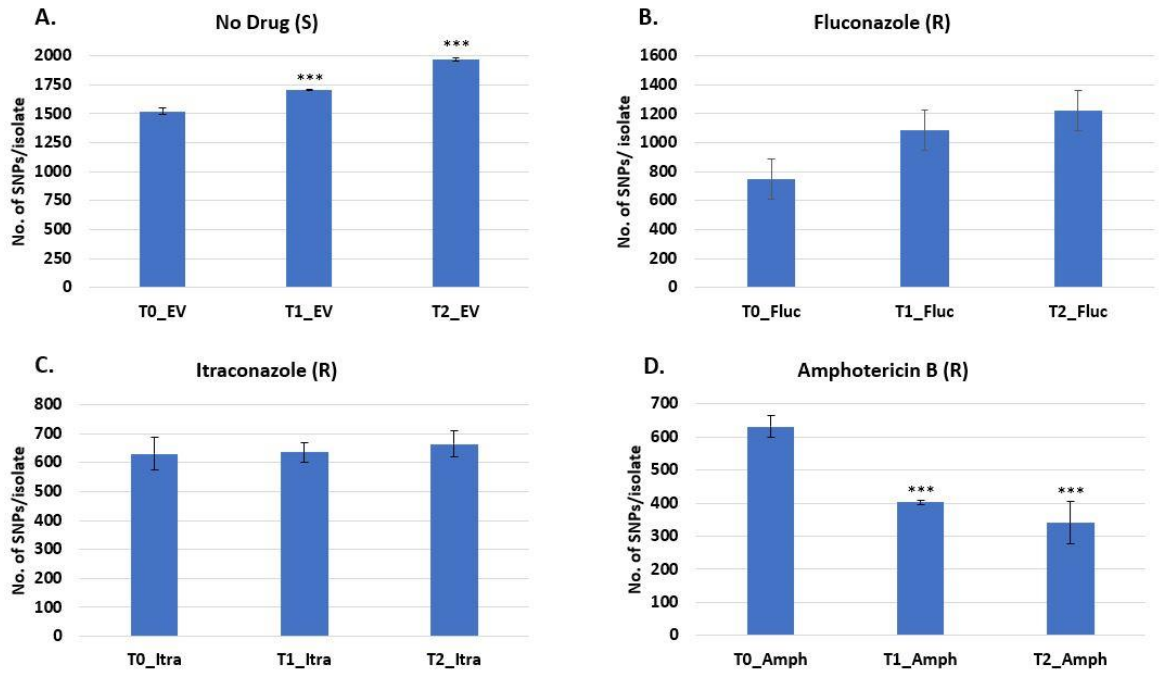

Figure 9* - Average number of SNPs per isolate excluding background mutations. A-D.** Average number of SNP's excluding background mutations present in T0, T1 and T2 evolved without drug (A.), with Fluconazole (B.), with Itraconazole (C.), with Amphotericin B (D.). Data represents the mean ± standard deviation of at least 5 independent isolates ($p<0.001$; **$p<0.01$; * $p<0.1$; t-test with 95% CI, relative to the strain T0). (S) corresponds to susceptible and (R) to resistant.

Next, we assessed the types of SNPs that occurred during the drug and drug-free evolutions in the three strains (Figure 10). A wide variety of types of SNPs were found, including intergenic variants, intragenic variant, missense variant, synonymous variant, intron variant, splice region variant and intron variant, splice region variant and synonymous variant, start lost, stop gained, stop lost, stop retained variant, splice region variant and stop retained variant, noncoding transcript exon variant, stop lost and splice region variant. These types were classified into five categories: Intergenic (intergenic region); Intronic (intragenic variant); Missense (missense variant); Synonymous (synonymous variant); and Others (intron variant; splice region variant and intron variant; splice region variant and synonymous variant; start lost; stop gained; stop lost; stop retained variant; splice region variant and stop retained variant; noncoding transcript exon variant; stop lost and splice region variant). Results showed that in the four conditions of evolution, the three strains have

a similar pattern, with the Intergenic category being the zone where the majority of SNPs appear (~65%), followed by Synonymous (~14%), Missense (~12%), Intronic (~8%) and Others (~1%).

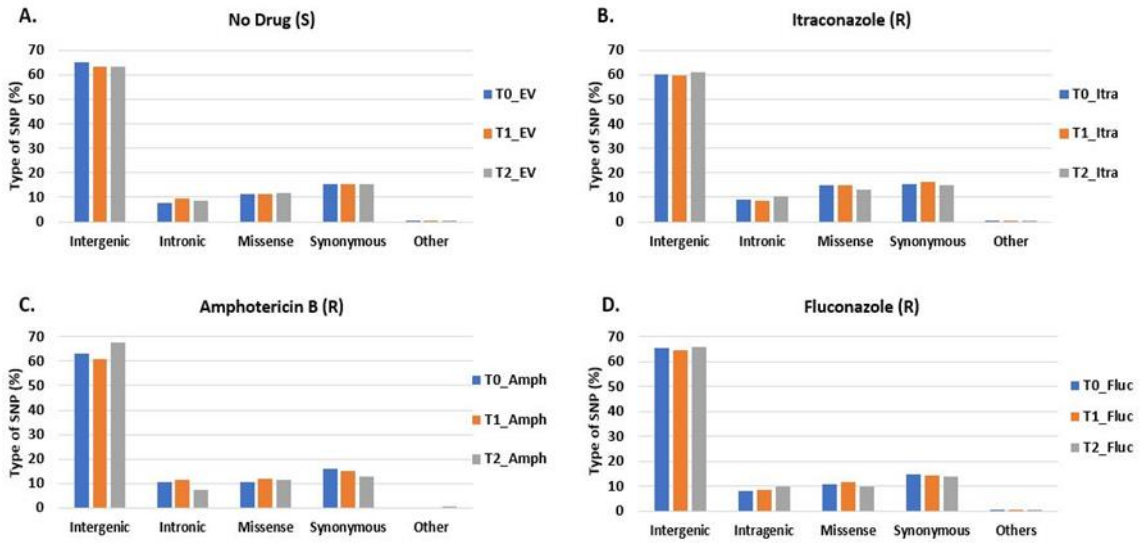

Figure 10 **- Types of SNPs**. A classification of the total SNPs without background mutations into Intergenic, Intragenic, Missense, Synonymous and Others. The distribution was similar between the 3 strains (T0; T1 and T2) under the four different conditions: evolution without drug (No Drug (S)); evolution with Itraconazole (Itraconazole (R)); evolution with Amphotericin B (Amphotericin B(R)) and evolution with Fluconazole (Fluconazole (R)). (S) corresponds to susceptible and (R) to resistant isolates.

After analysing the total number of SNPs without background mutations and the corresponding type of each SNP, we filtered the data to obtain a list of genes mutated in all isolates of each strain. This is a strict criterion that reduces the list of mutations that occur during evolution of multiple clones of both hypermistranslating and control strains but is essential to clarify the adaptive and mechanistic relevance of the multiple mutations. Only mutations that were present in the coding region (Itronic; Missense; Synonymous and Others) were addressed. Using the Gene Ontology (GO) tool provided by the Candida Genome Database platform, mutated genes of the three strains were assessed for their functional enrichment (Figure - 11) and functional categorization (Figure - 12 and 13) after evolution with and without drug.

In the drug-free evolution (Figure - 11A.) it was observed that mutated genes of T0 and T2 strains have a functional enrichment related to cell adhesion (23.50%) and biofilm formation (11.80%). The T1 strain has functional enrichment in cell adhesion (37.50%), biofilm formation (37.50%) and hyphal growth (21.40%) functions.

In the evolution with Itraconazole (Figure - 11B.) strain T0 presented functional enrichment in functions such as cell adhesion (46.20%), biofilm formation (38.50%), host interaction (23.10%) and cellular copper ion homeostasis (15.40%). In strain T1 there is a functional enrichment in cell adhesion (18.80%) and biofilm formation (25%) functions. Strain T2 presents a functional enrichment in cell adhesion (27.80%), biofilm formation (16.70%) and host interaction (11.10%) functions.

In the evolution with Fluconazole (Figure - 11C.) strain T0 presents functional enrichment in the biofilm formation function (18.20%). T1 strain presents functional enrichment in cell adhesion function (15.80%). T2 strain has functional enrichment in cell adhesion (36.40%), biofilm formation (36.40%) and hyphal growth (45.50%) functions.

In the evolution with Amphotericin B (Figure - 11D.) the enrichment occurred only in the cell adhesion (T0 – 27.30%; T1 – 18.90%) and biofilm formation (T0 – 18.90%; T1 – 18.90%) functions. The T2 strain does not show functional enrichment.

Overall, the pattern of enrichment was very similar among the different conditions of evolution and among the different strains, with mutations occurring in genes mostly related to cell adhesion, hyphal growth and biofilm formation.

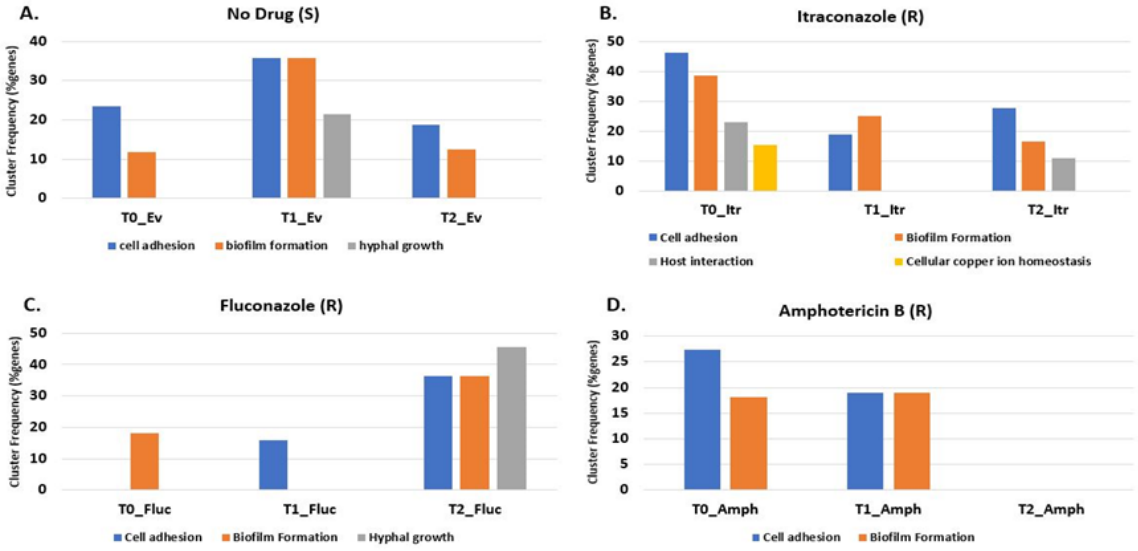

Figure 11 **- Functional enrichment of genes with intragenic mutations. A.** Functional enrichment of evolution without drug, where the functions cell adhesion and biofilm formation are present in all strains. **B.** Functional enrichment of evolution with Itraconazole, where the functions cell adhesion and biofilm formation are present in all strains. **C.** Functional enrichment of evolution with Itraconazole, where the functions cell adhesion and biofilm formation are present in all strains. **D.** Functional enrichment of evolution with Amphotericin B, where the functions cell adhesion and biofilm formation are present in all strains. GO term analysis was performed using the GO Term Analysis tool of CGD using a threshold of p-value<0.1. (S) corresponds to susceptible and (R) to resistant isolates.

We then categorized genes with mutations without performing functional enrichment. In drug-free evolution (Figure - 12A.), results showed that in strain T0, the highest frequency of mutated genes is in the category of unknown biological processes (35.30%), filamentous growth (29.40%) and response to stress (29.40%). In the case of strain T1, the categories of cell adhesion (35.70%), biological process involved in interspecies interaction between organisms (35.70%) and biofilm formation (35.70%) have the highest frequency of genes. The T2 strain has a higher frequency of mutated genes in the RNA metabolic process (25%) and biological process unknown (25%) categories.

In evolution with Amphotericin B (Figure - 12B.), the control T0 strain has the highest frequency of genes in the filamentous growth category (36.40%). In strain T1 there is a higher frequency in the categories of biological process unknown (40.50%), transport (21.60%) and filamentous growth (21.60%). In strain T2 the categories with the highest

frequency, 33.30%, are carbohydrate metabolic process, not yet annotated, lipid metabolic process, biological process unknown, and response to stress.

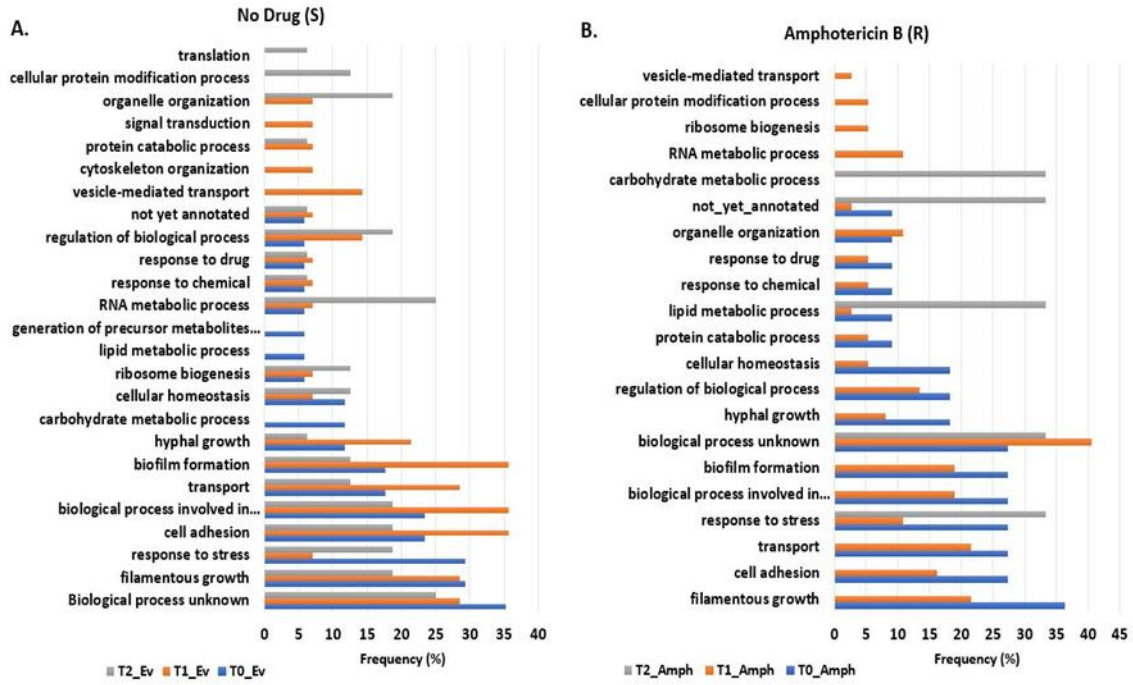

Figure 12 **- Functional analysis of genes with intragenic mutations.** Distribution of genes with SNPs in strains evolved without drug (A.) and with Amphotericin B (B.).

In the evolution with Fluconazole (Figure - 13A.), T0 strain has mutated genes belonging to the transport category (31.60%) and biological process unknown (31.60%). In strain T1, categories such as filamentous growth (45.50%), biological process unknown (36.40%) and transport (36.40%) have the highest frequency. In strain T2, the most frequent categories are filamentous growth (45.50%), biological process unknown (36.40%), cell adhesion (36.40%) and biological process involved in interspecies between interaction organisms (36.40%).

In evolution with Itraconazole (Figure - 13B.), T0 strain has mutated genes belonging to the biological process involved in interspecies interaction between organisms (46.20%), cell adhesion (46.20%), biofilm formation (38.50%) and biological process unknown (38.50%). T1 strain shows higher frequency in the transport category (37.50%). In T2 strain,

categories such as biological process involved in interspecies interaction between organisms (27.80%), cell adhesion (27.80%) and biological process unknown (27.80%) are the most frequent.

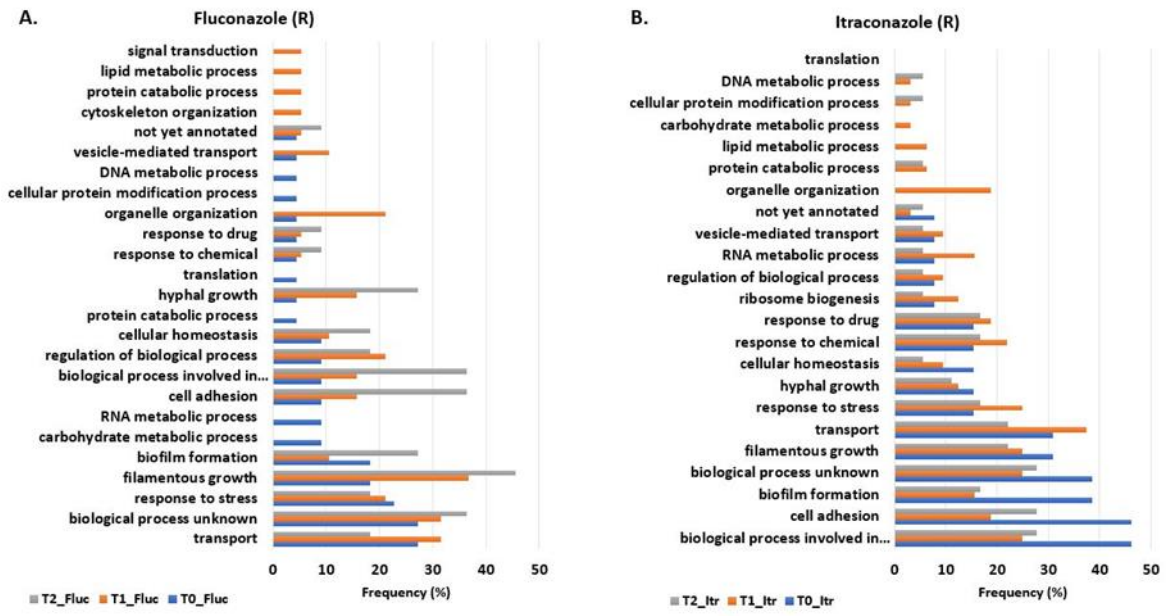

***Figure 13* - Functional analysis of genes with intragenic mutations.** Distribution of genes with SNPs in strains evolved with Fluconazole (A.) and Itraconazole (B.).

Of the different categories presented in the functional categorization, the focus was only on mutated genes in the categories of response to drug, response to chemicals, and response to stress (Table 3). These categories were chosen due to their direct relationship with the frequency of acquisition of resistance to the antifungal agents used. To dissect the role of mistranslation in the acquisition of resistance, we also focused our analysis on mutated genes that appear in hypermistranslating strains and not in the control strain in the four conditions of evolution (highlighted in red in Table 3). In the drug-free evolution, the hypermistranslating T1 strain has only the EAP1 gene mutated. In evolution with Fluconazole, hypermistranslating strains have the FMO1, LIP5, FGR6-4 and EAP1 genes with mutations in the coding region. In evolution with Itraconazole, hypermistranslating strains have FMO1, RPF2, GZF3, RSP5, PGA14, C4_05790W_A, LIP5, PHO112, FGR6-10, SYS3, FET31, and FGR6-3 genes with mutations. In evolution with Amphotericin B,

the focus is on the wild type strain as it presented a greater number of resistant isolates, so the wild type presented the ALS9, FGR28 and LIP5 genes that differ from the hypermistranslating strains. Functions of these genes and how they may contribute to acquisition of resistance will be discussed in section IV.

Table 3 - Genes with mutations belonging to categories such as response to drug, response to chemical and response to stress

Evolution	Strain	Genes
Without Drug	**T0**	ALS9; FGR28; HAL21; FGR6-10; FGR51
	T1	EAP1; FGR6-10
	T2	ALS9; FGR28; FGR6-10
Fluconazole	**T0**	ALS9; FGR28; FGR6-10; CR_03590C_A; FGR51
	T1	FMO1; FGR28; FGR6-4; LIP5; FGR6-10
	T2	EAP1; FGR28; FGR6-10
Itraconazole	**T0**	EAP1; ALS9; FGR51
	T1	FMO1; RPF2; GZF3; RSP5; EAP1; ALS9; PGA14; C4_05790W_A; LIP5; PHO112; FGR6-10; SYS3
	T2	FMO1; FET31; ALS9; FGR6-3; FGR6-10
Amphotericin B	**T0**	ALS9; FGR28; LIP5
	T1	
	T2	HAL21

2.1.2. Small Insertions/Deletions (INDELs)

The average number of Indels per isolate in strains T0, T1, T2, under the different conditions of evolution, was analysed using strain T0 as control. After excluding the background mutations, results showed that in the drug-free evolution (Figure - 14A.) the T0 strain (355 INDELs) presents a higher average number of INDELs per isolate compared to the T1 (270 INDELs) and T2 (292 INDELs) strains, although not statistically significant.

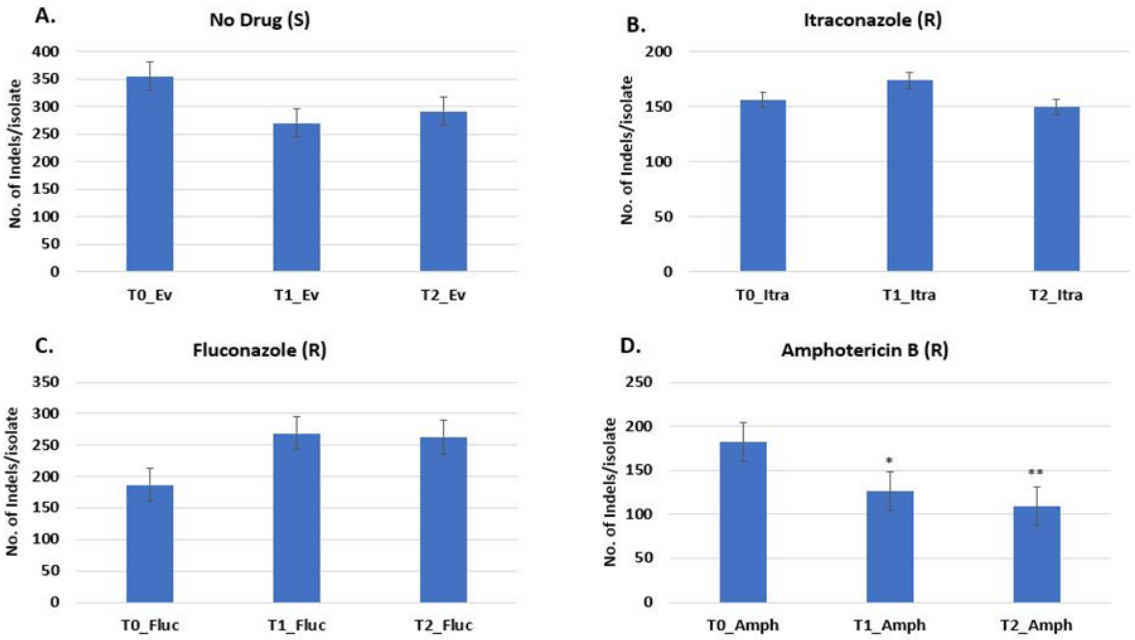

Figure 14 **- Average number of INDELs per strain. A-D.** Average number of INDELs excluding background mutations present in T0, T1 and T2 evolved without drug (A.), with Itraconazole (B.), with Fluconazole (C.), with Amphotericin B (D.). Data represents the mean ± standard deviation of at least 5 independent isolates (*** p<0.001; **p<0.01; * p<0.1; t-test with 95% CI, relative to the strain T0). (S) corresponds to susceptible and (R) to resistant.

In the evolution with Itraconazole (Figure 14B.), strain T1 had the highest average number of INDELs per isolate (174 INDELs) compared to T0 (156 INDELs), but T2 had the lowest number compared to the others (150 INDELs). In evolution with Fluconazole (Figure 14C.), strains T1 (269 INDELs) and T2 (263 INDELs) have a higher average number of INDELs per isolate compared to T0 (187 INDELs). With both azoles, results were not statistically significant.

In the evolution with Amphotericin B (Figure 14D.), there was a significant decrease in hypermistranslating strains T1 (127 INDELs) and T2 (109 INDELs) compared to control T0 (182 INDELs).

The types of INDELs present in the three strains under the four evolution conditions were analysed (Figure - 15). The following types of INDELs were found: frameshift variant, frameshift variant and start lost, frameshift variant and stop gained, intragenic variant, intergenic region, intron variant, conservative frame deletion, conservative inframe insertion, stop gained and conservative inframe insertion, stop gained and disruptive inframe

insertion, disruptive inframe deletion, disruptive inframe insertion, frameshift variant and stop lost, splice region variant and intron variant, noncoding transcript exon variant, frameshift variant and stop lost and splice region variant. These types of INDELs were organized into four distinct groups: intergenic (Intergenic region), frameshift (frameshift variant and start lost, frameshift variant and stop gained, frameshift variant and stop lost, frameshift variant and stop lost and splice region variant), intragenic (intragenic variant, intron variant, noncoding transcript exon variant) and inframe insertion/deletion (conservative inframe deletion, conservative inframe insertion, stop gained and conservative inframe insertion, stop gained and disruptive inframe insertion, disruptive inframe deletion; disruptive inframe insertion). Results show that under the four conditions, intergenic are the most abundant in the three strains, with approximately 65% in the drug-free and Itraconazole evolutions (Figure - 15A.-B.) and approximately 70% in the Fluconazole and Amphotericin B evolutions (Figure - 15C-D.). The other types are similarly distributed among the four conditions and the three strains, with frameshift with approximately 15%, intragenic with approximately 10% and inframe insertion/deletion accounting for approximately 9%.

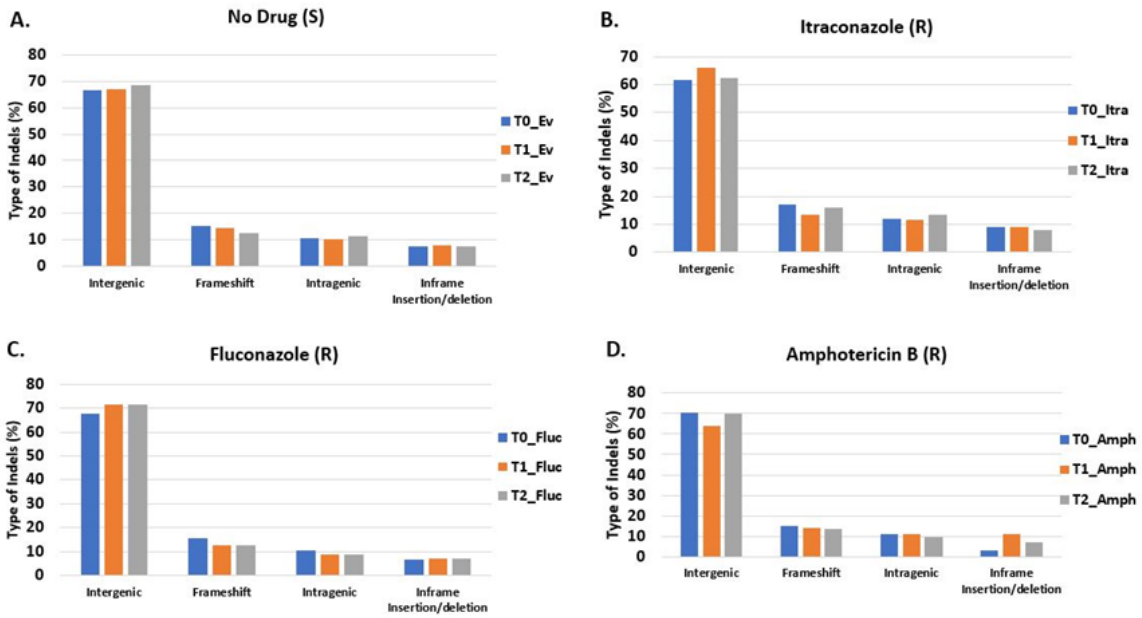

***Figure 15* - Types of INDELs.** A Classification of the total INDELs without background mutations into Intergenic, Intragenic, Frameshift and Inframe insertion/deletion. The distribution was similar between the 3 strains (T0; T1 and T2) under the four different conditions: evolution without drug (No Drug (S)); evolution with Itraconazole (Itraconazole (R)); evolution with Amphotericin B (Amphotericin B(R)) and evolution with Fluconazole (Fluconazole (R)).

Genes with INDELs were filtered to obtain a list of genes that were commonly mutated in all isolates of each strain under the different conditions. Focusing only on genes with INDELs present in their coding region (frameshift; intragenic and inframe insertion/deletion), their functional enrichment (Figure - 16) and functional categorization (Figure - 17 and 18) was assessed in conditions of evolution.

In the evolution without drug, as well as evolutions with fluconazole and itraconazole, there was no functional enrichment. However, in the evolution with Amphotericin B (Figure - 16), an enrichment of the cell redox homeostasis function (40%) was observed in the T0 strain. Strain T1 was enriched in cell adhesion (12.50%) and biofilm formation (8.30%) functions, while strain T2 did not show functional enrichment.

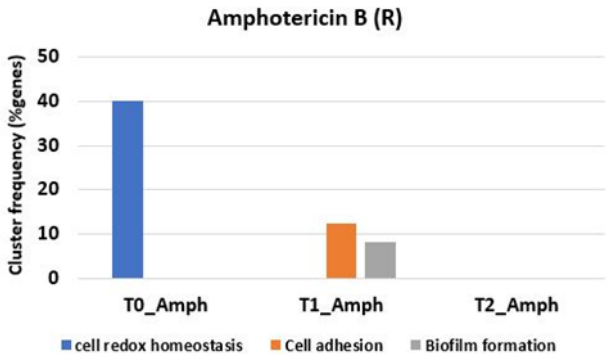

Figure 16 **- Functional enrichment of genes with intragenic INDELs.** Only evolution with Amphotericin B presented functional enrichment. GO term analysis was performed using the GO Term Analysis tool of CGD using a threshold of p-value<0.1.

In the functional categorization analysis, the T0 strain evolved without drug (Figure - 17A.) presented 100% of frequency in the not yet annotated category, while strains T1 and T2 presented 50% in categories such as response to stress and DNA metabolic process.

In evolution with Fluconazole (Figure - 17B.), the T0 strain had the highest frequency of genes in the response to stress category (40%). T1 and T2 strains had a 50% frequency in the remaining categories.

In evolution with Itraconazole (Figure - 18A.), strain T2 does not present gene frequency in any category. The T0 strain has 50% of its genes in the categories not yet annotated and biological processes unknown. In the case of the T1 strain, it has a higher frequency of genes in the categories of biological process unknown (50%), filamentous growth (50%), regulation of biological process (40%) and response to stress (40%).

In evolution with Amphotericin B (Figure - 18B.), the T0 strain has a higher frequency of genes in the cellular homeostasis (50%) and regulation of biological process (50%) categories. The T1 strain has the highest frequency of genes in the biological process unknown (41.70%), transport (25%) and response to stress (25%) categories. The T2 strain obtained 50% gene frequency in the categories not yet annotated, vesicle-mediated transport, transport, and organelle organization.

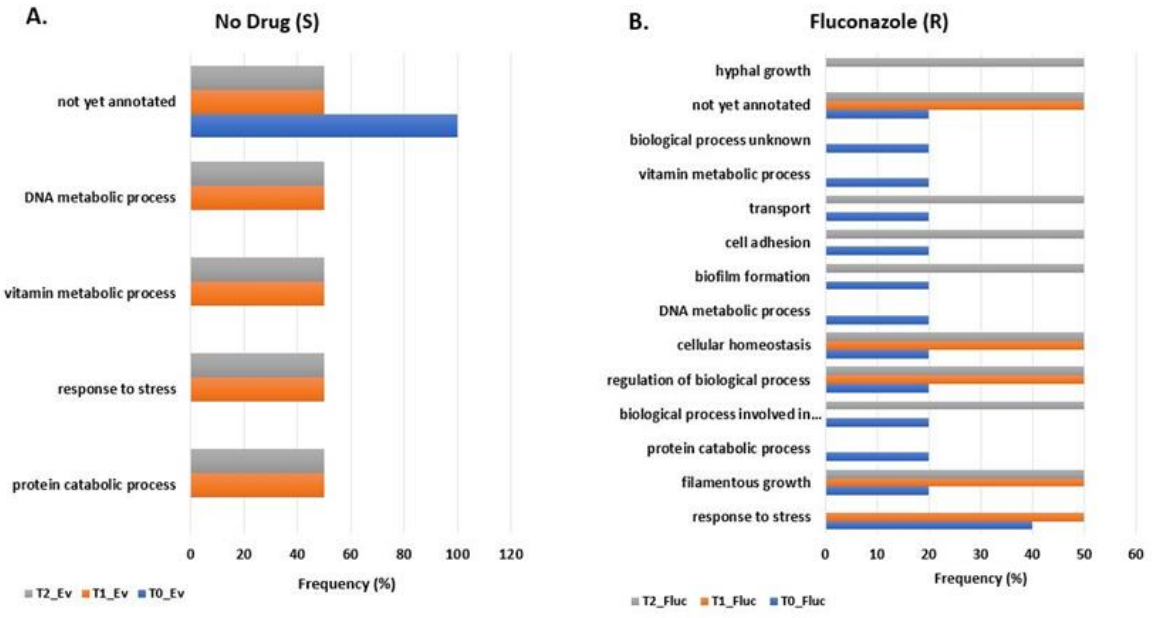

Figure 17 **- Functional analysis of genes with intragenic INDELs.** Distribution of genes with INDELs in strains evolved without drug (A.) and with Fluconazole (B.).

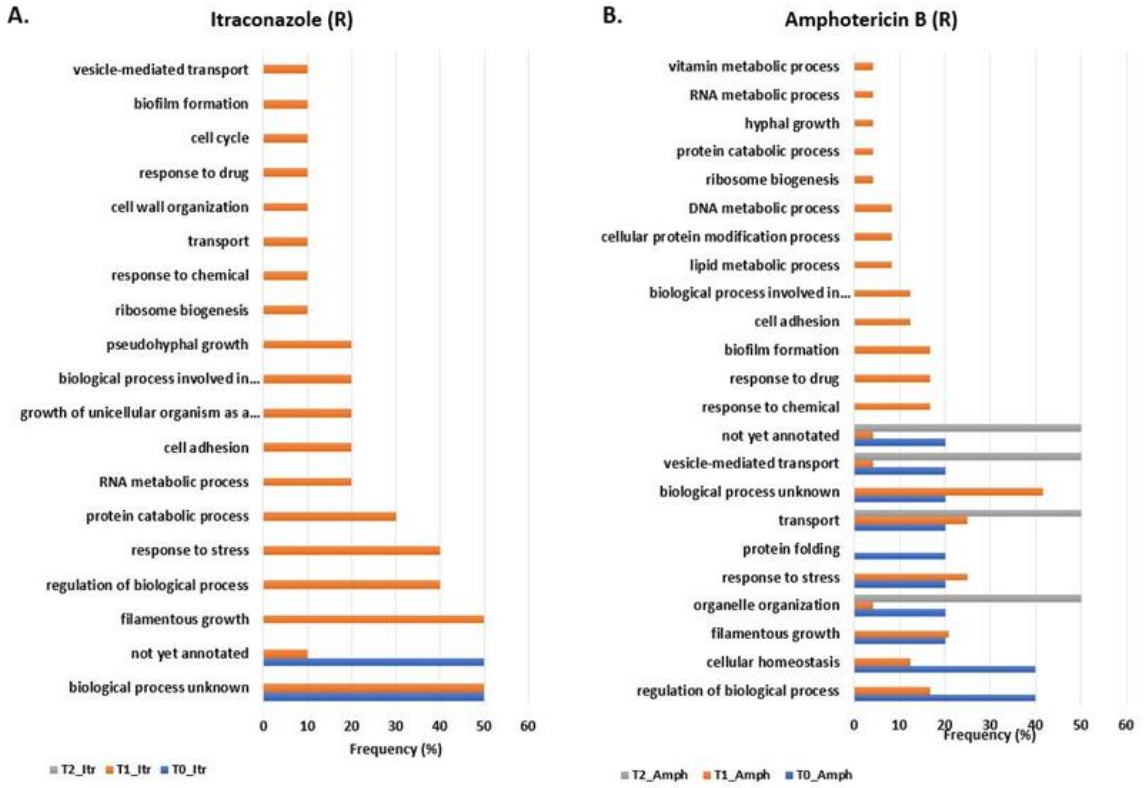

Figure 18 **- Functional analyses of genes with intragenic INDELs.** Distribution of genes with INDELs in strains evolved with Itraconazole (A.) and Fluconazole (B.).

Of the categories presented in the functional categorization, only the categories response to drug, response to chemical and response to stress were addressed, since the genes in these categories are directly related to acquisition of antifungal resistance. The table below (Table 4) shows the genes found in these categories in the different strains and conditions of evolution. By comparing the genes that appear in hypermistranslating strains to the control strain in the four conditions of evolution, we highlighted in red those mutated in high-mistranslating conditions. In drug-free evolution, the hypermistranslating strains T1 and T2 have the RIB7 gene mutated. In evolution with Fluconazole hypermistranslating strains don't present different genes comparing to wild type. In evolution with Itraconazole, T1 has the GZF3, PIN4 and DSE1 genes with INDELs. In evolution with Amphotericin B, where more isolates from the control strain T0 acquired resistance, no differences were found

between the wild type and the hypermistranslating ones. These genes and their functions will be discussed in section IV.

Table 4 **-** Genes with INDELs belonging to categories such as response to drug, response to chemical and response to stress

Evolution	Strain	Genes
Without Drug	**T0**	
	T1	RIB7
	T2	RIB7
Fluconazole	**T0**	EAP1; FGR28; RIB7
	T1	FGR28
	T2	
Itraconazole	**T0**	
	T1	GZF3; PIN4; DSE1
	T2	
Amphotericin B	**T0**	FGR28
	T1	FGR28
	T2	

2.2. Copy Number Variations

Analysis of copy number variations (CNVs) showed that before the experimental evolution (Figure - 19) the isolates of strains T0, T1 and T2 did not show any significant alteration in their chromosomes.

In drug-free evolution (Figure - 20), susceptible isolates from strains T0, T1 and T2 did not change significantly, but strain T1 shows small copy gains at the ends of chromosomes I-VII.

In the evolution with Amphotericin B (Figure - 21), resistant isolates from strains T0 and T2 showed a copy gain on all chromosomes I, III, and VII. In strain T1, only Chromosome I showed a copy gain.

In evolution with Itraconazole (Figure - 22), resistant isolates from T0 strain showed a copy gain in half of Chromosome IV (850100 bp – 1588700 bp) and on Chromosome R (0 - 1359700 bp), and a deletion in Chromosome R (1999000 bp – 2286237 bp). The T1 strain does not show significant changes in its chromosomes. Strain T2 has a deletion on

Chromosome IV (0 - 420400 bp), on Chromosome R (1999000 bp - 2286237 bp), and a gain on Chromosome R (0 to 1999000 bp).

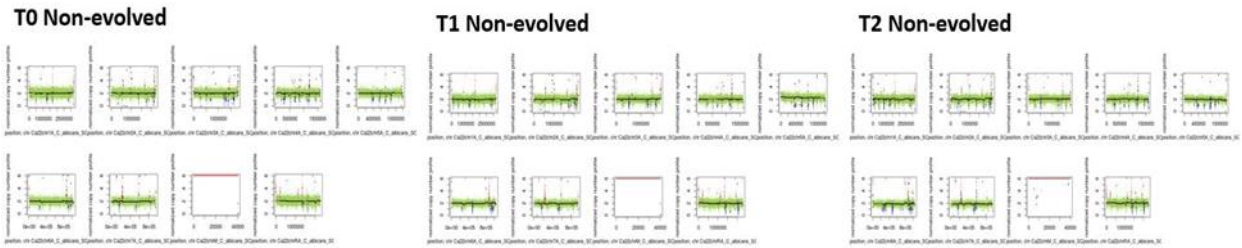

Figure 19 **- Copy number variations detected in non-evolved strains**. For each strain shown is the genome of an exemplificative isolate. Each box represents a chromosome I-VII, M and R. Chromosomal duplications are shown in red, deletion events in blue and green is normal. Non-evolved strains showed no significant CNVs.

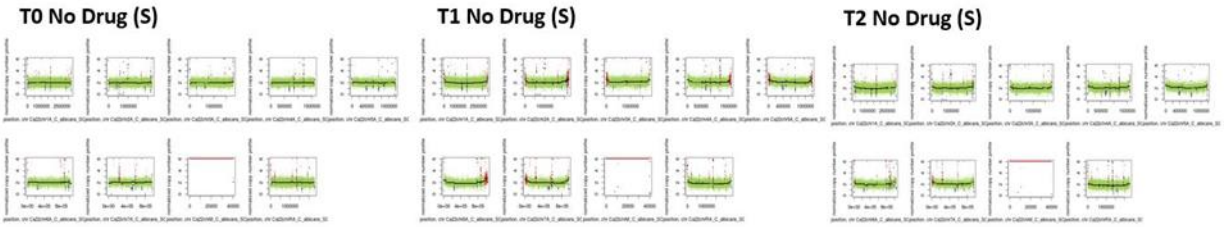

Figure 20 **- Copy number variations detected in evolved strains without drug.** For each strain shown is the genome of an exemplificative susceptible isolate. Each box represents a chromosome I-VII, M and R. Chromosomal duplications are shown in red, deletion events in blue and green is normal. Strains evolved without drug strains remain at normal number of CNV, with some duplication events in the edge of some chromosome, but not statistically significant.

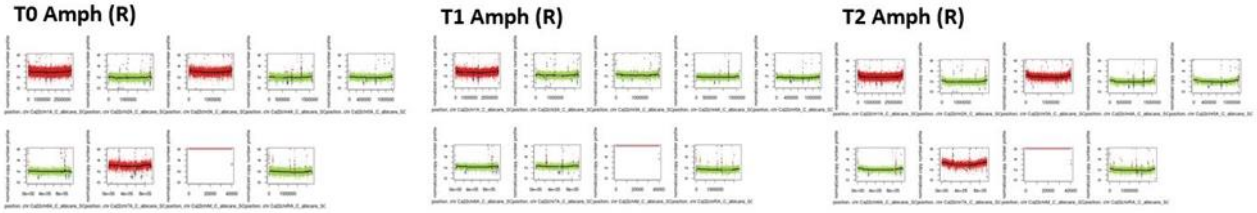

Figure 21 **- Copy number variations detected in strains evolved with Amphotericin B.** For each strain shown is the genome of an exemplificative resistant isolate. Each box represents a chromosome I-VII, M and R. Chromosomal duplications are shown in red, deletion events in blue and green is normal. Strains T0 and T2 have a duplication event in whole Chromosome I, III, VII. T1 strain has a duplication in whole Chromosome I.

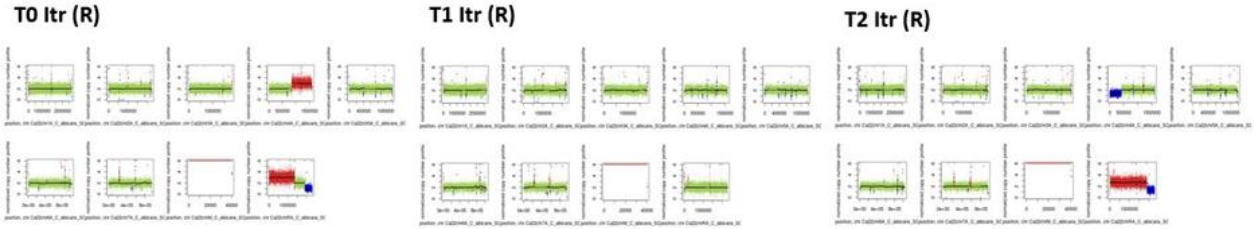

Figure 22 **- Copy number variations detected in strains evolved with Itraconazole.** For each strain shown is the genome of an exemplificative resistant isolate. Each box represents a chromosome I-VII, M and R. Chromosomal duplications are shown in red, deletion events in blue and green is normal. Strain T0 has a duplication in chromosome IV and chromosome R; and a deletion event in chromosome R. Strain T1 has no alterations. Strain T2 has a deletion event in chromosome IV and R, and a duplication in chromosome R.

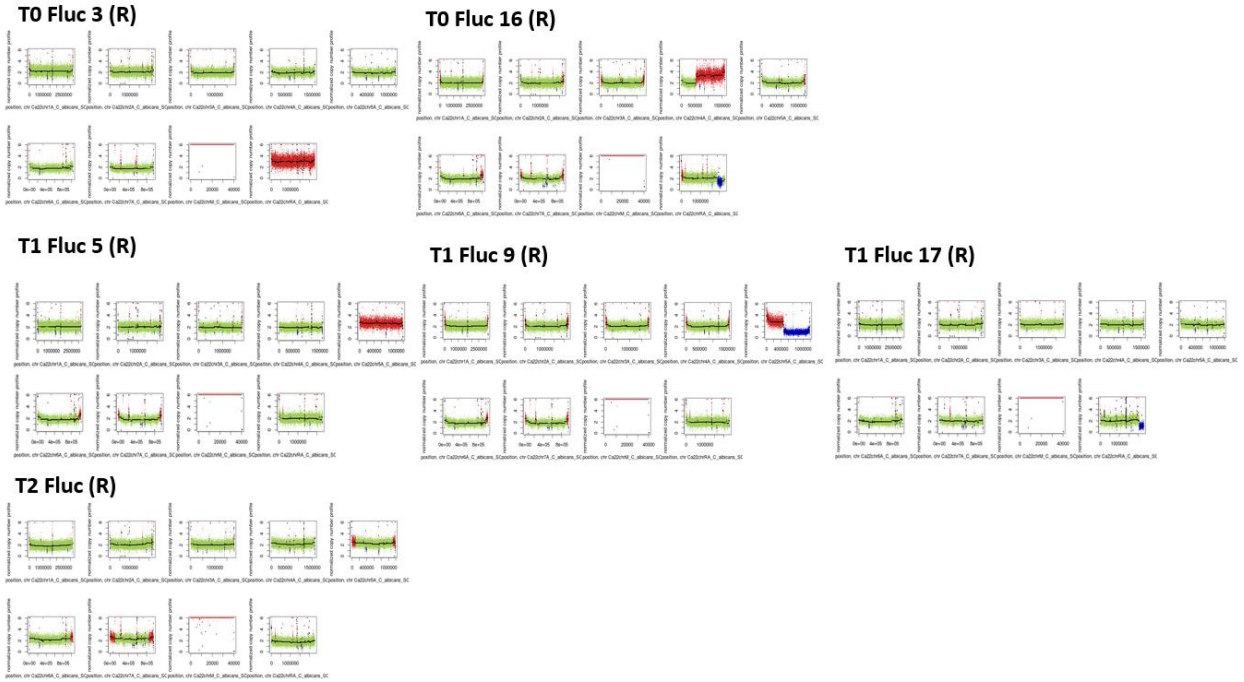

Figure 23 **- Copy number variations detected in strains evolved with Fluconazole.** For each strain shown is the genome of resistant isolates representing the variability of results. Each box represents a chromosome I-VII, M and R. Chromosomal duplications are shown in red, deletion events in blue and green is normal. Strain T0 is represented by isolates T0 Fluc 3 (R) and T0 Fluc 16 (R). T0 Fluc 3 (R) have a duplication in whole chromosome R and T0 Fluc 16 (R) have a duplication in chromosome IV and a deletion in chromosome R. Strain T1 is represent by isolates T1 Fluc 5 (R), T1 Fluc 9 (R) and T1 Fluc 17 (R). T1 Fluc 5 (R) have a duplication event in whole chromosome V; T1 Fluc 9 (R) have a duplication and a deletion in Chromosome V; and T1 Fluc 17 (R) have a deletion in chromosome R.

Unlike all other conditions, in evolution with Fluconazole (Figure 23) there was variation among the different resistant isolates of each strain, with no defined pattern of CNVs common among all isolates. In strain T0, isolate T0 Fluc 3 (R) showed a copy gain on the entire Chromosome R, and isolate T0 Fluc 16 (R) showed a copy gain in Chromosome IV in the range of 532300 bp to 1603259 bp, and a deletion on the Chromosome R in the range of 1623800 bp to 2136300 bp. In strain T1, isolate T1 Fluc 5 (R) had a copy gain on Chromosome V ranging from 0 to 466100 bp and a deletion ranging from 472000 bp to 1188100 bp; and isolate T1 Fluc 17 (R) had a deletion in Chromosome R ranging from 866700 bp to 2286237 bp. In strain T2, isolate T2 Fluc 9 (R) showed a copy gain in Chromosome V in the ranges from 0 to 466100 bp and 724900 bp to 1190100 bp, on Chromosome VI in the range of 780200 bp to 1031700 bp and on Chromosome VII in the ranges from 0 to 242900 bp and from 577600 bp to 948600 bp. In this case, all isolates that are not shown in Figure 23 did not show genomic alterations.

Genes that were present in the altered areas of the chromosomes of the three strains, under the three conditions of antifungal therapy, were categorised using the Gene Ontology (GO) tool (complete tables are shown in annex C). Categories were selected with a threshold above 10% frequency. When comparing the hypermistranslating strains with the control T0, it was found that in the evolution of Amphotericin B there were no aneuploidies that were different between the three strains. However, in the evolution with Itraconazole (Figure - 24) strain T2 presented monosomy on Chromosome IV (0–420 kb) and trisomy on Chromosome R (1360 kb to 1999) with genes mapped into cellular protein modification processes (IV – 12.40%, R – 12.10%), organelle organization (IV – 20.30%, R – 22.60%), protein catabolic process (R – 11.30%), regulation of biological process (IV – 19.80%, R – 24.80%), response to chemical (IV – 12%, R – 12.60%), response to stress (IV – 11.50%, R – 12.80%), ribosome biogenesis (IV – 13.40%, R – 14.80%), RNA metabolic process (IV – 18.40%, R – 20.30%), translation (IV – 14.70%, R – 12.60%), and transport (IV – 35.90%, R – 32.10%).

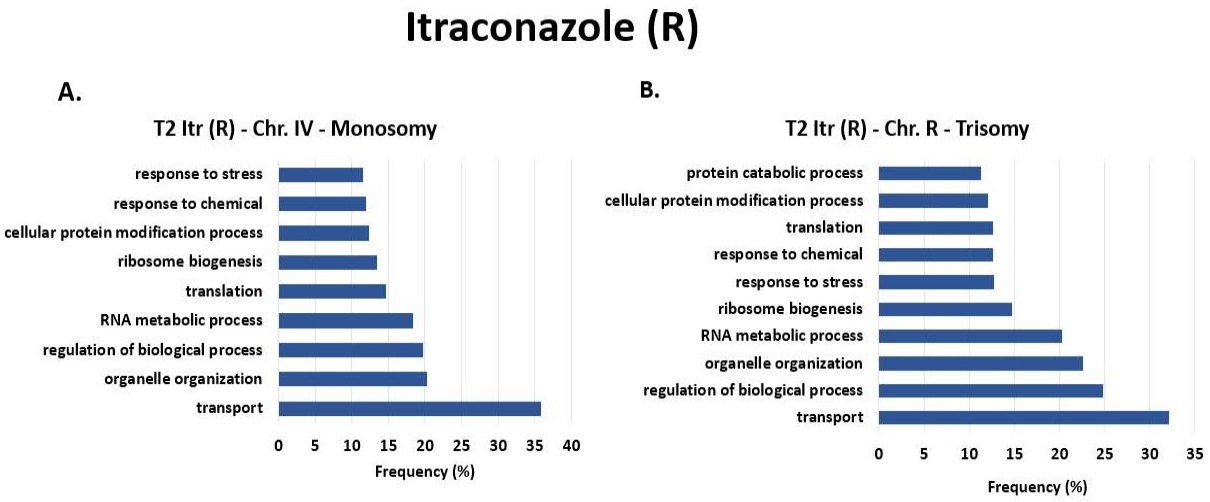

***Figure 24* – Functional analysis of genes with aneuploidies in evolution with Itraconazole. A.** Categorization of genes found in the monosomy presented on chromosome IV (0–420 kb) of strain T2. **B**. Categorization of genes found in the trisomy presented on the chromosome R (1360 kb to 1999) of the T2 strain.

In evolution with Fluconazole (Figure - 25) the isolates representing the T1 strain significantly differ from the control. The isolate T1 Fluc 5 (R) exhibited a trisomy across Chromosome V, with genes classified as cell cycle, cellular protein modification process, filamentous growth, organelle organization, protein catabolic process, regulation of biological processes, response to stress, ribosome biogenesis, RNA metabolic process, translation, and transport. Isolate T1 Fluc 9 (R) has a monosomy on chromosome V (472 kb to end) with genes categorised in the category's regulation of biological process (V-Tri-20.60%, V-Mono-23.60%), organelle organization (V-Tri-24.50%, V-Mono-20.90%), RNA metabolic process (V-Tri-22.50%, V-Mono-18.60%), translation (V-Tri-16.70%, V-Mono-13%), cellular protein modification process (V-Tri-13.70%, V-Mono-12.70%), response to chemical (V-Mono-12.40%), ribosome biogenesis (V-Tri-10.80%, V-Mono-11.50%), response to stress (V-Tri-12.70%, V-Mono-10.00%), cell cycle (V-Tri-10.80%) and transport (V-Tri-24.50%, V-Mono-25.70%). The T2 strain differs from T0 by presenting trisomy on Chromosome VI (780 kb to end) and Chromosome VII (0 to 253 kb and 578 kb to end) with genes categorised as cellular protein modification process (VI- 11.80%) filamentous growth (VI – 20.60%), organelle organization (VI – 17.60%, VII – 18.50%), protein catabolic process (VII – 10.80%), regulation of biological process (VI – 17.60%, VII – 18.50%), response to chemical (VI – 14.70%, VII – 18.50%), response to stress (VI – 11.80%, VII – 11.50%), ribosome biogenesis (VII – 10.00%), RNA metabolic process (VI

– 11.80%, VII – 20.80%), translation (VI – 11.80%), transport (VI – 44.10%, VII – 33.10%), response to drug (VI – 14.70%), biofilm formation (VI – 11.80%), hyphal growth (VI – 11.80%), biological process involved in interspecies between organisms (VI – 29.40%) and cell adhesion (VI – 11.80%). Genes mapped to categories such as response to chemical and response to stress will be further discussed in the next section.

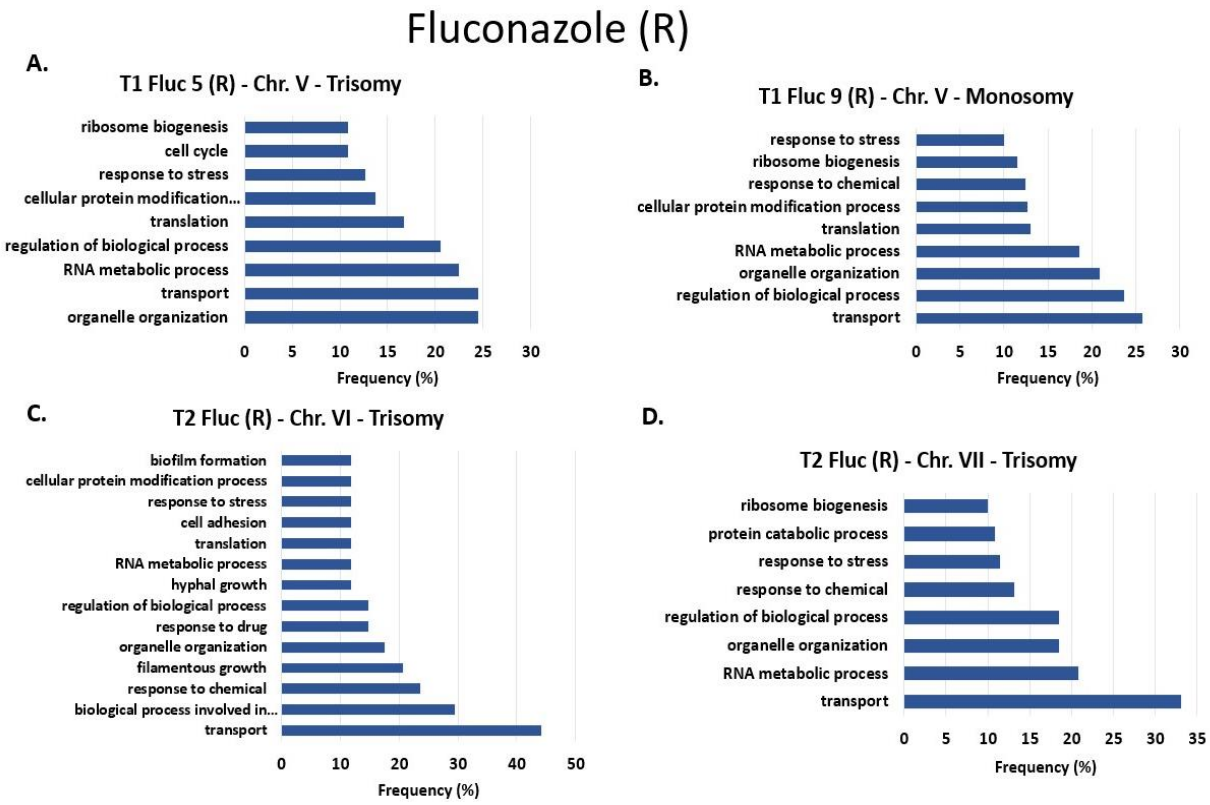

Figure 25 **- Functional analysis of genes with aneuploidies in evolution with Fluconazole. A.** Categorization of genes found in the trisomy presented on whole chromosome V of isolate T1 Fluc 5 (R). **B**. Categorization of genes found in the monosomy presented on the chromosome V (472 kb to end) of isolate T1 Fluc 9 (R) **C.** Categorization of genes found in the trisomy presented on chromosome VI (780 kb to end) of strain T2. **D.** Categorization of genes found in the trisomy presented on chromosome VII (0 to 253 kb and 578 kb to end) of strain T2.

IV. DISCUSSION

1. Effect of mistranslation on the acquisition of antifungal resistance during experimental evolution

Experimental evolution and MIC assessment results indicate that there is a relationship between mistranslation and the frequency in the acquisition of antifungal resistance. Increased levels of mistranslation appear to speed up the emergence of azole resistance but not polyene resistance. Weil and colleagues did a similar experimental evolution study where they evolved a strain of *Candida albicans* that has high levels of mistranslation to examine its influence on the acquisition of resistance to Fluconazole[107]. Their results showed that during drug-free evolution the wild-type and hypermistranslating strain remained susceptible until the end of evolution, while with Fluconazole the hypermistranslating strain gained resistance at a much earlier time point than the wild-type[107]. However, the Weil study only evolved one isolate of each strain and, therefore, there was no representativity to allow the drawing of definitive conclusions. Nonetheless, when comparing the data obtained in this study with data from Weil et al., both studies showed the same trend. There are no previous similar studies that demonstrate the relationship between mistranslation and the acquisition of resistance to Itraconazole or Amphotericin B, which makes this work the first to test this relationship.

Another aspect to be considered is the presence of cell aggregation and the hypha and pseudohypha phenotypes in strains T1 and T2, which prevented the determination of MIC in evolutions with and without Fluconazole. The EUCAST protocol is not efficient in the presence of filamentous phenotypes or cell aggregates. These phenotypes and the inability to assess MICs can be explained by the high mistranslation level present in strains T1 and T2 that is associated with filamentation and cell-cell aggregation. The phenotype change hypothesis was put forward in a study by Miranda et al[106]. In this study they inserted *S. cerevisiae* tRNALeu genes into *C. albicans* to increase mistranslation, and in their data, they observed that this strain showed morphogenesis[106]. A wide morphological variety was found and highly heterogeneous cell populations containing elongated ovoid cells, pseudohypha and true hypha were produced spontaneously and without external factors[106]. In the case of cell-cell aggregation, mistranslation is supposed to increase the effectiveness of adherence of ALS proteins. The Als glycoproteins are cell surface adhesins that have been

shown to facilitate *Candida albicans* cell-to-cell aggregation as well as adhesion to proteins and cells[123]. Miranda et al. did a study where they suggested that mistranslation has an influence on the increase of adherence in *C. albicans*[101]. In this study, one of the assays demonstrated that a *C. albicans* strain with 28% mistranslation (displaying 28% leucine incorporation rather than the usual 3% leucine incorporation) has a greater capacity to adhere to several abiotic and biotic substrates than a wild-type strain[101]. This result led them to study the surface proteins that have the adhesion function, in this case the ALS proteins, which have several ambiguous CUG codons in their genomic sequences[101]. Thus, they performed an assay where they inserted two different isoforms of *C. albicans* ALS3 into non-adherent *S. cerevisiae*, where in the CUG sites the Als3p-Leu isoform incorporates leucine, and the Als3p-Ser isoform incorporates serine[101]. *S. cerevisiae* expressing Als3p-Leu flocculated more than the strain expressing Als3p-Ser when cultured in liquid media, demonstrating that the variable translation of the CUG codon has a major impact on cell-cell adhesion[101]. Als3p's ability to bind to diverse substrates was similarly affected when leucine was substituted for serine[101]. Als3p-Leu-expressing *S. cerevisiae* cells demonstrated considerably better adhesion to polystyrene, fibronectin, vitronectin, and gelatine than Als3p-Ser-expressing cells[101]. Overall, the fact that the Als3p-Ser and Als3p-Leu isoforms have dramatically different adherence qualities suggests that CUG mistranslation has functional ramifications[101] that in this study hindered the measurement of precise minimal inhibitory concentrations.

2. Genomic alterations during experimental evolution without drug

MIC evaluation at the beginning and end of the drug-free evolution showed that isolates of both control and hypermistranslating strains are susceptible to all drugs. However, it is important to determine the effects of mistranslation in the genomes of isolates under study, because in response to environmental, nutritional, or immunological stress, mistranslation can increase cellular survival[124,125]. Changes in translational fidelity and consequently protein structures, for example, may be used by cells to monitor and adapt to adverse environmental circumstances, and the capacity to properly perceive and mount an effective response to stress is critical for cellular survival[124].

Results showed that hypermistranslating strains had a higher average number of SNPs per isolate than the wild-type strain. Strain T2 exhibited the highest number of SNPs per isolate among the hypermistranslating strains. The higher the rate of mistranslation, the more probable SNPs are to arise, according to this study. Because there has been few research on the link between SNP incidence and mistranslation, it is unclear how mistranslation affects SNP occurrence.[105,107] The functional enrichment of the altered genes revealed an enrichment of activities linked to virulence and pathogenicity, such as cell adhesion and biofilm formation on all strains with no difference between control and high-mistranslating strains. Only the hypermistranslating T1 strain showed differences to the wild-type strain in terms of functional enrichment with SNPs in genes belonging to hyphal growth. Furthermore, the genes were classified into categories such as response to stress, response to drug, response to chemical, filamentous growth, hyphal growth, biofilm formation and cell adhesion, all of which are linked to virulence factors and antifungal agent acquisition. These findings show that prior to exposure to antifungal treatments, mistranslation increases mutations in genes that are related to resistance to antifungal drugs.

Unlike the SNP results, data revealed that the wild-type strain has more INDELs than the hypermistranslating strains. It is uncertain how a rise in mistranslation levels reduces the frequency of INDELs. No statistically significant functional enrichment was detected in genes with INDELs. However, in terms of functional categorization, the two hypermistranslating strains had a high frequency of mutated genes in the response to stress category, which is linked to antifungal resistance acquisition, suggesting once again that mistranslation increases mutations in genes that are related to resistance to antifungal drugs.

In hypermistranslating strains mutations were found in genes that were not mutated in the control strain. In the analysis of SNPs, the hypermistranslating T1 strain presented mutations in the EAP1 gene. This gene encodes a glycosylphosphatidylinositol-anchored, glucan-cross-linked cell wall protein, which is involved in adhesion and biofilm formation *in vitro* and *in vivo*[126]. In the analysis of INDELs, both hypermistranslating strains presented mutations in the RIB7 gene. This gene has 5-amino-6-(5-phosphoribosylamino)uracil reductase activity and role in riboflavin biosynthetic process[120]. The importance of riboflavin synthesis in microbial pathogenesis has just lately been established. The synthesis of this vitamin in nutrient-poor host niches is needed for survival of various infection contexts and hence is vital for *C. albicans* virulence[127].

In short, in drug-free evolution no change was found in relation to CNVs and amount of INDELs, however it was found that the significant increase in SNPs and the occurrence of mutations in the EAP1 and RIB7 that are related to resistance and pathogenic mechanisms, suggest that mistranslation can have a significant impact on the acquisition of antifungal resistance.

3. Genomic alterations during experimental evolution with Azoles

3.1 Experimental evolution with Fluconazole

In the experimental evolution with Fluconazole there was no statistically significant changes in the number of SNPs and INDELs between the hypermistranslating strains and the control strain T0. Although there were no differences in the number of SNPS, the hypermistranslating strains had mutated genes that can be categorized in response to stress/drug/chemicals.

The hypermistranslating T1 and T2 strains showed mutations in genes that were not mutated in the wild type. In T1, genes FMO1, FGR6-4 and LIP5 had SNPs in the coding region. In T2, we found mutations in the EAP1 gene. The FMO1 gene encodes an oxidoreductase that, when mutated, confers hypersensitivity to the toxic analogue of ergosterol[120], however in this study this gene may have the opposite effect to what is described in the literature, that is, acquire resistance to azoles. The LIP5 gene is part of the family of secreted hydrolases, the lipases, consists of 10 members (LIP1–10)[128]. The LIP genes may have developed to adapt to *C. albicans*' constant interaction with the human host, and so may play essential roles throughout persistence and infection processes[128]. The FGR6-4 gene is part of the filamentous growth regulator (FGR) family genes, which are specific to the *C. albicans* species, and no relatives were found in *S. cerevisiae* or in any other biological model[129]. These genes control specific filament characteristics that are part of *C. albicans*' ability to colonise and proliferate in warm-blooded animals, the only known hosts for these organisms[129]. The filamentation is crucial for robust biofilm formation[5], because biofilm cells are difficult to destroy and have significant degrees of resistance to most antifungals used in clinical practice[130].

Unlike SNPs and INDELs, evolution with fluconazole did cause copy number variations in hypermistranslating strains that were not present in control T0. Chromosome

IV experienced a duplication, and chromosome R suffered a duplication and deletion during evolution of the wild-type strain, which is not shown in hypermistranslating strains. On the other hand, strains with higher levels of mistranslation suffered duplications and deletions in chromosomes V, VI, VII, and R. The hypermistranslating T1 strain has the same chromosome R deletion as the control strain. On the chromosome R is where the rDNA locus is located, which serve as hotspots for genome rearrangements that contribute to genomic and phenotypic plasticity. This deletion has already been observed in an *in vivo* evolution performed by Ford *et al*, which consisted of sequencing and analysing *Candida* isolates in patients with oral candidiasis[95]. Of the 43 isolates sequenced, the CNVs showed great variability and presented duplications on the same chromosomes as those observed in this work, but they did not present the deletions[95]. However, in the *in vitro* evolution carried out by Weil *et al*, its hypermistranslating clone presented the same deletions in the Chromosome R as those observed in this study[107]. Also, increased copy numbers of chromosomes VI have been added to the list of genomic rearrangements linked to fluconazole resistance in *C. albicans*, according to research by Hirakawa *et al*[83]. The same duplications were observed in this study.

In hypermistranslating T1 and T2 strains, aneuploidies were found in genes that are related to the traditional mechanisms of resistance to Fluconazole, involving TAC1 and ERG11 in Chromosome V. TAC1 is a Zn(2)-Cys(6) binuclear cluster transcriptional activator of drug-responsive genes such as ABC drug transporters CDR1 and CDR2[78]. This increase will likely increase the production of drug transporters to expel Fluconazole from the cell. In the literature and in these data, the duplication was only found in exposures to Fluconazole[66]. The lanosterol demethylase enzyme, which is the target of azole antifungals, is encoded by the ERG11 gene[71]. The ability of the azoles to bind to and inhibit Erg11 is altered by mutations in ERG11 that result in a point mutation, leading to resistance[71]. In the work by Flowers *et al*, 9 point mutations were found in the ERG11 gene (Y132F, K143R, F145L, S405F, D446E, G448E, F449V, G450E, and G464S) that contributed to resistance to Fluconazole[71]. In another study, Xiang *et al* found that A114S, Y132H, Y132F, K143R, Y257H, and K143Q point mutations contributed to resistance to Fluconazole and Voriconazole but found no significant differences in resistance to Itraconazole[72]. In addition to point mutations, overexpression of the ERG11 gene is related to overexpression of the UPC2 gene, conferring resistance to Fluconazole[76]. In this work, the Chromosome V of

hypermistranslating isolates underwent duplication which affects erg11 and likely its expression.

Overall, results suggest that SNPs and INDELs may not be responsible for the acquisition of resistance to fluconazole by hypermistranslating isolates. On the other hand, the variability of CNVs demonstrates that evolution with fluconazole causes large scale rearrangements that affect the traditional mechanisms of resistance acquisition, such as drug efflux and overexpression of the drug target.

3.2 Experimental evolution with Itraconazole

Analysis of the number of SNPs and INDELs during evolution with itraconazole showed that there are no statistically significant differences between the control T0 and the hypermistranslating strains. Although there were no differences in the number of SNPs and INDELs, some mutated genes related to response to drugs were specifically mutated in T1 and T2. The T1 strain had the FMO1, RPF2, GZF3, RSP5, PGA14, C4_05790W_A, LIP5, PHO112, FGR6-10, SYS3, PIN4 and DSE1 genes, while the T2 had the FMO1, FET31, FGR6-3 and FGR6-10 genes. From this set of genes, FMO1 and LIP5 were discussed in evolution with Fluconazole. The FGR6-3 and FGR6-10 genes belong to the filamentous growth regulator (FGR) family genes[129]. The PGA14 gene is GPI protein is known to be covalently integrated into the cell wall network or to stay connected to the plasma membrane[131]. They've been recommended for a variety of functions and might have a role in cell wall biosynthesis and remodelling[131]. They are hypothesised to have a role in adhesion and pathogenicity, as well as determining surface hydrophobicity and antigenicity[131].

The T1 strain had no changes in its chromosomes regarding CNVs, but strain T2 had a deletion on chromosome IV and a duplication on chromosome R that were not present in T0.

In the aneuploidies of the hypermistranslating T2 strain, genes that may be linked to acquisition of resistance were found, such as the DAG7 and ERG8 genes. Apart from being part of the ergosterol pathway, the ERG8 gene has never been studied in *C. albicans* as it is only referred to as an ortholog of the ERG8 gene from *S. cerevisiae*[120] and is a phosphomevalonate kinase[132]. ERG8 mutations in *C. albicans* have never been reported until our data showed a deletion in the gene. DAG7 gene encodes a secretory protein, in which

mutations confer hypersensitivity to toxic ergosterol analogues[133]. Our data showed a deletion in the DAG7 gene, however this deletion has never been reported as related to acquisition of resistance.

Other aneuploidies in T2 isolates affected genes encoding Heat shock proteins (Hsps) such as HSP60 and HSP104. The heat shock response is a conserved response among organisms to stressful situations such extreme heat, hunger, and oxidative damage[134,135]. Protein unfolding, and nonspecific protein aggregation can occur because of such stressors, causing cell death[5]. Hsps are produced by cells to avert this unfavourable outcome[134]. Hsps are abundant in *C. albicans* and play a role in a variety of physiological pathways, including calcium-calcineurin, MAPK, Ras1-cAMP-PKA, and cell cycle regulation signalling. Hsps client proteins are found in many signalling molecules in various pathways[136]. Furthermore, several studies have shown that Hsps contribute to antifungal drug resistance in *C. albicans* via modulation of various signalling pathways[136]. HSP60 is a mitochondrial HSP whose function is unknown[5]. In a previous study, an hsp60/HSP60 heterozygous mutant displayed enhanced susceptibility to high temperatures, suggesting that Hsp60 could be essential for thermal stress tolerance[137]. However, it is not known what relationship it could have to exposure to azoles. Heat shock, osmotic stress, hyperosmotic stress, and oxidative stress all stimulate the production of HSP104, a heat shock protein with chaperone and prion propagation properties[138,139]. No studies were found specifically on the influence of azoles on HSP104. However, Fiori et al showed that Hsp104 is necessary for effective resistant biofilm formation by constructing a hsp104 Δ/Δ mutant whose hyphae have structural abnormalities, look patchy and loose[140]. Also, others Hsps, such HSP90, are linked to resistance to antifungals. Reduced Hsp90 levels resulted in a significant reduction in matrix glucan levels, suggesting that Hsp90 may also play a role in biofilm azole resistance[141].

Overall, the data showed that hypermistranslating strains may have acquired resistance to Itraconazole through aneuploidies, altering genes that are not associated with traditional mechanisms of resistance. This is in contrast to results of fluconazole evolution where aneuploidies affected drug efflux and overexpression of the drug target.

4. Genomic alterations induced by experimental evolution with Amphotericin B

In evolution with the polyene Amphotericin B, results showed that the average number of SNPs per isolate is higher in control T0 strain than in hypermistranslating ones. This decrease highlights the results obtained from MICs, where strain T0 had a greater number of isolates to acquire resistance. In the functional enrichment, the T0 and T1 strains presented enrichment in the same functions, cell adhesion and biofilm formation, but the T0 strain presented greater enrichment in the cell adhesion function. These functions are linked to virulence and contribute to the acquisition of resistance. In the functional categorization, strain T0 and T1 presented gene frequencies in categories related to virulence and acquisition of resistance, such as response to drug, response to chemical, hyphal growth, biofilm formation, response to stress, cell adhesion and filamentous growth. The T2 strain only showed frequency in the response to stress category. The same pattern was observed in the INDELs analysis. The average number of INDELs per isolate was higher in T0 than in hypermistranslating strains.

During evolution with Amphotericin B the appearance of resistant isolates was most frequent in the control T0 strain, therefore we focused our analysis on genes that were specifically mutated in this strain. T0 resistant isolates revealed mutations in genes such as ALS9, FGR28 and LIP5. The FGR28 belong to the filamentous growth regulator (FGR) family genes[129]. The ALS (agglutinin-like sequence) gene family in *C. albicans* encodes eight large cell-surface glycoproteins with adhesive activity (Als1-Als7 and Als9)[38]. In vulvovaginal candidiasis, the ALS9 gene plays an adherence and initiation role in the pathogenic phase[142]. It also presented different sequences in the alleles, which could modify the protein's function[142]. Furthermore, the ALS9 gene was shown to be expressed in clinical vaginal fluid specimens and vaginal candidiasis model systems (murine vaginitis model and reconstituted human vaginal epithelium model)[143]. Mutations in genes of the ALS family are in accordance with the current literature that state that their conserved Ser/Thr-rich domain is prone to intergenic recombination between ALS homologues, but intragenic recombination may also occur, producing new genetic variants[53].

The analysis of CNVs showed that duplications in chromosomes I, III and VII occurred in all strains. T0 and T2 had duplications on the same chromosomes (I, III and VII) and strain T1 only had the duplication on chromosome I. Since aneuploidies were common between control and hypermistranslating strains, we can exclude this type of rearrangements

as a specific mechanism of strains with higher error rates. This is in sharp contrast to what happened during evolution with both azoles.

In short, results suggest that exposure to Amphotericin B decreases the occurrence of SNPs and INDELs at high levels of mistranslation and no differences were found between wild type strain and hypermistranslating strains in relation to CNVs.

V – CONCLUSIONS AND FUTURE PERSPECTIVES

In this work we analysed the genomes of three *C. albicans* strains, wild-type (T0) and hypermistranslating (T1, T2), evolved under different conditions of experimental evolution *in vitro*. This method aims to identify possible genomic alterations (SNPs, INDELs, CNVs) that occur at different levels of mistranslation and upon exposure to Amphotericin B, Fluconazole and Itraconazole. We also aimed to relate those genomic rearrangements with known resistance mechanisms and potentially identify new ones.

Our results suggest that mistranslation plays an important role in the acquisition of drug resistance, although differently depending on the type of antifungal that was used. Hypermistranslation caused more rapid and frequent evolution of azole resistance mediated through CNVs that affected distinct types of genes. Fluconazole resistant isolates showed aneuploidies affecting the classical drug efflux and ergosterol biosynthesis pathways, while itraconazole resistant isolates showed aneuploidies affecting transport. In the evolution with the polyene Amphotericin B, hypermistranslation seemed to delay acquisition of resistance since the control T0 strain showed a higher number of resistant isolates. These also showed a higher number of SNPs and INDELs but no CNVs when compared to hypermistranslating strains T1 and T2. Mutations affected mostly genes such as ALS9, FGR28 and LIP5 that are related to virulence factors, which hinders the action of antifungals or helping to acquire resistance.

It was not possible to carry out the study of loss of heterozygosity (LOH), despite being an important mechanism for acquiring resistance to Fluconazole. In the literature, the loss of heterozygosity in regions encoding ERG11, TAC1, or MRR1 is frequently described [81,82]. For future work, it is necessary to study the LOH that occurred during the four different experimental evolutions. Furthermore, mutations that were identified need to be validated.

To do so, null/null mutants of *C. albicans* and genetic engineering through the CRISPR system may be used to verify if the mutations that occurred in this work influenced the acquisition of resistance to antifungal agents. Transcriptome analysis via RNAseq will also be important to perform since in all conditions most mutations occurred in the intergenic zone (60%). Finally, this study showed that, by being a driver of mutagenesis, mistranslation accelerated the evolution of resistance to azoles and decreased evolution of resistance to polyenes. It would be important to perform similar studies with drugs belonging to the other major class of clinical antifungals, namely echinocandins such as caspofungin.

VI-Bibliography

1. Bongomin, F., Gago, S., Oladele, R. O. & Denning, D. W. Global and multi-national prevalence of fungal diseases—estimate precision. *Journal of Fungi* vol. 3 (2017).
2. Brown, G. D. *et al.* Hidden killers: Human fungal infections. *Science Translational Medicine* vol. 4 (2012).
3. Crous, P. W., Gams, W., Stalpers, J. A., Robert, V. & Stegehuis, G. *MycoBank: an online initiative to launch mycology into the 21st century*. *IN MYCOLOGY* vol. 50 www.indexfungorum.org. (2004).
4. Dadar, M. *et al.* Candida albicans - Biology, molecular characterization, pathogenicity, and advances in diagnosis and control – An update. *Microbial Pathogenesis* vol. 117 128–138 (2018).
5. Mayer, F. L., Wilson, D. & Hube, B. Candida albicans pathogenicity mechanisms. *Virulence* vol. 4 119–128 (2013).
6. Robbins, N., Caplan, T. & Cowen, L. E. Molecular Evolution of Antifungal Drug Resistance. (2017) doi:10.1146/annurev-micro-030117.
7. Pérez, J. C. Candida albicans dwelling in the mammalian gut. *Current Opinion in Microbiology* vol. 52 41–46 (2019).
8. Höfs, S., Mogavero, S. & Hube, B. Interaction of Candida albicans with host cells: virulence factors, host defense, escape strategies, and the microbiota. *Journal of Microbiology* vol. 54 149–169 (2016).
9. Sanguinetti, M., Posteraro, B. & Lass-Flörl, C. Antifungal drug resistance among Candida species: Mechanisms and clinical impact. *Mycoses* **58**, 2–13 (2015).
10. Gajdács, M., Dóczi, I., Ábrók, M., Lázár, A. & Burián, K. Epidemiology of candiduria and Candida urinary tract infections in inpatients and outpatients: Results from a 10-year retrospective survey. *Central European Journal of Urology* **72**, 209–214 (2019).
11. McManus, B. A. & Coleman, D. C. Molecular epidemiology, phylogeny and evolution of Candida albicans. *Infection, Genetics and Evolution* vol. 21 166–178 (2014).
12. Gonçalves, B. *et al.* Vulvovaginal candidiasis: Epidemiology, microbiology and risk factors. *Critical Reviews in Microbiology* vol. 42 905–927 (2016).
13. Kadosh, D. Control of Candida albicans morphology and pathogenicity by post-transcriptional mechanisms. *Cellular and Molecular Life Sciences* vol. 73 4265–4278 (2016).
14. Sobel, J. D. *Vulvovaginal candidosis*. *www.thelancet.com* vol. 369 www.thelancet.com (2007).
15. Brown, S. E. *et al.* The Vaginal Microbiota and Behavioral Factors Associated with Genital Candida albicans Detection in Reproductive-Age Women. *Sexually Transmitted Diseases* **46**, 753–758 (2019).
16. Basso, V., d'Enfert, C., Znaidi, S. & Bachellier-Bassi, S. From genes to networks: The regulatory circuitry controlling candida albicans morphogenesis. in *Current Topics in Microbiology and Immunology* vol. 422 61–99 (Springer Verlag, 2019).
17. Poulain, D. Candida albicans, plasticity and pathogenesis. *Critical Reviews in Microbiology* vol. 41 208–217 (2015).
18. Noble, S. M., Gianetti, B. A. & Witchley, J. N. Candida albicans cell-type switching and functional plasticity in the mammalian host. *Nature Reviews Microbiology* vol. 15 96–108 (2017).

19. Cottier, F. & Hall, R. A. Face/Off: The Interchangeable Side of Candida Albicans. *Frontiers in Cellular and Infection Microbiology* vol. 9 (2020).
20. Warenda, A. J. & Konopka, J. B. Septin function in Candida albicans morphogenesis. *Molecular Biology of the Cell* **13**, 2732–2746 (2002).
21. Sudbery, P., Gow, N. & Berman, J. The distinct morphogenic states of Candida albicans. *Trends in Microbiology* vol. 12 317–324 (2004).
22. Witchley, J. N. *et al.* Candida albicans Morphogenesis Programs Control the Balance between Gut Commensalism and Invasive Infection. *Cell Host and Microbe* **25**, 432-443.e6 (2019).
23. Carlisle, P. L. *et al. Expression levels of a filament-specific transcriptional regulator are sufficient to determine Candida albicans morphology and virulence*. www.pnas.orgcgidoi10.1073pnas.0804061106 (2008).
24. Jansons' And, V. K. & Nickerson, W. J. *Chlamydospore of Candida albicans*. *JOURNAL OF BACTERIOLOGY* (1970).
25. Martin, S. W., Douglas, L. M. & Konopka, J. B. Cell cycle dynamics and quorum sensing in Candida albicans chlamydospores are distinct from budding and hyphal growth. *Eukaryotic Cell* **4**, 1191–1202 (2005).
26. Anderson, J., Mihalik, R. & Soll, D. R. *Ultrastructure and Antigenicity of the Unique Cell Wall Pimple of the Candida Opaque Phenotype*. *JOURNAL OF BACTERIOLOGY* vol. 172 (1990).
27. Douglas, L. J. *Candida biofilms and their role in infection*. http://timi.trends.com (2003).
28. Tao, L. *et al.* Discovery of a "White-Gray-Opaque" Tristable Phenotypic Switching System in Candida albicans: Roles of Non-genetic Diversity in Host Adaptation. *PLoS Biology* **12**, (2014).
29. Liang, S. H. *et al.* Hemizygosity Enables a Mutational Transition Governing Fungal Virulence and Commensalism. *Cell Host and Microbe* **25**, 418-431.e6 (2019).
30. Pande, K., Chen, C. & Noble, S. M. Passage through the mammalian gut triggers a phenotypic switch that promotes Candida albicans commensalism. *Nature Genetics* **45**, 1088–1091 (2013).
31. Zdanavičienė, E., Sakalauskienė, J., Gleiznys, A., Gleiznys, D. & Žilinskas, J. *Host responses to Candida albicans. A review*. *Baltic Dental and Maxillofacial Journal* vol. 19 (2017).
32. Wächtler, B., Wilson, D., Haedicke, K., Dalle, F. & Hube, B. From attachment to damage: Defined genes of Candida albicans mediate adhesion, invasion and damage during interaction with oral epithelial cells. *PLoS ONE* **6**, (2011).
33. Zhu, W. & Filler, S. G. Interactions of Candida albicans with epithelial cells. *Cellular Microbiology* vol. 12 273–282 (2010).
34. Chaffin, W. L. Candida albicans Cell Wall Proteins . *Microbiology and Molecular Biology Reviews* **72**, 495–544 (2008).
35. Moyes, D. L., Richardson, J. P. & Naglik, J. R. Candida albicans-epithelial interactions and pathogenicity mechanisms: Scratching the surface. *Virulence* **6**, 338–346 (2015).
36. Gaur, N. K. & Klotz, S. A. *Expression, Cloning, and Characterization of a Candida albicans Gene, ALA1, That Confers Adherence Properties upon Saccharomyces cerevisiae for Extracellular Matrix Proteins*. *INFECTION AND IMMUNITY* vol. 65 (1997).
37. Sheppard, D. C. *et al.* Functional and structural diversity in the Als protein family of Candida albicans. *Journal of Biological Chemistry* **279**, 30480–30489 (2004).
38. Hoyer, L. The ALSgene family ofCandida albicans. *TRENS in Microbiology* **9**, (2001).
39. Modrzewska, B. & Kurnatowski, P. *Review articles Adherence of Candida sp. to host tissues and cells as one of its pathogenicity features 1*. *Annals of Parasitology* vol. 61 (2015).
40. Wächtler, B. *et al.* Candida albicans-epithelial interactions: Dissecting the roles of active penetration, induced endocytosis and host factors on the infection process. *PLoS ONE* **7**, (2012).
41. Dalle, F. *et al.* Cellular interactions of Candida albicans with human oral epithelial cells and enterocytes. *Cellular Microbiology* **12**, 248–271 (2010).
42. Phan, Q. T. *et al.* Als3 is a Candida albicans invasin that binds to cadherins and induces endocytosis by host cells. *PLoS Biology* **5**, 0543–0557 (2007).
43. Phan, Q. T., Fratti, R. A., Prasadarao, N. v., Edwards, J. E. & Filler, S. G. N-cadherin mediates endocytosis of Candida albicans by endothelial cells. *Journal of Biological Chemistry* **280**, 10455–10461 (2005).
44. Sun, J. N. *et al.* Host cell invasion and virulence mediated by Candida albicans Ssa1. *PLoS Pathogens* **6**, (2010).
45. Naglik, J. R., Challacombe, S. J. & Hube, B. Candida albicans Secreted Aspartyl Proteinases in Virulence and Pathogenesis . *Microbiology and Molecular Biology Reviews* **67**, 400–428 (2003).

46. Kumamoto, C. A. Molecular mechanisms of mechanosensing and their roles in fungal contact sensing. *Nature Reviews Microbiology* vol. 6 667–673 (2008).
47. Brand, A. *et al.* Hyphal Orientation of Candida albicans Is Regulated by a Calcium-Dependent Mechanism. *Current Biology* **17**, 347–352 (2007).
48. Brand, A. & Gow, N. A. Mechanisms of hypha orientation of fungi. *Current Opinion in Microbiology* vol. 12 350–357 (2009).
49. Brand, A. *et al.* An internal polarity landmark is important for externally induced hyphal behaviors in Candida albicans. *Eukaryotic Cell* **7**, 712–720 (2008).
50. Fanning, S. & Mitchell, A. P. Fungal biofilms. *PLoS pathogens* **8**, (2012).
51. Finkel, J. S. & Mitchell, A. P. Genetic control of Candida albicans biofilm development. *Nature Reviews Microbiology* vol. 9 109–118 (2011).
52. Ene, I. v., Bennett, R. J. & Anderson, M. Z. Mechanisms of genome evolution in Candida albicans. *Current Opinion in Microbiology* vol. 52 47–54 (2019).
53. Dunn, M. J. & Anderson, M. Z. To repeat or not to repeat: Repetitive sequences regulate genome stability in candida albicans. *Genes* vol. 10 (2019).
54. Todd, R., Wikoff, T. D., Forche, A. & Selmecki, A. Genome plasticity inCandida albicansisdriven by long repeat sequences. *eLife* **8**, (2019).
55. Selmecki, A., Forche, A. & Berman, J. Genomic plasticity of the human fungal pathogen Candida albicans. *Eukaryotic Cell* vol. 9 991–1008 (2010).
56. Legrand, M., Jaitly, P., Feri, A., d'Enfert, C. & Sanyal, K. Candida albicans: An Emerging Yeast Model to Study Eukaryotic Genome Plasticity. *Trends in Genetics* vol. 35 292–307 (2019).
57. Bennett, R. J. The parasexual lifestyle of Candida albicans. *Current Opinion in Microbiology* vol. 28 10–17 (2015).
58. Perry, A. M., Hernday, A. D. & Nobile, C. J. Unraveling how candida albicans forms sexual biofilms. *Journal of Fungi* vol. 6 (2020).
59. Guan, G. *et al.* Environment-induced same-sex mating in the yeast Candida albicans through the HSF1–HSP90 pathway. *PLoS Biology* **17**, (2019).
60. Gintjee, T. J., Donnelley, M. A. & Thompson, G. R. Aspiring Antifungals: Review of Current Antifungal Pipeline Developments. *Journal of Fungi* **6**, 28 (2020).
61. Vallières, C., Raulo, R., Dickinson, M. & Avery, S. v. Novel combinations of agents targeting translation that synergistically inhibit fungal pathogens. *Frontiers in Microbiology* **9**, (2018).
62. Tscherner, M. & Kuchler, K. A histone acetyltransferase inhibitor with antifungal activity against CTG clade Candida species. *Microorganisms* **7**, (2019).
63. Carolus, H., Pierson, S., Lagrou, K. & van Dijck, P. Amphotericin b and other polyenes—discovery, clinical use, mode of action and drug resistance. *Journal of Fungi* vol. 6 1–20 (2020).
64. Santos, G. C. de O. *et al.* Candida infections and therapeutic strategies: Mechanisms of action for traditional and alternative agents. *Frontiers in Microbiology* vol. 9 (2018).
65. Houšť, J., Spížek, J. & Havlíček, V. Antifungal drugs. *Metabolites* vol. 10 (2020).
66. Ksiezopolska, E. & Gabaldón, T. Evolutionary emergence of drug resistance in candida opportunistic pathogens. *Genes* vol. 9 (2018).
67. Yong, J., Zu, R., Huang, X., Ge, Y. & Li, Y. Synergistic Effect of Berberine Hydrochloride and Fluconazole Against Candida albicans Resistant Isolates. *Frontiers in Microbiology* **11**, (2020).
68. Su, S. *et al.* Antifungal Activity and Potential Mechanism of Panobinostat in Combination With Fluconazole Against Candida albicans. *Frontiers in Microbiology* **11**, (2020).
69. Lupetti, A., Danesi, R., Campa, M., del Tacca, M. & Kelly, S. Molecular basis of resistance to azole antifungals. *TRENSS in Molecular Medicine* **8**, (2002).
70. Shapiro, R. S., Robbins, N. & Cowen, L. E. Regulatory Circuitry Governing Fungal Development, Drug Resistance, and Disease. *Microbiology and Molecular Biology Reviews* **75**, 213–267 (2011).
71. Flowers, S. A., Colón, B., Whaley, S. G., Schuler, M. A. & David Rogers, P. Contribution of clinically derived mutations in ERG11 to azole resistance in Candida albicans. *Antimicrobial Agents and Chemotherapy* **59**, 450–460 (2015).
72. Xiang, M. J. *et al.* Erg11 mutations associated with azole resistance in clinical isolates of Candida albicans. *FEMS Yeast Research* **13**, 386–393 (2013).
73. Berkow, E. L. & Lockhart, S. R. Fluconazole resistance in Candida species: A current perspective. *Infection and Drug Resistance* vol. 10 237–245 (2017).
74. Morio, F., Pagniez, F., Lacroix, C., Miegeville, M. & le pape, P. Amino acid substitutions in the Candida albicans sterol δ5,6-desaturase (Erg3p) confer azole resistance: Characterization of two

novel mutants with impaired virulence. *Journal of Antimicrobial Chemotherapy* **67**, 2131–2138 (2012).
75. Cowen, L. E., Sanglard, D., Howard, S. J., Rogers, P. D. & Perlin, D. S. Mechanisms of antifungal drug resistance. *Cold Spring Harbor Perspectives in Medicine* **5**, (2015).
76. MacPherson, S. *et al.* Candida albicans zinc cluster protein Upc2p confers resistance to antifungal drugs and is an activator of ergosterol biosynthetic genes. *Antimicrobial Agents and Chemotherapy* **49**, 1745–1752 (2005).
77. Morschhäuser, J. *et al.* The transcription factor Mrr1p controls expression of the MDR1 efflux pump and mediates multidrug resistance in Candida albicans. *PLoS Pathogens* **3**, 1603–1616 (2007).
78. Coste, A. T., Karababa, M., Ischer, F., Bille, J. & Sanglard, D. TAC1, transcriptional activator of CDR genes, is a new transcription factor involved in the regulation of Candida albicans ABC transporters CDR1 and CDR2. *Eukaryotic Cell* **3**, 1639–1652 (2004).
79. Tsao, S., Rahkhoodaee, F. & Raymond, M. Relative contributions of the Candida albicans ABC transporters Cdrlp and Cdr2p to clinical azole resistance. *Antimicrobial Agents and Chemotherapy* **53**, 1344–1352 (2009).
80. Siikala, E. *et al.* Persistent Candida albicans colonization and molecular mechanisms of azole resistance in autoimmune polyendocrinopathy-candidiasis-ectodermal dystrophy (APECED) patients. *Journal of Antimicrobial Chemotherapy* **65**, 2505–2513 (2010).
81. Coste, A. *et al.* A mutation in Tac1p, a transcription factor regulating CDR1 and CDR2, is coupled with loss of heterozygosity at chromosome 5 to mediate antifungal resistance in Candida albicans. *Genetics* **172**, 2139–2156 (2006).
82. Selmecki, A., Forche, A. & Berman, J. *Aneuploidy and Isochromosome Formation in Drug-Resistant Candida albicans*. www.sciencemag.org/cgi/content/full/313/5785/367/DC1 (2006).
83. Hirakawa, M. P., Chyou, D. E., Huang, D., Slan, A. R. & Bennett, R. J. Parasex generates phenotypic diversity de novo and impacts drug resistance and virulence in candida albicans. *Genetics* **207**, 1195–1211 (2017).
84. Arendrup, M. C. & Perlin, D. S. Echinocandin resistance: An emerging clinical problem? *Current Opinion in Infectious Diseases* vol. 27 484–492 (2014).
85. Castanheira, M., Messer, S. A., Jones, R. N., Farrell, D. J. & Pfaller, M. A. Activity of echinocandins and triazoles against a contemporary (2012) worldwide collection of yeast and moulds collected from invasive infections. *International Journal of Antimicrobial Agents* **44**, 320–326 (2014).
86. Huang, W. *et al.* Lipid flippase subunit Cdc50 mediates drug resistance and virulence in Cryptococcus neoformans. *mBio* **7**, (2016).
87. Walker, L. A., Gow, N. A. R. & Munro, C. A. Fungal echinocandin resistance. *Fungal Genetics and Biology* **47**, 117–126 (2010).
88. Jensen, R. H. *et al.* Stepwise emergence of azole, echinocandin and amphotericin B multidrug resistance in vivo in Candida albicans orchestrated by multiple genetic alterations. *Journal of Antimicrobial Chemotherapy* **70**, 2551–2555 (2015).
89. Martel, C. M. *et al.* A clinical isolate of Candida albicans with mutations in ERG11 (encoding sterol 14α-demethylase) and ERG5 (encoding C22 desaturase) is cross resistant to azoles and amphotericin B. *Antimicrobial Agents and Chemotherapy* **54**, 3578–3583 (2010).
90. Vandeputte, P. *et al.* A nonsense mutation in the ERG6 gene leads to reduced susceptibility to polyenes in a clinical isolate of Candida glabrata. *Antimicrobial Agents and Chemotherapy* **52**, 3701–3709 (2008).
91. Spampinato, C. & Leonardi, D. Candida infections, causes, targets, and resistance mechanisms: Traditional and alternative antifungal agents. *BioMed Research International* vol. 2013 (2013).
92. Hope, W. W., Tabernero, L., Denning, D. W. & Anderson, M. J. Molecular mechanisms of primary resistance to flucytosine in Candida albicans. *Antimicrobial Agents and Chemotherapy* **48**, 4377–4386 (2004).
93. Revie, N. M., Iyer, K. R., Robbins, N. & Cowen, L. E. Antifungal drug resistance: evolution, mechanisms and impact. *Current Opinion in Microbiology* vol. 45 70–76 (2018).
94. Dunkel, N. & Morschhäuser, J. Loss of heterozygosity at an unlinked genomic locus is responsible for the phenotype of a Candida albicans sap4Δ sap5Δ sap6Δ mutant. *Eukaryotic Cell* **10**, 54–62 (2011).
95. Ford, C. B. *et al.* The evolution of drug resistance in clinical isolates of candida albicans. *eLife* **2015**, 1–27 (2015).
96. Cowen, L. E., Anderson, J. B. & Kohn, L. M. Evolution of drug resistance in Candida albicans. *Annual Review of Microbiology* vol. 56 139–165 (2002).

97. Anderson, J. B. *et al. Mode of Selection and Experimental Evolution of Antifungal Drug Resistance in Saccharomyces cerevisiae*. www.stanford.edu/group/yeast_deletion_ (2003).
98. Cowen, L. E. *et al. Population genomics of drug resistance in Candida albicans*. www.pnas.orgcgidoi10.1073pnas.102291099 (2002).
99. Santos, M. A. S., Gomes, A. C., Santos, M. C., Carreto, L. C. & Moura, G. R. The genetic code of the fungal CTG clade. *Comptes Rendus - Biologies* vol. 334 607–611 (2011).
100. Bezerra, A. R. *et al.* The role of non-standard translation in Candida albicans pathogenesis. *FEMS Yeast Research* vol. 21 (2021).
101. Miranda, I. *et al.* Candida albicans CUG mistranslation is a mechanism to create cell surface variation. *mBio* **4**, (2013).
102. Schwartz, M. H. & Pan, T. Function and origin of mistranslation in distinct cellular contexts. *Critical Reviews in Biochemistry and Molecular Biology* vol. 52 205–219 (2017).
103. Gomes, A. C. *et al.* A genetic code alteration generates a proteome of high diversity in the human pathogen Candida albicans. *Genome Biology* **8**, (2007).
104. Rocha, R., José, P., Pereira, B., Santos, M. A. S. & Macedo-Ribeiro, S. Unveiling the structural basis for translational ambiguity tolerance in a human fungal pathogen. (2011) doi:10.1073/pnas.1102835108/-/DCSupplemental.
105. Bezerra, A. R. *et al.* Reversion of a fungal genetic code alteration links proteome instability with genomic and phenotypic diversification. *Proceedings of the National Academy of Sciences of the United States of America* **110**, 11079–11084 (2013).
106. Miranda, I. *et al.* A genetic code alteration is a phenotype diversity generator in the human pathogen Candida albicans. *PLoS ONE* **2**, (2007).
107. Weil, T. *et al.* Adaptive Mistranslation Accelerates the Evolution of Fluconazole Resistance and Induces Major Genomic and Gene Expression Alterations in Candida albicans. *mSphere* **2**, (2017).
108. Coste, A. *et al.* A mutation in Tac1p, a transcription factor regulating CDR1 and CDR2, is coupled with loss of heterozygosity at chromosome 5 to mediate antifungal resistance in Candida albicans. *Genetics* **172**, 2139–2156 (2006).
109. Lohberger, A., Coste, A. T. & Sanglard, D. Distinct roles of Candida albicans drug resistance transcription factors TAC1, MRR1, and UPC2 in virulence. *Eukaryotic Cell* **13**, 127–142 (2014).
110. Dunkel, N., Blaß, J., Rogers, P. D. & Morschhäuser, J. Mutations in the multi-drug resistance regulator MRR1, followed by loss of heterozygosity, are the main cause of MDR1 overexpression in fluconazole-resistant Candida albicans strains. *Molecular Microbiology* **69**, 827–840 (2008).
111. Andrews, S. FastQC: a quality control tool for high throughput sequence data. (2010).
112. Bolger, A. M., Lohse, M. & Usadel, B. Trimmomatic: A flexible trimmer for Illumina sequence data. *Bioinformatics* **30**, 2114–2120 (2014).
113. Li, H. & Durbin, R. Fast and accurate long-read alignment with Burrows-Wheeler transform. *Bioinformatics* **26**, 589–595 (2010).
114. Danecek, P. *et al.* Twelve years of SAMtools and BCFtools. *GigaScience* **10**, (2021).
115. Picard Toolkit. Broad Institute, GitHub Repository. (2019).
116. van der Auwera, G. & O'Connor, B. *Genomics in the Cloud: Using Docker, GATK, and WDL in Terra* . (O'Reilly Media, 2020).
117. Selmecki, A. M. *et al.* Polyploidy can drive rapid adaptation in yeast. *Nature* **519**, 349–351 (2015).
118. Cingolani, P. *et al.* A program for annotating and predicting the effects of single nucleotide polymorphisms, SnpEff: SNPs in the genome of Drosophila melanogaster strain w1118; iso-2; iso-3. *Fly* **6**, 80–92 (2012).
119. Boeva, V. *et al.* Control-FREEC: A tool for assessing copy number and allelic content using next-generation sequencing data. *Bioinformatics* **28**, 423–425 (2012).
120. Skrzypek, M. *et al.* The Candida Genome Database (CGD). *incorporation of Assembly 22, systematic identifiers and visualization of high throughput sequencing data* (2017).
121. Arendrup, M. C. *et al.* Method for the determination of broth dilution minimum inhibitory concentrations of antifungal agents for yeasts. *EUCAST antifungal MIC method for yeasts* 1–21 (2020).
122. Ciudad, T., Hickman, M., Bellido, A., Berman, J. & Larriba, G. Phenotypic consequences of a spontaneous loss of heterozygosity in a common laboratory strain of Candida albicans. *Genetics* **203**, 1161–1176 (2016).
123. Klotz, S. A. *et al.* Candida albicans Als proteins mediate aggregation with bacteria and yeasts. *Medical Mycology* **45**, 363–370 (2007).

124. Mohler, K. & Ibba, M. Translational fidelity and mistranslation in the cellular response to stress. *Nature Microbiology* vol. 2 (2017).
125. Wang, X. & Pan, T. Methionine Mistranslation Bypasses the Restraint of the Genetic Code to Generate Mutant Proteins with Distinct Activities. *PLoS Genetics* **11**, (2015).
126. Li, F. *et al.* Eap1p, an adhesin that mediates Candida albicans biofilm formation in vitro and in vivo. *Eukaryotic Cell* **6**, 931–939 (2007).
127. Demuyser, L., Palmans, I., Vandecruys, P. & van Dijck, P. Molecular Elucidation of Riboflavin Production and Regulation in Candida albicans, toward a Novel Antifungal Drug Target. *mSphere* **5**, (2020).
128. Hube, B. *et al.* Secreted lipases of Candida albicans: Cloning, characterisation and expression analysis of a new gene family with at least ten members. *Archives of Microbiology* **174**, 362–374 (2000).
129. Uhl, M. A., Biery, M., Craig, N. & D.Jonhson, A. Haploinsufficiency-based large-scale forward geneticanalysis of filamentous growth in the diploid humanfungal pathogen C.albicans. *The EMBO Journal* **22**, 2668–2678 (2003).
130. Lee, J. H., Kim, Y. G., Gupta, V. K., Manoharan, R. K. & Lee, J. Suppression of fluconazole resistant Candida albicans biofilm formation and filamentation by methylindole derivatives. *Frontiers in Microbiology* **9**, (2018).
131. de Groot, P. W. J., Hellingwerf, K. J. & Klis, F. M. Genome-wide identification of fungal GPI proteins. *Yeast* **20**, 781–796 (2003).
132. Houten, S. M. & Waterham, H. R. Nonorthologous gene displacement of phosphomevalonate kinase. *Molecular Genetics and Metabolism* **72**, 273–276 (2001).
133. Sorgo, A. G. *et al.* Effects of fluconazole on the secretome, the wall proteome, and wall integrity of the clinical fungus candida albicans. *Eukaryotic Cell* **10**, 1071–1081 (2011).
134. Lindquist, S. *Heat-shock proteins and stress tolerance in microorganisms*. (1992).
135. Lindquist, S. *THE HEAT-SHOCK RESPONSE*. www.annualreviews.org (1986).
136. Gong, Y., Li, T., Yu, C. & Sun, S. Candida albicans heat shock proteins and Hsps-associated signaling pathways as potential antifungal targets. *Frontiers in Cellular and Infection Microbiology* vol. 7 (2017).
137. Leach, M. D., Stead, D. A., Argo, E. & Brown, A. J. P. Identification of sumoylation targets, combined with inactivation of SMT3, reveals the impact of sumoylation upon growth, morphology, and stress resistance in the pathogen Candida albicans. *Molecular Biology of the Cell* **22**, 687–702 (2011).
138. Zenthon, J. F., Ness, F., Cox, B. & Tuite, M. F. The [PSI+] prion of Saccharomyces cerevisiae can be propagated by an Hsp104 orthologue from Candida albicans. *Eukaryotic Cell* **5**, 217–225 (2006).
139. Enjalbert, B. *et al.* Role of the Hog1 Stress-activated Protein Kinase in the Global Transcriptional Response to Stress in the Fungal Pathogen Candida albicans □ D. *Molecular Biology of the Cell* **17**, 1018–1032 (2006).
140. Fiori, A. *et al.* The heat-induced molecular disaggregase Hsp104 of Candida albicans plays a role in biofilm formation and pathogenicity in a worm infection model. *Eukaryotic Cell* **11**, 1012–1020 (2012).
141. Robbins, N. *et al.* Hsp90 governs dispersion and drug resistance of fungal biofilms. *PLoS Pathogens* **7**, (2011).
142. Razavi, T. *et al.* Investigating the expression of ALS2 and ALS9 genes along with allele frequency of ALS9 in patients with vulvovaginal candidiasis. *Infection, Genetics and Evolution* **82**, (2020).
143. Cheng, G. *et al.* Comparison between Candida albicans agglutinin-like sequence gene expression patterns in human clinical specimens and models of vaginal candidiasis. *Infection and Immunity* **73**, 1656–1663 (2005).
144. Bennett, R. J. Coming of age-sexual reproduction in Candida species. *PLoS Pathogens* **6**, (2010).
145. Morio, F., Jensen, R. H., le Pape, P. & Arendrup, M. C. Molecular basis of antifungal drug resistance in yeasts. *International Journal of Antimicrobial Agents* **50**, 599–606 (2017).

VII-Annexes

Annex A

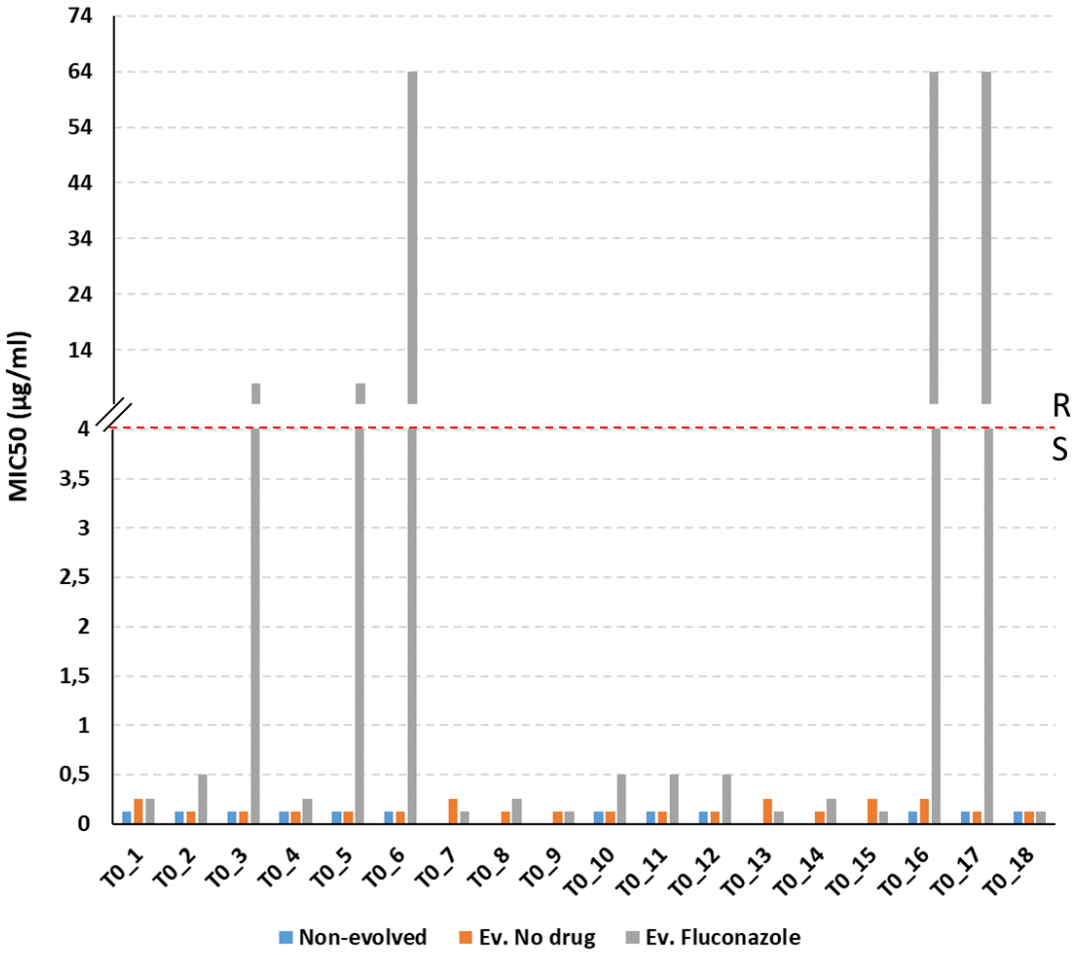

Figure 1 **- Minimal inhibitory concentration of strain T0.** The graph represents the minimum inhibitory concentration (MIC) of 18 isolates of T0 strain in the non-evolved condition (blue), evolved without drug (orange) and evolved with Fluconazole (grey). If the MIC result is greater than 4 µg/mL the isolate is resistant (R) and if it is less than 4 µg/mL the isolate is susceptible (S).

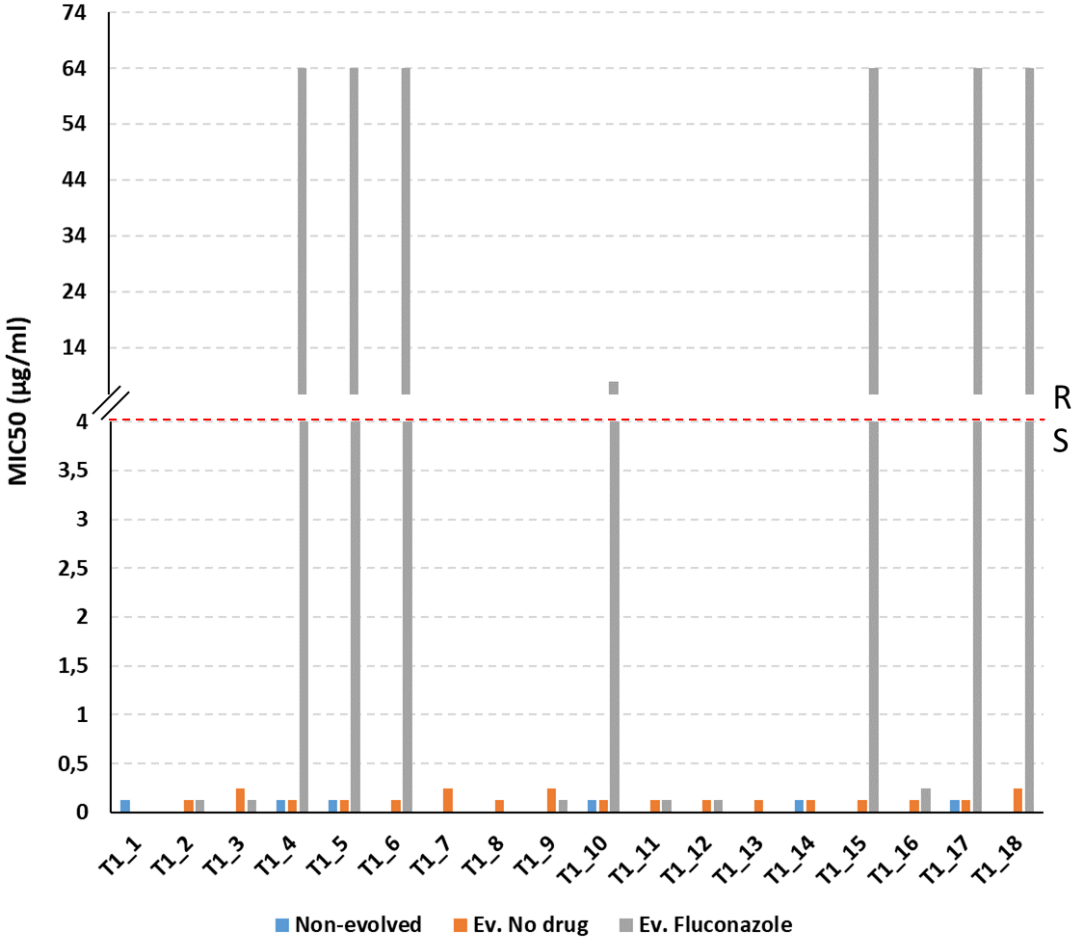

Figure 2 **- Minimal inhibitory concentration of strain T1.** The graph represents the minimum inhibitory concentration (MIC) of 18 strain T1 isolates in the non-evolved condition (blue), evolved without drug (orange) and evolved with Fluconazole (grey). If the MIC result is greater than 4 µg/mL the isolate is resistant (R) and if it is less than 4 µg/mL the isolate is susceptible (S).

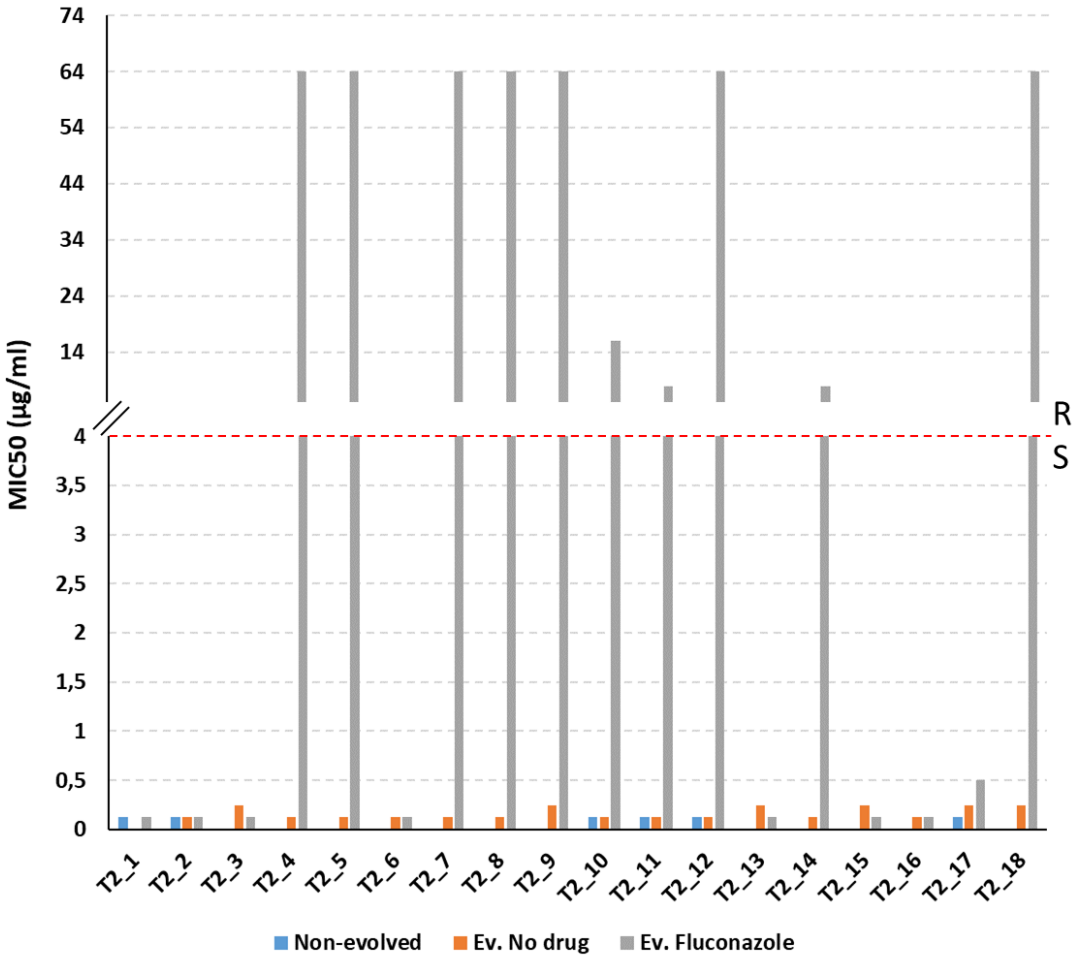

Figure 3 **- Minimal inhibitory concentration of strain T2.** The graph represents the minimum inhibitory concentration (MIC) of 18 strain T2 isolates in the non-evolved condition (Blue), evolved without drug (orange) and evolved with Fluconazole (grey). If the MIC result is greater than 4 µg/mL the isolate is resistant (R) and if it is less than 4 µg/mL the isolate is susceptible (S).

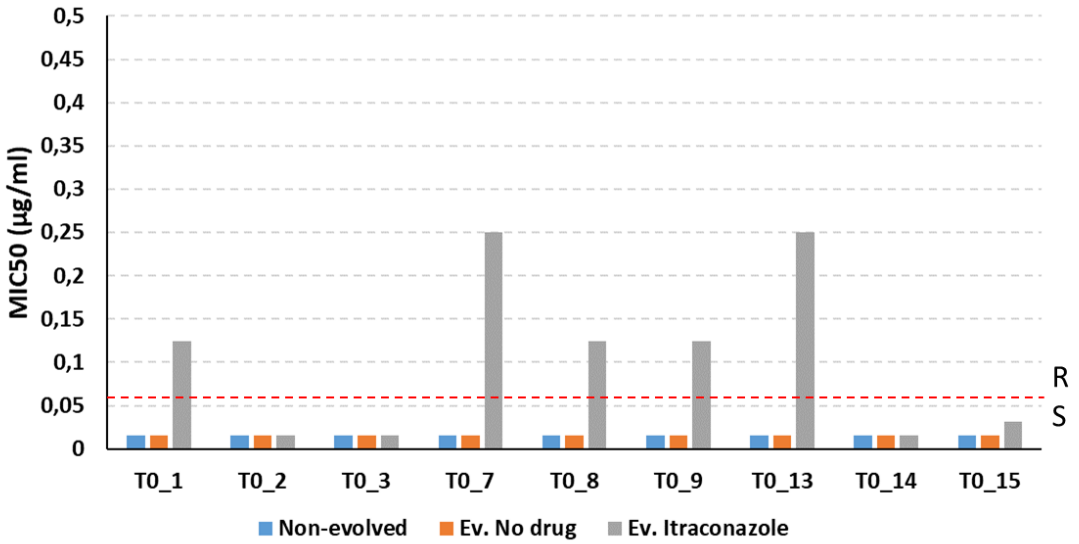

***Figure 4* - Minimal inhibitory concentration of strain T0.** The graph represents the minimum inhibitory concentration (MIC) of 9 strain T0 isolates in the non-evolved condition (blue), evolved without drug (orange) and evolved with Itraconazole (grey). If the MIC result is greater than 0.06 µg/mL the isolate is resistant (R) and if it is less than 0.06 µg/mL the isolate is susceptible (S).

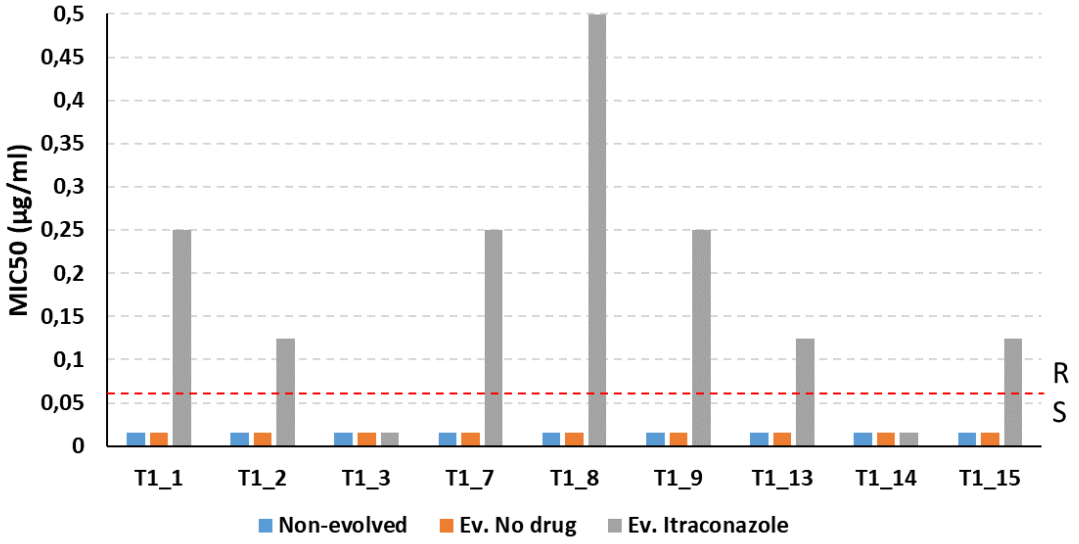

***Figure 5* - Minimal inhibitory concentration of strain T1.** The graph represents the minimum inhibitory concentration (MIC) of 9 strain T1 isolates in the non-evolved condition (blue), evolved without drug (orange) and evolved with Itraconazole (grey). If the MIC result is greater than 0.06 µg/mL the isolate is resistant (R) and if it is less than 0.06 µg/mL the isolate is susceptible (S).

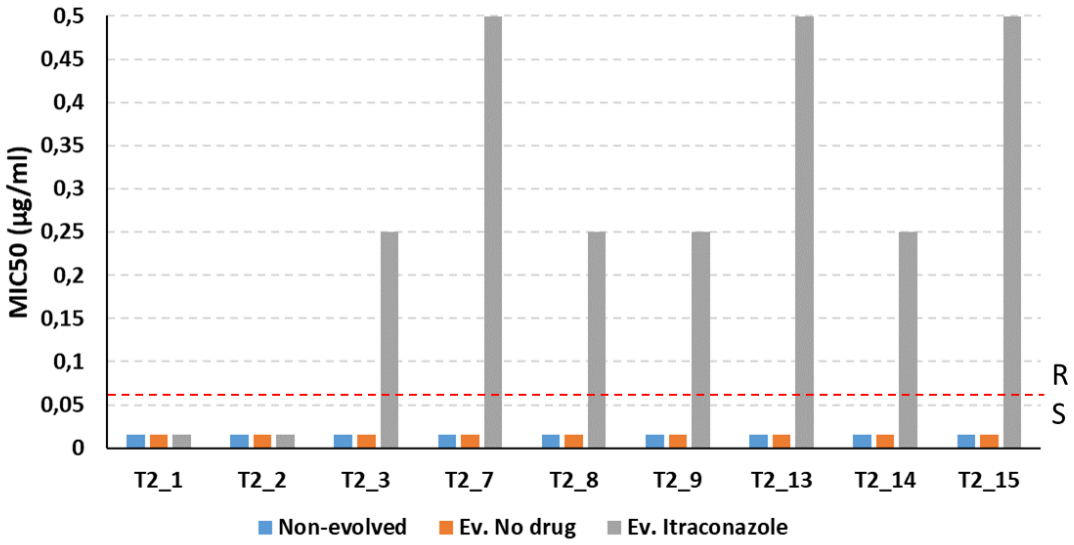

***Figure 6* - Minimal inhibitory concentration of strain T2.** The graph represents the minimum inhibitory concentration (MIC) of 9 strain T2 isolates in the non-evolved condition (blue), evolved without drug (orange) and evolved with Itraconazole (grey). If the MIC result is greater than 0.06 µg/mL the isolate is resistant (R) and if it is less than 0.06 µg/mL the isolate is susceptible (S).

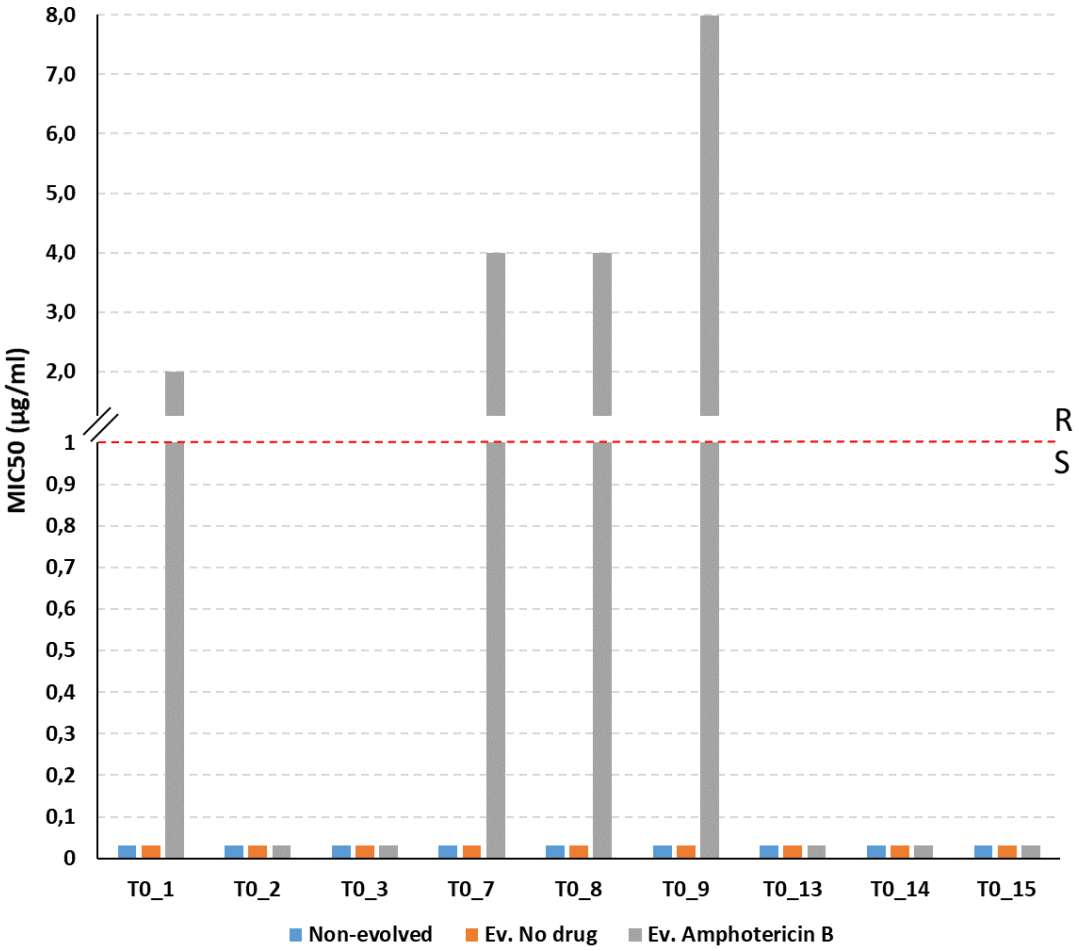

Figure 7 **- Minimal inhibitory concentration of strain T0.** The graph represents the minimum inhibitory concentration (MIC) of 9 strain T0 isolates in the non-evolved condition (blue), evolved without drug (orange) and evolved with Amphotericin B (grey). If the MIC result is greater than 1 µg/mL the isolate is resistant (R) and if it is less than 1 µg/mL the isolate is susceptible (S).

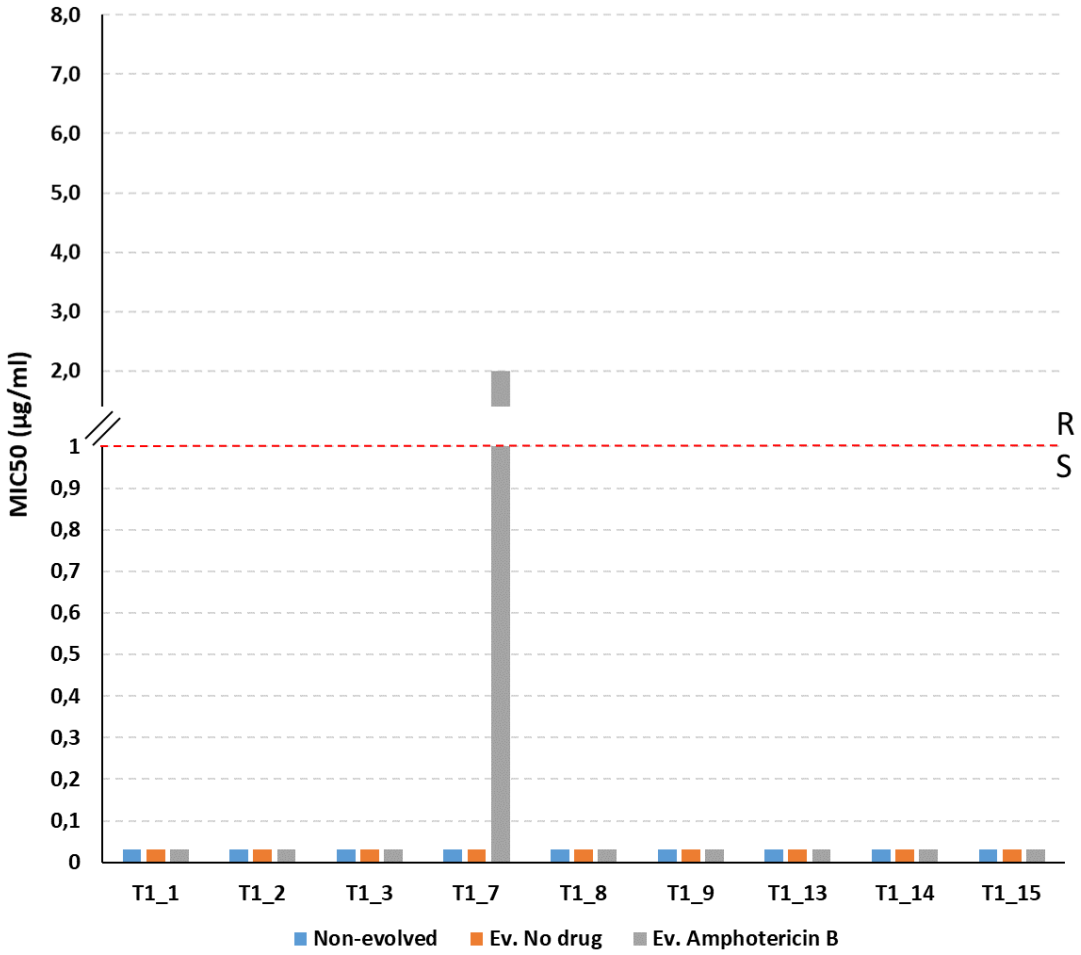

Figure 8 **- Minimal inhibitory concentration of strain T1.** The graph represents the minimum inhibitory concentration (MIC) of 9 strain T1 isolates in the non-evolved condition (blue), evolved without drug (orange) and evolved with Amphotericin B (grey). If the MIC result is greater than 1 µg/mL the isolate is resistant (R) and if it is less than 1 µg/mL the isolate is susceptible (S).

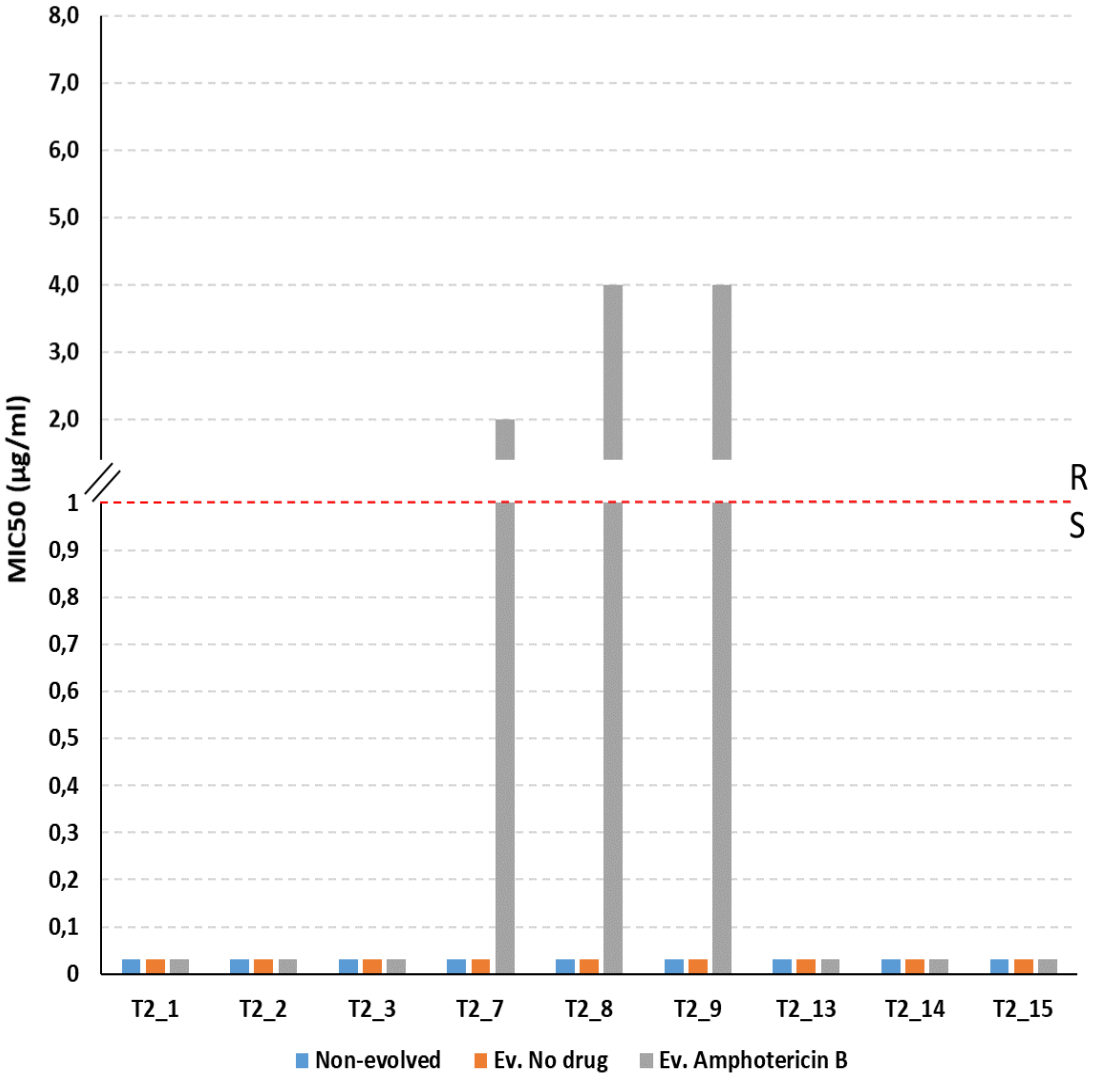

***Figure 9* - Minimal inhibitory concentration of strain T2.** The graph represents the minimum inhibitory concentration (MIC) of 9 strain T2 isolates in the non-evolved condition (blue), evolved without drug (orange) and evolved with Amphotericin B (grey). If the MIC result is greater than 1 µg/mL the isolate is resistant (R) and if it is less than 1 µg/mL the isolate is susceptible (S).

Annex B

Table 1 **-** Number of reads, % mapped reads and genome coverage from each isolate that was sequenced in evolution with Fluconazole.

		ID	genome coverage	#Reads	%Mapped reads
T0	**Non-evolved**	T0_1	119.2	11943039	99.4
		T0_3	111.9	11205562	91.6
		T0_6	118.0	11812485	99.4
		T0_16	115.0	11523205	99.4
	Evolved	T0_Ev_1	117.6	11740610	99.4
		T0_Ev_3	126.0	12545084	99.4
		T0_Ev_5	127.6	12699904	99.3
		T0_Ev_16	136.8	13646364	99.4
		T0_Ev_17	125.9	12549116	99.3
	Fluconazole	T0_Fluc_1	104.6	10447674	99.4
		T0_Fluc_3	99.0	9859802	99.4
		T0_Fluc_5	106.6	10626165	99.4
		T0_Fluc_6	121.5	12130390	99.4
		T0_Fluc_16	124.9	12423401	99.4
		T0_Fluc_17	121.7	12134032	99.4
T1	**Non-evolved**	T1_2	129.4	12933836	99.4
		T1_4	124.3	12398131	99.4
		T1_5	131.1	13204827	99.3
		T1_6	117.1	11707657	99.4
		T1_15	142.7	14251155	99.4
		T1_17	135.2	13480346	99.4
		T1_18	144.5	14419649	99.4
	Evolved	T1_Ev_4	136.0	13553244	99.4
		T1_EV_5	191.2	19338883	99.3
		T1_Ev_6	124.0	12355922	99.4
		T1_Ev_15	127.7	12749616	99.4
	Fluconazole	T1_Fluc_5	115.4	11675272	98.9
		T1_Fluc_9	133.8	13339126	99.5
		T1_Fluc_17	112.0	11152242	99.4
		T1_Fluc_18	120.8	12057081	99.4
T2	**Non-evolved**	T2_1	134.5	13445596	99.4
		T2_7	143.0	14266854	99.4
		T2_10	128.9	12880604	99.4
		T2_12	146.0	14565678	99.4
		T2_18	136.4	13631964	99.4
	Evolved	T2_Ev_10	114.9	11466736	99.4
		T2_Ev_12	133.5	13346381	99.4
		T2_Ev_14	139.5	13927304	99.5
		T2_Ev_18	129.8	12935426	99.4

	Fluconazole	T2_Fluc_1	155.3	15473547	99.4
		T2_Fluc_4	134.3	13382838	99.4
		T2_Fluc_5	136.7	13646641	99.4
		T2_Fluc_7	132.4	13197915	99.4
		T2_Fluc_8	134.1	13376113	99.4
		T2_Fluc_9	111.1	11097452	99.4
		T2_Fluc_11	114.0	11384854	99.4
		T2_Fluc_12	137.0	13656547	99.4
		T2_Fluc_14	114.9	11445919	99.4
		T2_Fluc_18	123.2	12283607	99.4

Table 2 - Number of reads, % mapped reads and genome coverage from each isolate that was sequenced in evolution with Itraconazole.

		ID	**genome coverage**	**#Reads**	**%Mapped reads**
T0	**Non-evolved**	T0_9	110.1	11454241	99.2
	Evolved	T0_Ev_9	42.9	6242720	99
	Itraconazole	T0_ITR_1	36.2	5284351	98.9
		T0_ITR_7	40.6	5933029	98.9
		T0_ITR_8	36.6	5348441	99
		T0_ITR_9	39.6	5791803	98.8
		T0_ITR_13	33.4	4882206	98.7
T1	**Non-evolved**	T1_9	149.8	15632299	98.9
	Evolved	T1_Ev_7	44.2	6442731	98.7
	Itraconazole	T1_ITR_1	37.1	5417627	99
		T1_ITR_7	122.7	18036426	98.6
		T1_ITR_8	35.4	5178828	98.8
		T1_ITR_9	31.3	4574718	98.9
		T1_ITR_13	38.7	5649482	99
T2	**Non-evolved**	T2_9	184.4	19217223	99.1
	Evolved	T2_Ev_9	57.0	8316965	98.5
	Itraconazole	T2_ITR_7	37.4	5450699	98.5
		T2_ITR_8	44.5	6492127	98.9
		T2_ITR_9	43.5	6351598	98.8
		T2_ITR_13	42.1	6152168	98.8
		T2_ITR_15	46.6	6814086	98.9

Table 3 **-** Number of reads, % mapped reads and genome coverage from each isolate that was sequenced in evolution with Amphotericin B.

		ID	genome coverage	#Reads	%Mapped reads
T0	**Non-evolved**	T0_9	110.1	11454241	99.2
	Evolved	T0_Ev_1	39.8	5799144	98.8
		T0_Ev_7	48.5	7073807	98.9
		T0_Ev_8	42.5	6198667	99
		T0_Ev_9	42.9	6242720	99
	Amphotericin B	T0_Amph_1	63.6	9231373	98.5
		T0_Amph_7	65.7	9549695	98.3
		T0_Amph_8	71.1	10338476	98.3
		T0_Amph_9	74.5	10804426	98.6
T1	**Non-Evolved**	T1_9	149.8	15632299	98.9
	Evolved	T1_Ev_7	44.2	6442731	98.7
	Amphotericin B	T1_Amph_7	81.8	11877200	98.6
T2	**Non-Evolved**	T2_9	184.4	19217223	99.1
	Evolved	T2_Ev_7	59.0	8602515	98.4
		T2_Ev_8	53.6	7801951	98.5
		T2_Ev_9	57.0	8316965	98.5
	Amphotericin B	T2_Amph_7	105.5	15323854	98.3
		T2_Amph_8	100.0	14496065	98.4
		T2_Amph_9	104.2	15137547	98.5

Annex C

Table 4 - Functional categorization of genes presents on CNVs from evolution with Itraconazole.

Itraconazole (R)						
Chr.	Region	Aneuploidy	GO	T0 Itr (R)	T1 Itr (R)	T2 Itr (R)
IV	850 kb to end	Trisomy	cellular protein modification process	v		
			organelle organization	v		
			protein catabolic process	v		
			regulation of biological process	v		
			response to chemical	v		
			response to stress	v		
			ribosome biogenesis	v		
			RNA metabolic process	v		
			transport	v		
R	0 to 1360 kb	Trisomy	cellular protein modification process	v		v
			organelle organization	v		v
			protein catabolic process	v		v
			regulation of biological process	v		v
			response to chemical	v		v
			response to stress	v		v
			ribosome biogenesis	v		v
			RNA metabolic process	v		v
			translation	v		v
			transport	v		v
R	1348 kb to end	Monosomy	cellular protein modification process	v		v
			organelle organization	v		v
			protein catabolic process	v		v
			regulation of biological process	v		v
			response to chemical	v		v
			response to stress	v		v
			ribosome biogenesis	v		v
			RNA metabolic process	v		v
			transport	v		v
IV	0 to 420 kb	Monosomy	cellular protein modification process			v
			organelle organization			v
			regulation of biological process			v
			response to chemical			v
			response to stress			v
			ribosome biogenesis			v
			RNA metabolic process			v
			translation			v
			transport			v
R	1360 kb to 1999 kb	Trisomy	cellular protein modification process			v
			organelle organization			v
			protein catabolic process			v
			regulation of biological process			v
			response to chemical			v
			response to stress			v
			ribosome biogenesis			v
			RNA metabolic process			v
			translation			v
			transport			v

Table 5 - Functional categorization of genes presents on CNVs from evolution with Amphotericin B.

Amphotericin B (R)						
Chr.	Region	Aneuploidy	GO	T0 Amph (R)	T1 Amph (R)	T2 Amph (R)
I	Whole	Trisomy	cellular protein modification process	v	v	v
			organelle organization	v	v	v
			protein catabolic process	v	v	v
			regulation of biological process	v	v	v
			response to chemical	v	v	v
			response to stress	v	v	v
			ribosome biogenesis	v	v	v
			RNA metabolic process	v	v	v
			translation	v	v	v
			transport	v	v	v
III	Whole	Trisomy	cellular protein modification process	v		v
			filamentous growth	v		v
			organelle organization	v		v
			protein catabolic process	v		v
			regulation of biological process	v		v
			response to chemical	v		v
			response to stress	v		v
			ribosome biogenesis	v		v
			RNA metabolic process	v		v
			translation	v		v
			transport	v		v
VI	Whole	Trisomy	organelle organization	v		v
			regulation of biological process	v		v
			response to chemical	v		v
			response to stress	v		v
			ribosome biogenesis	v		v
			RNA metabolic process	v		v
			translation	v		v
			transport	v		v

Table 6 **-** Functional categorization of genes presents on CNVs from evolution with Fluconazole.

Fluconazole (R)									
Chr.	Region	Aneuploidy	GO	T0 Fluc 3 (R)	T0 Fluc 16 (R)	T1 Fluc 5 (R)	T1 Fluc 9 (R)	T1 Fluc 17 (R)	T2 Fluc (R)
R	Whole	Trisomy	cellular protein modification process	v					
			organelle organization	v					
			protein catabolic process	v					
			regulation of biological process	v					
			response to chemical	v					
			response to stress	v					
			ribosome biogenesis	v					
			RNA metabolic process	v					
			translation	v					
			transport	v					
IV	532 kb to end	Trisomy	cellular protein modification process		v				
			organelle organization		v				
			protein catabolic process		v				
			regulation of biological process		v				
			response to chemical		v				
			response to stress		v				
			ribosome biogenesis		v				
			RNA metabolic process		v				
			transport		v				
R	1624 kb to 2136 kb	Monosomy	cellular protein modification process		v				
			organelle organization		v				
			protein catabolic process		v				
			regulation of biological process		v				
			response to chemical		v				
			response to stress		v				
			ribosome biogenesis		v				
			RNA metabolic process		v				
			transport		v				
			vesicle-mediated transport		v				
V	Whole	Trisomy	cell cycle			v			
			cellular protein modification process			v			
			organelle organization			v			
			regulation of biological process			v			
			response to stress			v			
			ribosome biogenesis			v			
			RNA metabolic process			v			
			translation			v			
			transport			v			
V	0 to 466 kb	Trisomy	cell cycle			v	v		
			cellular protein modification process			v	v		
			filamentous growth			v	v		
			organelle organization			v	v		
			regulation of biological process			v	v		
			response to chemical			v	v		
			response to stress			v	v		
			ribosome biogenesis			v	v		
			RNA metabolic process			v	v		
			translation			v	v		
			transport			v	v		
V	472 kb to end	Monosomy	cellular protein modification process				v		
			organelle organization				v		
			regulation of biological process				v		
			response to chemical				v		
			response to stress				v		
			ribosome biogenesis				v		
			RNA metabolic process				v		
			translation				v		
			transport				v		
R	866 kb to 2286 kb	Monosomy	transport		v		v	v	
			organelle organization		v		v	v	
			response to stress		v		v	v	
			regulation of biological process		v		v	v	
			protein catabolic process		v		v	v	
			RNA metabolic process		v		v	v	
			ribosome biogenesis		v		v	v	
			response to chemical		v		v	v	
			cellular protein modification process		v		v	v	
			filamentous growth		v		v	v	
			translation		v		v	v	
V	0 to 466 kb 969 kb to 1190 kb	Trisomy	cell cycle			v			v
			cellular protein modification process			v			v
			filamentous growth			v			v
			organelle organization			v			v
			regulation of biological process			v			v
			response to chemical			v			v
			response to stress			v			v
			ribosome biogenesis			v			v
			RNA metabolic process			v			v
			translation			v			v
			transport			v			v
VI	780 kb to end	Trisomy	biofilm formation						v
			biological process involved in interspecies interaction between organisms						v
			cell adhesion						v
			cellular protein modification process						v
			filamentous growth						v
			hyphal growth						v
			organelle organization						v
			regulation of biological process						v
			response to chemical						v
			response to drug						v
			response to stress						v
			RNA metabolic process						v
			translation						v
			transport						v
VII	0 to 253 kb 578 kb to end	Trisomy	organelle organization						v
			protein catabolic process						v
			regulation of biological process						v
			response to chemical						v
			response to stress						v
			ribosome biogenesis						v
			RNA metabolic process						v
			transport						v